Synthesis and *in vitro* Assessment of Chemically Modified siRNAs Targeting *BCL2* that Contain 2'-Ribose and Triazole-Linked Backbone Modifications

Gordon Hagen

Faculty of Science, *University of Ontario Institute of Technology*

Oshawa, ON, Canada

August, 2015

A thesis submitted to the University of Ontario Institute of Technology

in partial fulfillment of the requirements of the degree of Master of

Science in Applied Bioscience

Abstract

Short interfering RNAs (siRNAs) are biomolecules used for post-transcriptional gene regulation, and therefore hold promise as a future therapeutic by silencing gene expression of overexpressed deleterious genes. Chemically modifying the RNA structure is used to overcome the inherent limitations of the RNA structure. This project investigated the ability of a library of chemically modified siRNAs to target, *in vitro*, the therapeutically relevant oncogene, *BCL2*, by combining 2'-ribose sugar modifications with a novel triazole-linked backbone modification, previously described by our group. Solid support phosphoramidite chemistry was used to incorporate chemical modifications at various positions within anti-*BCL2* siRNAs. *In vitro* effects were evaluated through qPCR, cell viability, nuclease stability, and an immunological ELISA assay. Our results indicate that these unique modifications are well tolerated within RNAi and show enhanced activity and stability over natural siRNAs, while also improving upon inherent issues of immunological stimulation.

Acknowledgments

I would like acknowledge my supervisor Dr. Jean-Paul Desaulniers for welcoming me into his research group and being a part of such an exciting and fulfilling research project. Dr. Desaulniers sparked my interest in scientific research when I took bio-organic chemistry during my undergraduate degree, he opened up my eyes to what is possible with chemistry applied to biology and how exciting and multidisciplinary scientific research can be. Dr. Desaulniers was my biggest inspiration to start on the path I am now set on. I have found a purpose because of Dr. Desaulniers inspiration, and it has been a pleasure to work under his supervision for the past two years. Working under his supervision and guidance had given me many opportunities to learn and grow. Not only has he given me the opportunity to do exciting cutting edge research be he has given me the opportunity to co-author on 2015 ACS Med. Chem. Lett. publication, to give an oral presentation of my research at the 2014 QOMSBOC research conference, and most recently a first author publication with RSC Med. Chem. Comm. For these opportunities I am forever grateful.

I would like to thank my committee members Dr. Yuri Bolshan and Dr. Janice Strap. Dr. Bolshan has helped me deepen my appreciation for synthetic organic chemistry. His vast knowledge of the subject has helped me develop my synthetic organic skills not only practically but also written and oral communication and especially challenging reaction mechanisms. Dr. Strap I would like to thank for always supporting me, helping guide me with biological experiments and critically questioning and analyzing my methods & results and challenging me to become a more critical and thoughtful scientist.

I need acknowledge all of the research groups who let me use their labs, equipment, and guidance to complete my research: Dr. Forrester, Dr. Green-Johnson, Dr. Bonetta, and Dr. Jones-Taggart. Thank you for putting up with me always coming in and out of your labs! I would also like to acknowledge the chemistry staff at this school for helping with the NMR instrument, reagents, and general guidance: Dr. Zenkina, Dr. Coulter, Dr. Darcy Burns, Genevieve Barnes, and Clayton Jakins. I would also like to thank Ed Courville from the science stores for being so patient with me and always willing to help me source new materials and suppliers, you help was integral in the completion of my thesis.

None of my progress would have been possible without the help from everyone in Dr. Desaulniers research group. I firstly would like to thank Tim Efthymiou for laying down the foundation upon which my project was built upon; without your pioneering work in the lab and development of the methods my project would not have existed. I need to thank Brandon Peel and Chris McKim for being the greatest mentors I could have asked for. You both showed me everything in lab, taught me how to use the equipment, and do every existing procedure, but more importantly you were great friends and companions to me. We really worked together as a team because of the comradery we shared and accomplished so much together. Thank you both for keeping me positive and always encouraging me to work hard and stay on task while still having fun. Special thanks to all of the undergraduates who have worked alongside me throughout my stay: Kalai Krishnamurthy, Blake Roberts, Jocelyn Anderson, Jessica Pauze and Sebastian Robert. You were all very motivated and positive people, it was a pleasure working with you all and your help has been invaluable to me.

Another important acknowledgement to make is to everyone in the APBS program at UOIT, it was a pleasure to work in such a positive and collaborative environment. Special thanks to Dr. Isaac Shim for constantly troubleshooting with me while I struggled with molecular biology, Sandra Clarke for helping me with every step of my ELISA assay, Matthew Baxter for helping with synthetic organic chemistry, and Christina Adams for her constant support, collaborative brainstorming and all the help with my writing.

Finally I would like to acknowledge all of my friends and family who have supported me throughout my academic career. My parents, grandparents and my sister, thank you for your unwavering encouragement and support. Thank you so much for always believing in me, and propping me up when I got discouraged. This would not have been possible without all of your help. I would like to thank everyone who took me in while I was at university, my aunt and uncle, the Adams family and Shannen Johnston. Financially I would not have been able to attend post-secondary education without you. For taking me in and letting me be a part of your lives I am forever grateful; without your support post-secondary education would not have been a reality for me.

Lastly, I would like to thank NSERC for the funding that enabled me to conduct research at UOIT.

Table of Contents

List of Figures

List of Tables

List of Schemes

List of Appendix Figures

List of Abbreviations

18s 18 rRNA

A Adenine

A-1 Bcl-2-related Protein A1

Ago Argonaute Protein

Amp Ampicillin

APS Ammonium Persulfate

AS Antisense

ASO Antisense Oligonucleotide

ATF Activating Transcription Factor

ATP Adenosine Triphosphate

BAD BCL-2-Associated Death Promoter

BAK BCL-2-Antagonist/Killer

BAX BCL-2-Associated X Protein

BCL-2 B-Cell Lymphoma Protein 2

BCL-XL B-Cell Lymphoma Extra Large

BH3 BCL-2 Homology 3

BID BH3 Interacting-Domain Death Agonist

BIK BCL-2-Interacting Killer

BO Boranophosphate Backbone

BOK BCL-2-Related Ovarian Killer

bp Base-Pair

C Cytosine

C18 Octadecyl Carbon Chain-Bonded Silica Column

CD Circular Dichroism

cDNA Complementary DNA or Copy DNA

CH_2Cl_2 Dichloromethane

CHS Chalcone Synthase

CPG Controlled Pore Glass

Cq Quantification Cycle

C_tU Cytosine-Triazole Linked-Uracil

C_tUCH Cytosine-Triazole Linked- Uracil Cholesterol

DEPC Diethylpyrocarbonate (diethyl dicarbonate)

DIPEA *N*, *N*-Diisopropylethylamine

DMAP 4-(Dimethylamino)pyridine

DMF *N*, *N*-Dimethylformamide

DMSO Dimethylsulfoxide

DMT 4,4’-Dimethoxytrityl

DMT-Cl 4,4'-Dimethoxytrityl Chloride

DNA Deoxyribonucleic Acid

ds Double-Stranded

dT Deoxythymidine

EDTA Ethylenediaminetetraacetic Acid

EMAM Methylamine 40% wt. in H2O and Methylamine 33% wt. in Ethanol 1:1

EMEM Eagle's Minimum Essential Medium

ESI Q-TOF MS Electrospray Ionization Time-Of-Flight Mass Spectrometry

ESI-HRMS Electrospray Ionization High-Resolution Mass Spectrometry

Et Ethyl

Et2O Diethyl Ether

EtOAc Ethyl Acetate

EtOH Ethanol

FBS Fetal Bovine Serum

FDA The Food and Drug Administration

G Guanine

GAPDH Glyceraldehyde 3-phosphate Dehydrogenase

HCC Hepatocellular Carcinoma

HPLC High-Performance Liquid Chromatography

HRP Horseradish Peroxidase

IC_{50} Half Maximal Inhibitory Concentration

IDT Integrated DNA Technologies

IFN-α Interferon Alpha

IL-6 Interleukin 6

LNA Locked Nucleic Acid

m/z Mass-to-Charge Ratio

MCL-1 Induced Myeloid Leukemia Cell Differentiation Gene

Me Methyl

MeOH Methanol

MID Middle Domain

miRNA Micro-interfering RNA

mRNA Messenger RNA

MWCO Molecular-Weight Cut Off

MyD88 Myeloid Differentiation Primary Response Gene 88

NaOAc Sodium Acetate

NF-κB Nuclear Factor Kappa-Light-Chain-Enhancer of Activated B Cells

NMR Nuclear Magnetic Resonance

NRT No Reverse Transcriptase

nt Nucleotide

NTC No Template Control

NTP Nucleoside Triphosphate

OD Optical Density

OH Hydroxyl

***O*-Me** *O*-Methyl

***O*-MOE** Methoxyethyl

p53 phosphoprotein p53

PAGE Polyacrylamide Gel Electrophoresis

PAZ Piwi Argonaute Zwille Domain

P-Bodies Processing Bodies

PBMC A Peripheral Blood Mononuclear Cell

PBS Phosphate Buffered Saline

PCR Polymerase Chain Reaction

PEG Polyethylene Glycol

PIWI P-Element-Induced Wimpy Testis-Interacting Domain

PKR Double-Stranded RNA-Dependent Protein Kinase

PNA Peptide Nucleic Acid

Pre-miRNA Precursor miRNA

Pri-miRNA Primary miRNA

PS Phosphorothioate

qPCR Quantitative Real Time Polymerase Chain Reaction

RIG-1 Retinoic Acid Inducible Protein 1

RISC RNA-Induced Silencing Complex

RLC RISC Loading Complex

RNA Ribonucleic Acid

RNAi RNA Interference

RNase A Ribonuclease A

RNase H Ribonuclease H

RNase III Ribonuclease III

rt. Room Temperature

RT-PCR Reverse Transcription Polymerase Chain Reaction

shRNA Short Hairpin RNA

siRNA Short Interfering RNA

ss Single Stranded

T Thymine

TAE Tris-base, Acetic Acid and EDTA.

TBAF Tetrabutylammonium Fluoride

TBDMS or TBS *tert*-Butyldimethylsilyl

TBE Tris/Borate/EDTA

TBS-Cl *tert*-Butyldimethylsilyl Chloride

TCA Trichloroacetic Acid

TEA Triethylamine

TEG Triethylene Glycol

TEMED Tetramethylethylenediamine

THF Tetrahydrofuran

TLC Thin-Layer Chromatography

TLR Toll-Like Receptor

T*m* Melting Temperature

TMB 3,3′,5,5′-Tetramethylbenzidine

TNF-α Tumor Necrosis Factor Alpha

TOM Triisopropylsilyloxymethyl

TRBP *trans*-Activating Response RNA Binding Protein

TRIF TIR-domain-containing adapter-inducing interferon-β

U Uracil

UNA Unlocked Nucleic Acid

UTR Untranslated Region

UtU Uracil-Triazole-Uracil Dimer

UV Ultraviolet

wt Wild-Type

XTT (2,3-Bis-(2-Methoxy-4-Nitro-5-Sulfophenyl)-2H-Tetrazolium-5-Carboxanilide

Chapter 1: Literature Review

1.1 The "New" Central Dogma of Molecular Biology: RNAi

DNA into RNA into protein; the central dogma of molecular biology. This term was first coined in 1958 by the co-discoverer of DNA, Dr. Francis Crick, and was used to describe the flow of genetic information through biological systems (Crick, 1970). DNA serves as the storage of genetic information and provides the instructions for every function within the cell. RNA acts as an intermediate messenger, carrying the information of DNA to be translated into proteins. Proteins are the macromolecules which perform many of the biochemical reactions within the cell. The general idea of the central dogma still holds true today but our understanding has become somewhat more nuanced and less restrictive than DNA-RNA-Protein. RNA is a versatile biological macromolecule which seems to violate the classical understanding of the central dogma. RNA can be reverse transcribed into DNA (Baltimore, 1970; Temin & Mizutani, 1970), replicated into RNA (Koonin, et al., 1989) and can either up or down-regulate RNA and DNA expression (Li, et al., 2006; Hannon, 2002). The role of RNA within the central dogma of molecular biology is now more than a simple messenger, as it plays a key role in gene regulation.

Understanding RNA's role within the cell is a quickly growing area of research since the discovery of RNA interference (RNAi). The first hint of RNA interference was reported by Napoli, Lemieux and Jorgensen (1990). The aim of the study was to overexpress chalcone synthase gene (*CHS*) in petunias. This was accomplished through the introduction of the *CHS* gene using copy DNA (cDNA) via Agrobacterium *tumefaciens*

transformation. However, by introducing the gene they found the messenger RNA (mRNA) levels of the corresponding gene to be 50-fold lower than expected, and postulated this down-regulation was caused by a yet unknown mechanism. This unexpected result arose again in 1992 when researchers discovered mRNA depletion when the cDNA of a homologous mRNA sequences was introduced into the plant host (Romano & Macino, 1992). Soon, this unexplained phenomenon was observed in animals when Guo and Kemphues (1995) incubated C. *elegans* with sense and anti-sense RNA oligonucleotides corresponding to an endogenous mRNA. At the time, anti-sense mRNA was a known phenomenon, but the unexpected result was when the sense RNA, which could not hybridize with the endogenous mRNA, was still degraded. These findings overturned the conventional wisdom of the time by going against the central dogma. Fire and Mello (1998) followed up these studies by investigating the exact causes of this apparent RNA suppression, trying to tease apart the factors affecting this phenomenon. In their study they found that single stranded RNA (ssRNA) alone were not able to affect mRNA levels; but when ssRNA of the sense strand was injected into the animals, followed by the antisense strand (or the other way around) mRNA levels were diminished (hybridization of the ssRNA to form dsRNA occurred *in vivo*). This observation suggested that dsRNA, not ssRNA, was the trigger of this biological process (Fire, et al., 1998). The impact of this paper was enormous, sparking a new field of research and leading to a Nobel Prize for Fire and Mello in 2006 (less than a decade after their initial publication).

The next major step in RNAi was the elucidation of the exact trigger. Hamilton and Baulcombe (1999) postulated that at some point, the dsRNA must dissociate the sense

strand and use the anti-sense strand to bind the targeted mRNA. Through investigation of mRNA knock-down induced by viruses in plants models, they detected 25 nucleotide long antisense RNAs present, which they postulated are derived from a dsRNA source, causing the silencing (Hamilton & Baulcombe, 1999). The definitive proof of small dsRNA causing RNA interference was determined by Elbashir and collogues (2001). By incubating Drosophila cell extracts with dsRNA of various nucleotide lengths they demonstrated that synthetic 21- and 22-nt dsRNAs, with 3′ overhanging ends, act as the trigger for sequence-specific mRNA degradation. This served as the basis in which siRNAs are still designed, with a few minor refinements.

Concurrently, while the exact details of siRNAs were being investigated the RNAi pathway was discovered in a variety of eukaryotic taxa, including: animals, fungi, plants, and protozoa. Based on phylogenetic analysis, the most recent common ancestor of all eukaryotes most likely possessed an early RNAi pathway, indicating that RNAi is an ancient and conserved biological mechanism (Cerutti & Casas-Mollano, 2006). This lead to the understanding that RNAi is a broad biological pathway endogenously conserved within most, if not all, eukaryotes and this pathway included much more than the small interfering RNA.

1.2 RNAi Pathway

RNAi is an endogenous pathway which starts in the genome of an organism. Within the genome of eukaryotic organisms there are genes whose sole purpose is to be transcribed into non-coding RNA which only serve to regulate mRNA within the cell. These RNA are responsible for development, response to stress, and response to viral infections. As much as 5% of the human genome serves the sole purpose of encoding and producing

over 1000 of these regulatory RNAs; these regulatory RNAs govern the expression of over 30% of all genes (MacFarlane & Murphy, 2010). It has even been recently stated that the complexity of an organism is directly correlated to the number of regulatory RNAs present within the genome (Berezikov, 2011).

RNAi begins in the nucleus; a long RNA is transcribed and is known as the primary micro-interfering RNA transcript (pri-miRNA). Pri-miRNAs are typically over 1000 nucleotides in length and contain several secondary structures throughout. This pri-miRNA is then processed by a complex of proteins known as the microprocessor unit. The microprocessor unit is comprised of two key proteins, Dorsha and Pasha. Pasha is a dsRNA binding protein and Dorsha is a ribonuclease class III family enzyme with endonuclease capabilities. Dorsha cleaves the pri-miRNA into the precursor miRNA (pre-miRNA). The resulting pre-miRNA is typically 65-70 nucleotides in length and contains a distinctive double stranded stem-loop secondary structure and is immediately transported out of the nucleus and into the cytoplasm through a nuclear pore with the aid of transport facilitators Exprotin-5 and RanGTP (Lund & Dahlberg, 2006).

Once in the cytoplasm, the pre-miRNA is taken up by a protein known as Dicer, which cleaves the pre-miRNA into a fully mature micro interfering RNA (miRNA). It is at this point in the RNAi pathway which exogenous siRNAs and endogenous miRNAs converge. The resultant RNA is a duplex roughly 21-25 nucleotides long, with a 2 nucleotide overhang at each 3’-end of the duplex and a phosphate group at each 5’-end of the duplex. The duplex itself has an A-type helical secondary structure (Chiu & Rana, 2002; Schwarz, et al., 2003).

The next steps of the RNAi pathway are still an area of contention, but the leading theory is that Dicer recruits a double stranded RNA binding protein (TRBP) and together associate with argonaute (Ago) to form the RISC-loading complex (RLC). The dsRNA is then loaded into Ago, with one of the the 3'-ends associating with the PAZ domain and the 5'-phosphate end associating with the MID domain. The loading step is concurrent with strand selection, where one strand dissociates and the other is retained by Ago (Fabian & Sonenberg, 2010). The retained strand is the anti-sense, which is complementary to the mRNA target (this strand is known as the guide strand). The discarded strand is the equivalent sense strand to the mRNA target and is known as the passenger strand.

The basis for strand selection is based on the thermodynamics of the duplex sequence, the least thermodynamically stable 5'-end of the dsRNA is incorporated into Ago and the other strand is dissociated. This phenomenon is called the thermodynamic asymmetry principal (Kawamata & Tomari, 2010). Once the RNA is loaded into Ago, the protein complex is considered active and is known as the RNA-induced silencing complex (RISC).

RISC then undergoes cellular surveillance, scanning for a complementary sequence to the guide strand. Nucleotides 2-8 (counting from the 5'-end) of the guide strand initiate binding to the complementary sequence this is known as the seed region (Jackson, et al., 2006) (Ui-Tei, et al., 2008). This seed region does not need to have exact molecular complementarity with the target mRNA, but the extent of base-pairing does affect the subsequent silencing steps. If there is perfect complementation, and Ago2 is utilized over

the other Ago proteins, RISC undergoes canonical RNAi. If there are mismatches within the seed region, RISC undergoes non-canonical RNAi (Fabian & Sonenberg, 2010).

Canonical RNAi involves Ago2 and perfect seed sequence complementarity and is considered the "main" pathway of silencing. When RISC finds the complement mRNA sequence Ago2 will cleave the target mRNA sequence through its endoribonuclease III activity, cleaving the phosphodiester bond through hydrolysis resulting in 3′-hydroxyl and 5′-phosphate terminus products (Martinez & Tuschl, 2004). The RISC can continue its gene suppression by binding to and degrading any complementary mRNA sequences it encounters (Figure 1).

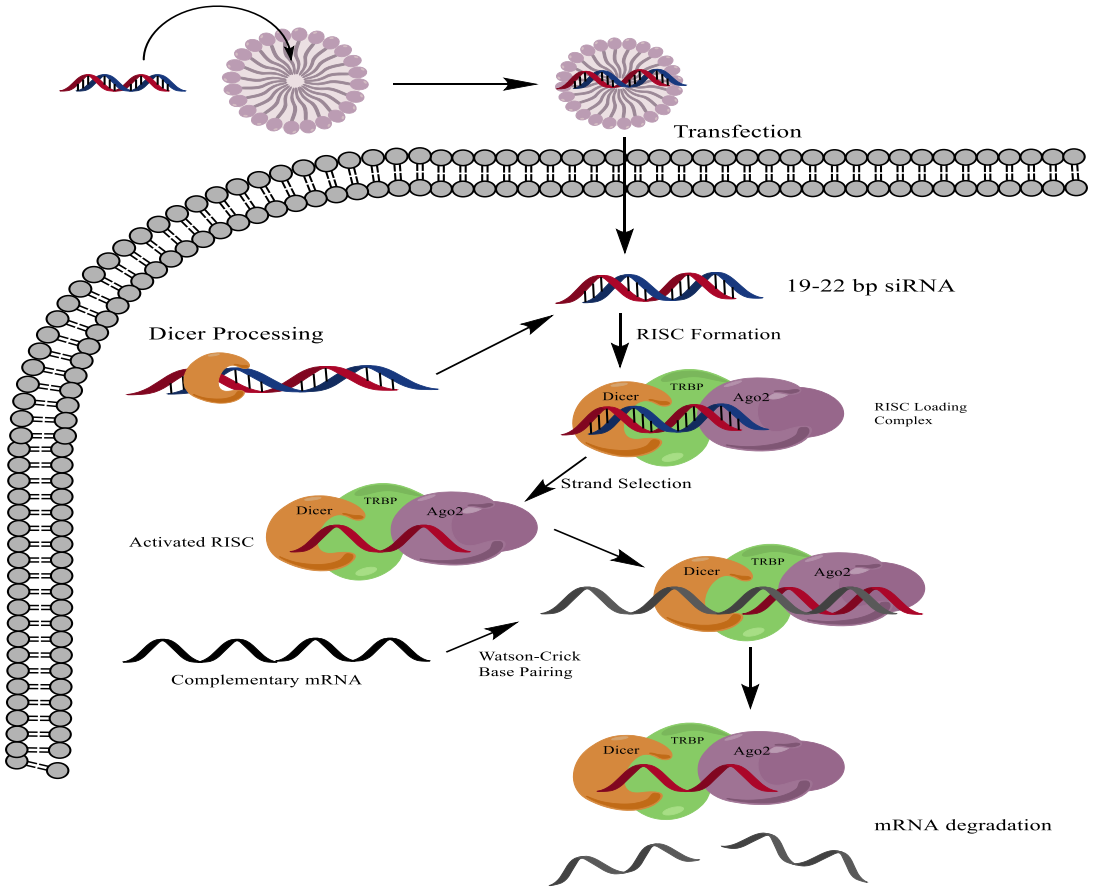

Figure 1 - Simplified schematic of canonical RNAi. Adapted from (Wilson & Doudna, 2013).

Non-canonical RNAi involves any of the other Ago proteins. There are four unique argonaute proteins found within humans, Ago1 through 4 (Doi, et al., 2003). They share common amino acid sequences yet only Ago2 has cleavage activity (Meister, et al., 2004). The other three Ago proteins do not contain a conserved catalytic tetrad within the PIWI domain of Ago2, which is the required for its slicing activity (Faehnle, et al., 2013). The RISC complex will bind its mRNA target and then associate with several other proteins and localize in processing bodies (P-bodies) within the cytoplasm. The P-bodies repress translation and enhance mRNA turnover via de-adenylation and de-capping proteins (Braun, et al., 2013). The details of the exact mechanisms, the protein players, protein interaction, molecular timing, and the importance of P-bodies has yet to be determined (Wilson & Doudna, 2013).

This molecular pathway is not only essential for the development and health of all eukaryotic organisms but through the use of exogenous siRNAs, this pathways has opened up doors which were once thought impossible in areas of biological research and potential therapeutics.

1.3 Application of siRNAs

The discovery of RNAi and the development of functional synthetic siRNAs has caused a revolution in basic biological research. SiRNAs can be used as a general tool for eukaryotic gene function studies, and have quickly become a popular tool for researchers across the globe. Researchers have been quick to adopt RNAi tools because of their relative ease to study gene function within eukaryotic organisms. A benefit of using

RNAi is its transient gene knockdown in adult mammalian organisms. Because of this transient gene knockdown, siRNAs can overcome the limitations that classical approaches cannot accomplish, due to embryonic lethal mutations which can occur through classical genetics (Brummelkamp & Bernards, 2003). SiRNAs can be used to test hypotheses of gene function, for validation of targets for potential therapeutics, for the analysis of protein pathways, to investigate gene redundancy, to generate libraries of siRNAs to perform functional screening of genes, and finally as a possible therapeutic.

SiRNAs can be used to validate gene function and investigate protein pathways within complex eukaryotic organisms. Researchers can make predictions of mammalian gene function through the use of comparative homology searches with genes whose functions are known in model organisms. In many cases, testing the accuracy of these predictions can be accomplished using siRNAs. One of the earliest applications of siRNAs in the study of gene function was by Kennerdell and Cathew (1998). Shortly after the discovery of RNAi they used dsRNA to study the role of *frizzled* and *frizzled 2* within the wingless pathway in Drosophila. Within a couple years, the utility of siRNA as a tool was expanded further by Burns, et al. (2004). In their study, they generated a library of siRNAs by constructing a set of retroviral vectors encoding 23,742 distinct siRNAs, which target 7,914 different human genes. The library was then used to discover five new genes which were key modulators of p53-dependent cellular proliferation arrest. This study clearly demonstrated the ability of RNAi for functional screens for complex eukaryotic organisms.

SiRNAs can also be used to validate targets for potential therapeutics. One of the first examples of using siRNA to validate therapeutic targets was by Li, et al. (2003). They

used siRNAs to reduce cyclin E expression in hepatocellular carcinoma (HCC) cells and, as expected, the cyclin E siRNA promoted apoptosis of HCC cells and blocked cellular proliferation *in vitro*. In *in* vivo mice models, cyclin E siRNAs inhibited HCC tumor growth in nude mice validating the *in vitro* results and highlighting the potential for creating drugs targeting cyclin E. This had lead into siRNAs being used as a viable therapeutic.

SiRNAs are able to be designed based solely on the mRNA sequence of the desired target. Therefore, any biological target can potentially become druggable through the use of siRNAs. This provides a distinct advantage over small molecule drug design, which is time consuming, vastly expensive, and a fortuitous process (Hughes, et al., 2011). It has also been stated that only 10-15% of all proteins are considered druggable by small molecules due to the complex structure and interactions of proteins *in vivo* (Griffith, et al., 2013). As such, there is great hope in siRNAs becoming a viable therapeutic option because of their distinct advantage over traditional small molecule drug design.

1.4 Limitations of siRNAs

Although siRNA based therapeutics seems like an ideal way to manage and treat disease, there are several important therapeutic limitations associated with siRNAs. The most glaring limitations include off-target effects/undesired strand selection, innate immune response to foreign nucleic acids, serum nuclease stability, and suitable delivery methods. These limitations will need to be overcome before siRNAs can be developed into a viable therapeutic.

Although siRNAs are tailored to match the sequence of the target mRNA, there are still off-target effects associated with siRNA administration. Off-target effects are when the siRNA knocks down an unintended mRNA sequence, which usually results in an undesired phenotypic effect. When researches design siRNAs sequence homology is considered when picking the target sequence. Sequence homology searches are performed to try to eliminate overt cross-reactivity. Yet, sequence homology alone is not able to fully predict the actual risk of off-target effects for the siRNAs. There are two major factors for unexpected off-target effects, one being the nature of the seed region of the siRNA and the other being improper strand selection by RISC.

The seed region of the siRNA is responsible for finding and complementing the target mRNA and is only 7 nucleotides in length (nucleotides 2–8 at the 5′-end of the guide strand). As such, the overall identity of the siRNA or the target mRNA makes little to no contribution to determining whether the expression of a particular gene will be affected. Instead, off-targeting is associated with the presence of one or more perfect 3'-untranslated region (UTR) matches with the seed region of the siRNA (Birmingham, et al., 2006). Therefore, when designing an siRNA, it is best to design based on the seed region complementation to the UTR of the target mRNA sequence to help mitigate unwanted off-target effects. The other major reason for unintended off-target effects is improper strand selection by RISC. Strand selection is based on the thermodynamic asymmetry rule, which states that the least thermodynamically stable 5’-end of the dsRNA is incorporated into Ago and the other strand is dissociated (Kawamata & Tomari, 2010). Therefore the sequence of the siRNA affects the likelihood of proper strand selection; an ideal sequence would contain low GC content around the 5’-end and

high GC content around the 3'-end of the antisense strand. If the siRNA duplex does not follow the asymmetry principal, the improper strand is likely to be incorporated into RISC, which can lead to knockdown of an unintended mRNA target. Taken together, the siRNA sequence must be carefully designed to try to avoid off-target effects.

Another major hurdle for siRNA therapeutics is host recognition and immune activation. SiRNA duplexes can activate the innate immune response in humans resulting in the secretion of high levels of inflammatory cytokines such as tumor necrosis factor alpha (TNF-α), interleukin-6 (IL-6), and interferon-alpha (IFN-α) (Hornung, et al., 2005; Judge et al., 2005). The human immune system has evolved sophisticated innate defences against foreign nucleic acids (Krieg, et al., 1995). The innate immune response to siRNAs is either through a toll-like receptor (TLR)-mediated response or a non-TLR mediated response (Robbins, et al., 2009).

There are thirteen known toll-like receptors in humans, three of which are capable of sensing RNAs (TLR 3, 7 and 8). These TLRs are located intracellularly and normally respond to nucleic acids by directly binding the RNA/DNA of viral invaders or by the nucleic acids from invading pathogens as they are released from lysosomes. TLR 3 is not only found intracellularly but it is also located on the outer membrane and can detect foreign nucleic acids outside of the cell (Kawai & Akira, 2011; Ozinsky, et al., 2000). TLR 7 and TLR 8 indiscriminately recognize dsRNA and ssRNA, simply recognizing the phosphate ribose backbone and uracil bases of ribonucleic acids (Diebold, et al., 2006). When TLR 7 or TLR 8 are stimulated by RNA they associate with the adaptor protein MyD88, forming a signaling complex (Takeda & Akira, 2005). The signal transduction leads to the nuclear translocation of NF-κB, causing the activation of transcription factors

responsible for up-regulating the expression of IFN-α and TNF-α, primary pro-inflammatory cytokines (Akira & Takeda, 2004; Kawai & Akira, 2006). TLR 3 is somewhat unrelated to TLR 7 or TLR 8 as it is genetically distinct, is expressed on the cellular surface as well as intracellularly, and activates a distinct signaling pathway. TLR 3 does not associate with the adaptor protein MyD88 but rather the TRIF adaptor protein, which eventually triggers a positive feedback mechanism starting with the secretion of IFN-α and β which then signal back to the cell causing the up-regulation other IFN-inducible genes, leading to the production of additional IFN-α (Kawai & Akira, 2006). The activated TLR 3/TRIF complex also triggers a signal cascade which leads to the activation of NF-κB, ATF, and c-Jun transcription factors which in turn induce the secretion of pro-inflammatory cytokines such as IL-6 and TNF-α (Kawai & Akira, 2006).

In addition to TLRs there are non-TLRs within the cytoplasm which trigger the innate immune response. The two major proteins are dsRNA-binding protein kinase (PKR) and RIG-1. PKR is a protein found within the cytoplasm which has a N-term dsRNA binding domain and a C-term kinase domain. When it binds dsRNAs, the PKRs will dimerize and autophosphorylate. This event starts a signal transduction pathway which leads to NF-κB activation, which in turn up-regulates pro-inflammatory cytokines (Feng, et al., 1992; Balachandran, et al., 2000; García, et al., 2007). The other major non-TLR protein is retinoic acid-inducible gene (RIG-1). RIG-1 is a cytoplasmic RNA helicase which acts as a sensor of viral RNA via binding and activation by either single-stranded or double-stranded RNA (Marques, et al., 2006; Pichlmair, et al., 2006). When RIG-1 binds to dsRNA, it triggers a cascade which leads to the activation of NF-κB leading to the production of primary interferons (Kawai, et al., 2005).

Overall, the presence of dsRNA, including siRNAs, causes the activation of the innate immune system, leading to the secretion of pro-inflammatory cytokines. These pro-inflammatory cytokines cause traditional inflammation symptoms: pain, increased body temperature (fever), redness, and swelling. The presence of siRNA could potentially trigger a runaway positive feedback loop causing systemic inflammatory response syndrome. Systemic inflammatory response causes whole body inflammation, leading to organ malfunction and damage and can be life threatening (Bone, et al., 1992; Teijaro, et al., 2014).

Because of the potential for severe immune response to RNA, siRNA therapeutics must proceed with the utmost caution before human trials are conducted. The precedent set by the TeGenero disaster in 2006 has made therapeutic companies more cautious when proceeding human trials of novel bio-pharmaceuticals. The TeGenero disaster involved an experimental antibody, which showed no immune stimulation in pre-clinical trials, administered to six healthy male volunteers at very low doses. Within an hour, all six displayed systemic inflammatory response characterized by a rapid induction of proinflammatory cytokines showing symptoms of: headache, nausea, diarrhea, erythema, vasodilatation, and hypotension. Within 24 hours, all six patients became critically ill, experiencing renal failure, widespread activation of the clotting cascade, complete depletion of lymphocytes/monocytes and organ failure (Suntharalingam, et al., 2006). Due to the unforeseen immunological outcome of the TeGenero disaster siRNA therapeutics must proceed with caution, as they are known to illicit an innate immune response.

Beyond the biological consequences of off-target effects and innate immune activation siRNAs also face the challenge of being degraded by nuclease enzymes. Once siRNAs are administered in an *in vivo* system, they are immediately targeted by serum endo and exoribonucleases, specifically ribonuclease-A (Haupenthal, et al., 2006; Turner, et al., 2007). The 2'-OH of the ribose sugar is essential for catalytic activity of ribonucleases as the 2'-OH then nucleophilically attacks the phosphate, resulting in a 2', 3'-cyclic phosphodiester, where the 5'-nucleotide leaves as the truncated product (Raines, 1998). In a comprehensive analysis by Hong, et al. (2010), the nuclease stability of 125 unique and unmodified dsRNAs was assessed in human and fetal calf serum. Mapping of the cleavage events occurring in serum treatment revealed two areas of vulnerability, UA/UA and CA/UG sites, and further solidified RNase A's role in siRNA degradation. SiRNAs propensity of being readily degraded in the presence of ribonucleases presents a major limitation that must be overcome to develop a potential siRNA therapeutic.

Nucleases are not the only challenge to siRNAs after administration; biodistribution and delivery to target cells are other challenges facing siRNA therapeutics. Administered siRNAs have poor tissue-targeting, a low propensity to target specific cells, and low cellular permeability. Systematic studies of the pharmacokinetic properties of oligonucleotides and siRNAs *in vivo* have shown that, once administered, siRNAs tend to accumulate in the kidneys and the liver but are noticeably absent in the central nervous system (Juliano, et al., 1999). Further investigation, using *in vivo* animal systems have shown that less than 1% of the administered siRNA will make it to the targeted tissues (Mescalchin, et al., 2007), demonstrating that siRNAs are not effective at reaching target tissues. Another problem is, due to siRNAs large molecular weight (~13 kDa) and

polyanionic nature (~40 negative phosphate charges), naked siRNAs do not effectively cross the cell membrane on their own. As such, siRNA therapeutics will not be effective therapeutics until these delivery and biodistribution issues can be overcome (Juliano, et al., 2009).

1.5 Chemical Modifications of siRNAs to Overcome Therapeutic Barriers

While these therapeutic challenges facing siRNA therapeutics seem daunting and more than enough to rule out siRNA as a future therapeutic, the challenges, however, are not insurmountable and the answer lies within the chemical structure of RNA. By chemically modifying the native structure of RNA, many of the therapeutic limitations can be diminished, making siRNA therapy a viable therapeutic option. Changing the chemical structure of oligonucleotides to overcome practical therapeutic challenges has been widely studied and well established for many years. In the 1970s, it was discovered that synthetic oligonucleotides, which were complementary to a mRNA sequence, could arrest the translation process *in vivo* (Stephenson & Zamecnik, 1978; Zamecnik & Stephenson, 1978). Since their discovery, anti-sense oligonucleotides (ASOs) have been thoroughly investigated with the hopes of developing a therapeutic. Recently, this work has led to two FDA approved oligonucleotide therapeutics: Fomivirsen and Mipomersen (Athyros, et al., 2008). ASOs successful approval has highlighted the need for chemical modification to be successful and gain FDA approval, as both commercially available oligonucleotides contain a plethora of modifications throughout their structure (Geary, et al., 2002; Hair, et al., 2013). As such, much of what has been learned from ASOs can be applied to siRNA design to help overcome therapeutic limitations associated with oligonucleotide based therapies.

Many chemical modifications are rationally designed, allowing for specific alterations of many of the inherent properties of native oligonucleotides and thus changing their biological application and potency. These modifications can help minimize off-target effects, modulate duplex structure/conformation, incur nuclease resistance, and reduce immunostimulatory properties.

Chemical modifications can be grouped into three broad categories: (1) internucleotide backbone modifications (Deleavey & Damha, 2012), (2) sugar modifications (Prakash, 2011), and (3) nucleobase modifications (Herdewijn, 2000). Each group has unique advantages and disadvantages when used in oligonucleotide design and varying effects in terms of overcoming the therapeutic limitations.

Chemical modification of the nucleobase is a modification employed in oligonucleotide design to alter thermal stability, reduce immune activation, and help limit off-target effects. Nucleobase modifications also include incorporation of novel fluorophores that can be used for studying nucleic acid-containing systems (Wilhelmsson, 2010). Figure 2 illustrates a selection of nucleobase modifications employed in oligonucleotide design.

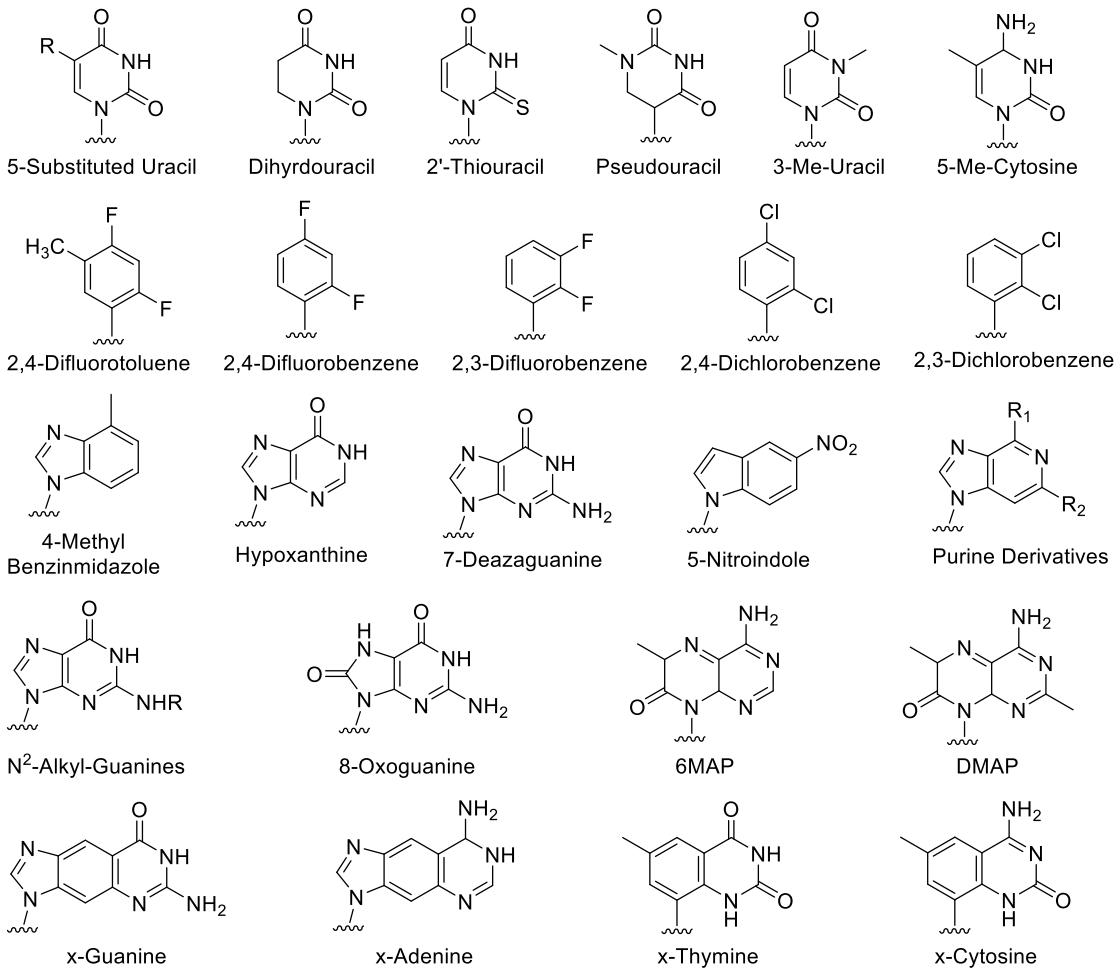

Figure 2 – Chemical structures of select nucleobase modifications.

Most nucleobase modifications alter duplex thermal stability, sugar conformation, and hydrogen-bonding properties of the duplex, all of which modulate the thermodynamics of duplex formation. These modifications can either maintain classical hydrogen bonding through nitrogen and oxygen heteroatoms or lack classical hydrogen bond donating groups completely while still maintaining base pair complementation (Peacock, et al., 2011). Due to the thermodynamic modulation that base modifications incur upon duplex formation, they can be incorporated into siRNAs to tailor sequences to better meet the

thermodynamic asymmetry principal, increasing potency and helping to reduce inappropriate strand selection (Addepalli, et al., 2010).

Sugar modifications are the most common chemical modifications used in oligonucleotide design and as such are the best understood and studied chemical modifications. This is because the effects of the sugar modification can be understood in terms of nucleotide sugar puckering preferences and thus the biological significance can be inferred (Deleavey & Damha, 2012). Sugar puckering has a large effect upon the thermodynamics of the duplex which in turn affects secondary structure, binding affinity toward complementary strands and enzyme interactions. Most modified ribose sugar derivatives either adopt conformations characterized as either RNA-like north conformation (C3'-endo, C2'-exo), or DNA-like south conformation (C2'-endo, C3'-exo) (Figure 3) (Altona & Sundaralingam, 1972; Blackburn, et al., 2006).

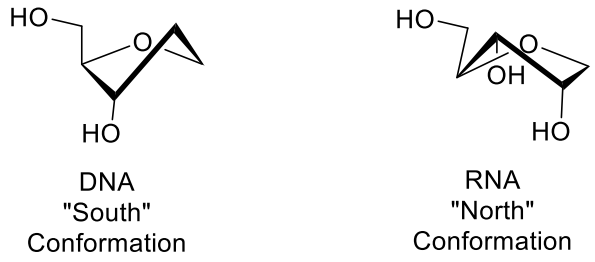

Figure 3 – Ribose sugar puckering conformations of DNA and RNA.

In B-form, dsDNA sugars adopt the ‘‘south’’ puckering, whereas in A-form dsRNA sugars prefer the ‘‘north’’ conformation. The cellular enzymes involved in the RNAi pathway can only tolerate duplexes in the A-form conformation. Thus, it is important to

have chemical modifications which help stabilize the duplex in A-form helical conformations. There are a vast array of sugar modifications compatible with oligonucleotide design, which can have either stabilizing or destabilizing effects upon the duplex (Figure 4).

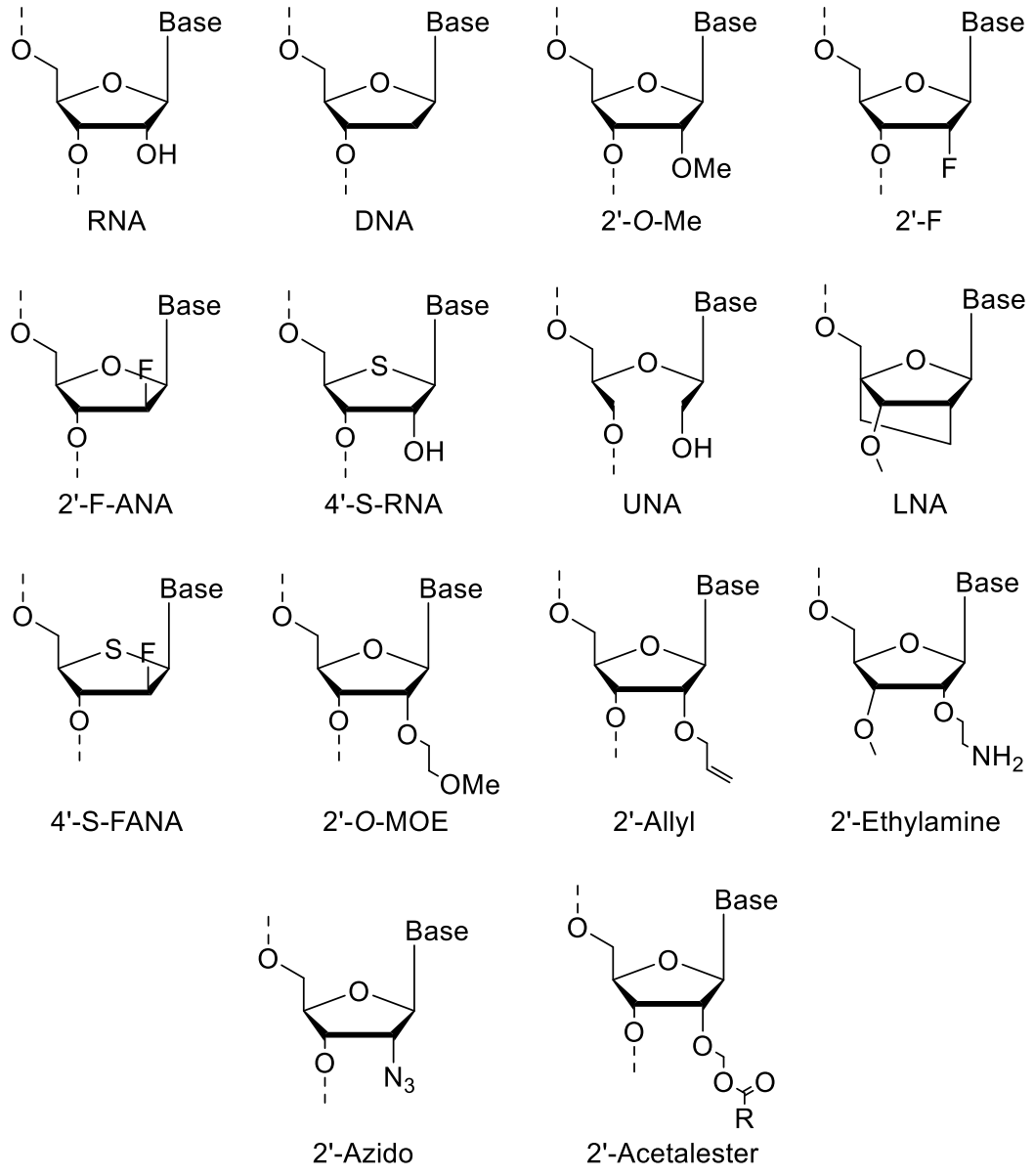

Figure 4 – Chemical structures of select sugar modifications.

Among the various sugar modifications the two modifications which have garnered the most attention, and are the most used modifications in oligonucleotide design: the 2'-O-Methyl (2'-*O*-Me) and the 2'-Fluoro (2'-F) modifications (Prakash, et al., 2005). These modifications are well tolerated within the RNAi pathway and have shown to increase potency of gene knockdown (Wu, et al., 2014). They have a high amount of resistance to nuclease degradation and thus, higher blood serum half-life (Volkov, et al., 2009; Chounga, et al., 2006). These modifications also incur thermodynamic stabilization, helping stabilize the A-form RNA helix (Majlessi, et al., 1998). Because of their stabilizing nature, they can be placed logically within the siRNA duplex to help aid in strand selection by following the thermodynamic asymmetry principal (Manoharan, 1999; Kawamata & Tomari, 2010). Among these benefits, these 2'-modifications also show innate immune evasion *in vitro* and *in vivo*. Native siRNAs are strong activators of the immune response, yet small amounts of 2'-modification can diminish immune response completely (Judge, et al., 2006). On-top of all these beneficial properties of 2'-*O*-Me and 2'-F modifications, they can also be combined with other modifications to further enhance these therapeutic properties, improving potency, immune evasion, nuclease stability, and overall tolerance within the RNAi pathway (Wu, et al., 2014).

Beyond sugar modifications, another common chemical modification that has been successfully incorporated into siRNAs is internucleotide backbone modifications. There is a significant variety of backbone modifications, ranging from subtle one atom changes to a complete redesign of the molecular architecture (Figure 5). Two of the more common backbone modifications include, phosphorothioate nucleic acids (PS RNA) and

boranophosphate nucleic acids (BO RNA); other backbone modifications are not as widely used.

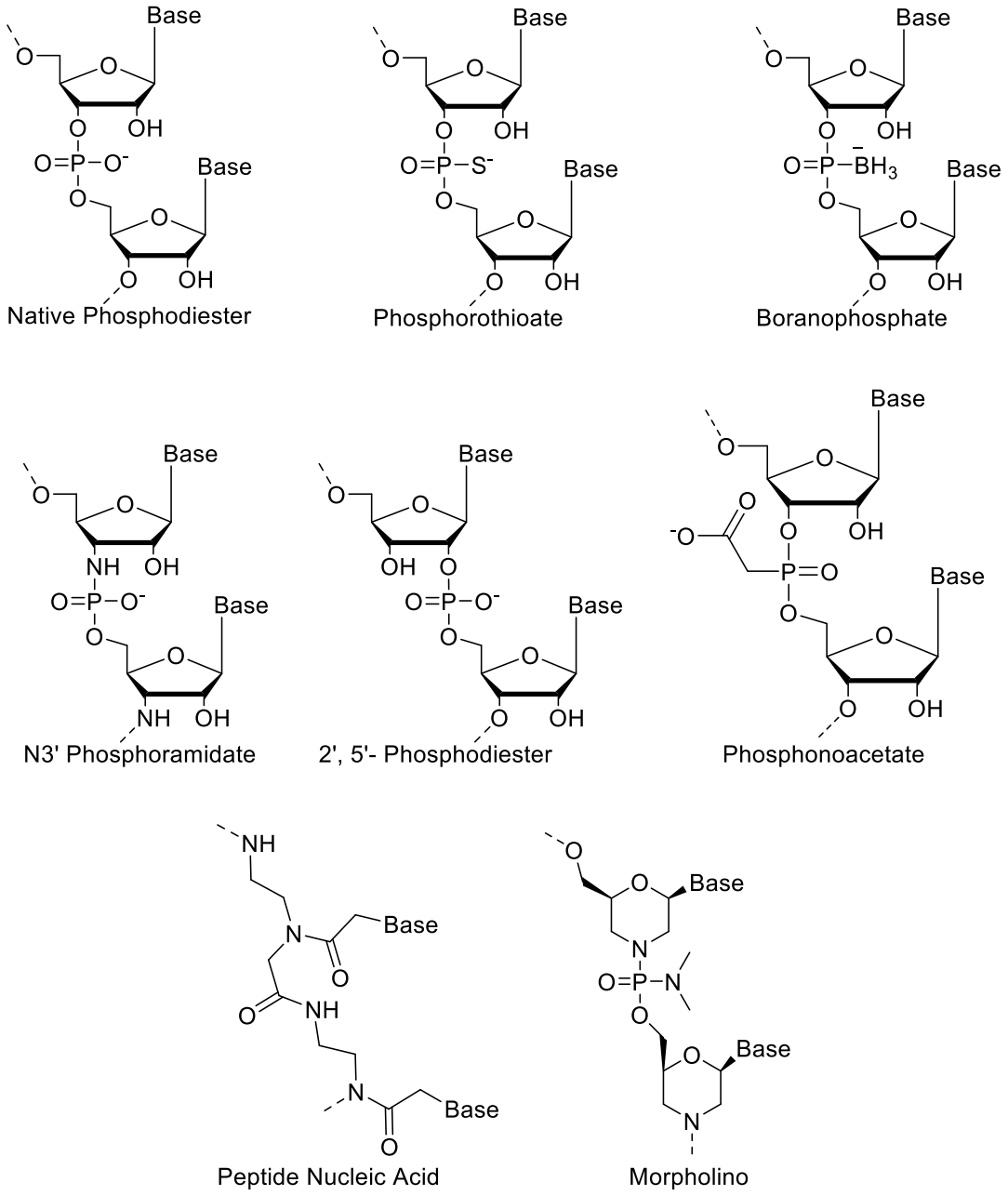

Figure 5 – Chemical structures of select internucleotide backbone modifications.

The phosphorothioate (PS) linkage, where sulfur substitutes one of the non-bridging phosphate oxygen (Eckstein, 2002), is one of the most popular chemical modifications used for siRNA design. The PS linkage shows substantial resistance to nucleases and is widely used in siRNA design and has some affinity for serum albumin helping the biodistribution and increasing circulation time *in vivo* (Watanabe, et al., 2006; Geary, et al., 2001). PS-modified AONs can also be taken up by cells without the use of transfection or electroporation (Stein, et al., 2010). However, this modification is not without its problems, as PS linkages have shown to have toxicity issues and diminished siRNA activity when compared to native siRNAs (Bennett & Swayze, 2010).

Another common modification of the phosphate backbone is the introduction of a boron atom in place of one of the non-bridging oxygen atoms to create a boron-phosphorous linkage, boranophosphate (BO). This modification has shown improved gene silencing activity at lower concentrations relative to either PS siRNAs or native siRNAs and enhanced resistance to degradation by nucleases, but they are limited in their uses because of suboptimal synthetic methods (Hall, et al., 2004).

Peptide nucleic acids (PNAs) are another widely studied backbone modification. PNAs have a neutral backbone oligonucleotide mimic, in which the pyrimidine and purine bases are connected through a methylene carbonyl linker to an amino ethyl glycine backbone and are able to form stable duplexes with complementary base pairing (Egholm, et al., 1993). They also exhibit significant nuclease and protease resistance (Demidov, et al., 1994). Since the discovery of PNAs, a wide variety of PNA analogs have been developed and studied for oligonucleotide and siRNA applications (Pensato, et al., 2007). Their success is somewhat limited by their low solubility in aqueous environment and their

poor cellular uptake, thus further modification of the PNA backbone is needed to perfect a therapeutically viable chemical modification (Pellestor & Paulasova, 2004).

1.6 Triazole-Linked Backbone Modification

Despite all the success of the various chemical modifications there is still no universal chemical modification used to overcome all therapeutic limitations. Thus, there is still a need to develop novel chemical modifications. The triazole functionality has been used by researchers to develop novel RNA backbone modifications through the use of click chemistry. Click chemistry was pioneered by Sharpless in 2001 (the Cu(I)-catalyzed adaptation of Huisgen's 1,3-dipolar [3 + 2] azide-alkyne (CuAAC) cycloaddition), and has nearly become ubiquitous within the field of synthetic [bio]chemistry due to its speed, versatility, simplicity, regioselectivity, its broad range of applications, and its low toxicity within biological systems (Wang, et al., 2003; Wu, et al., 2004). One such modification is the PNA-like triazole-linked nucleic acid developed by Efthymiou and Desaulniers (2011) (Figure 6).

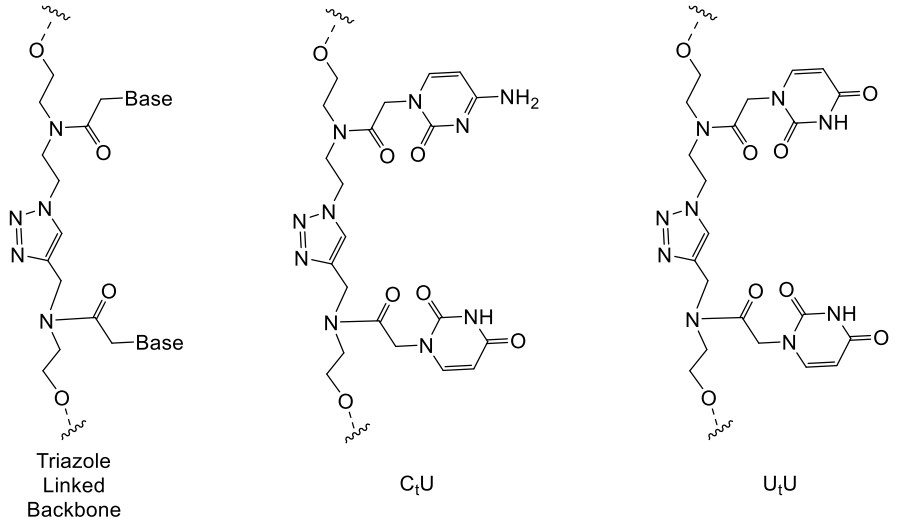

Figure 6 – Chemical structure of the triazole-linked nucleic acid.

The rationale for designing a triazole linked backbone modification was to help overcome the limitations caused by the polyanionic structure of the native phosphodiester linkage; click chemistry can introduce a neutrally-charged and physiologically stable heterocycle at this site. Another desirable property associated with the 1, 2, 3-triazole is its ability to form hydrogen bonds through N_2 and N_3 of the heterocycle, which could allow triazole-linked RNAs to interact with biological molecules such as blood-serum proteins (Zhang, et al., 2013).

Efthymiou and collogues demonstrated that triazole based phosphoramidites were compatible with solid support nucleotide synthesis and successfully incorporated into RNA oligonucleotides. The modified oligonucleotides were then able to form stable duplexes with A-form helical conformation with slightly destabilizing effects (Efthymiou & Desaulniers, 2011). The triazole backbone functionality was then incorporated into siRNA duplexes and tested for their ability to perform gene knockdown in a eukaryotic system. Their nuclease resistance was also assessed via incubation with serum nucleases for various time frames. SiRNAs containing the triazole backbone functionality were able to retain potent and dose dependent gene knock-down comparable to wild-type siRNAs. They also showed greatly enhanced nuclease stability compared to native siRNAs when the triazole was placed in an overhang position (Efthymiou, et al., 2012). Efthymiou and Desaulniers were able to demonstrate that the triazole backbone functionality was a viable candidate for siRNA design to help overcome therapeutic limitations.

To further expand the utility of the triazole backbone modification it will be combined with 2'-ribose sugar modifications. Combining different classes of chemical

modifications is an area of research that is broadly ignored. Combining the phosphothioate backbone modification with 2'-ribose modifications is one of the only investigated combinations of modifications. Kraynack & Baker (2006), investigated siRNAs containing 2'-*O*-Me modifications in conjunction with phosphothioate backbone. They found that by incorporating a modified 2'-*O*-Me sense strand in combination with PS modifications, the siRNA duplex had increased resistance to degradation by nucleases, as well as prolonged serum retention while still retaining potent gene silencing activity. They postulated that by using 2'-*O*-Me modifications in conjunction with PS there may be increased target specificity by eliminating sense-strand-induced off-target gene silencing. This is thought to be due to the modulation of the thermodynamics of the duplex to help follow the thermodynamic asymmetry principal (Kawamata & Tomari, 2010). One of the two only commercially available oligonucleotide therapeutics (Mipomersen) also combines sugar modifications with backbone modifications, demonstrating that combinations of chemical modifications may be the key for overcoming therapeutic limitations. Thus, by combining 2'-ribose modifications with triazole backbone modifications for the design of siRNAs, this project hopes to inform future chemical modification patterns which would improve the therapeutic properties of potential siRNA therapeutics.

1.7 Cancer: Perfect Candidate for siRNA therapy

SiRNA's are poised to spark the next great revolution in cancer therapeutics. The medical industry is trying to move towards personalized medicine for the treatment of cancers (Hudson, 2013; Patel, et al., 2013) and siRNA therapy is tailored to meet the needs of personalized cancer medicine (Wu, et al., 2014). Cancer is the prime target for RNAi to

make its breakthrough as a therapeutic, as cancer is defined as unregulated cell growth and division caused by the mutation and misregulation of specific genes (Hanahan & Weinberg, 2000). Because siRNAs can be designed to knockdown any gene of interest based on the target mRNA sequence, the potential personalization of cancer therapeutics seems within grasp.

In a landmark publication in 2000, Hanahan and Weinberg described the molecular hallmarks of cancer, which was further refined in 2011 (Hanahan & Weinberg, 2000 and 2011). They summarize the molecular events which cause normal cells to become tumorigenic, categorized into six distinct categories: resistance of apoptosis, abundant cellular division signals, evasion of growth suppressor signals, tissue invasion/metastasis, replicative immortality and induction of angiogenesis. Through high-throughput DNA sequencing analyses of cancer cell genomes, each of these six phenotypic characteristics are explained by mutations within somatic cells. Thus, cancer is a disease characterized by aberrant gene expression.

These mutations can be characterized into two distinct categories, oncogenes and tumor suppressor genes. Oncogenes can be considered gain of function mutations whereas tumor suppressor genes are loss of function mutations (Lee & Muller, 2010).

Tumor suppressor genes (also known as anti-oncogenes) are genes which code for proteins which have a dampening or repressive effect on the regulation of the cell cycle or promote apoptosis and sometimes both (Weinberg, 1991). Tumor suppressor gene mutations are considered recessive mutations because both alleles code for the protein, and thus both genes must be mutated to cause a phenotypic effect. When tumor

suppressor genes are activated they lead to one of the molecular hallmarks of cancer. Due to their nature they are considered loss of function mutations.

On the other hand, oncogenes, are considered gain of function dominant mutations. Oncogenes evolve from proto-oncogenes. Proto-oncogenes are genes which code for regulatory proteins which help regulate the cellular life cycle, usually implicated in cellular differentiation or help regulate cell growth. These mutations are considered dominant mutations because it only requires one allele to become mutated for the phenotypic effect to be observed. Once these proto-oncogenes become mutated they overexpress their protein products which leads the cell to display one of the molecular hallmarks of cancer.

One such oncogene is the *BCL2* oncogene. The oncogenic mutation, which causes bcl-2 to become irresponsive to apoptotic signals, is a genomic translocation event which moves the *BCL2* gene from chromosome 18 to 14. This translocation links the *BCL2* to a highly expressed immunoglobulin locus, leading to excessive expression (Tsujimoto, et al., 1984; Cory & Adams, 2002).

Bcl-2 has a nuanced role within the cell as it is a key regulator of both apoptosis and autophagy; precariously maintaining the balancing between the two cellular states.

Autophagy is a lysosomal degradation pathway which is responsible for digestion and recycling of bulk cellular components, such as organelles, ribosomes and protein aggregates. Autophagy is induced by nutrient and energy deprivation and metabolic stress. When autophagy is highly activated—due to excess cellular stress—it can lead to cell death. This cellular process is known as type-II programmed cell death. Bcl-2 plays a direct role in autophagic regulation by binding and inhibiting Beclin-1, a protein which

promotes autophagy (Pattingre, et al., 2005). A proof of concept study, demonstrating bcl-2s role in autophagic cell death, was published by Akar, et al. (2008). The authors knocked-down bcl-2 using siRNA and monitored autophagy levels, and as bcl-2 was knocked down, autophagic cell death increased.

Bcl-2 plays an important regulatory role in apoptosis through its interactions with bcl-2 family proteins (Bcl-xl, Bcl-w Mcl-1, and A1). Bcl-2 family proteins are inhibitors of apoptosis by supressing pro-apoptotic proteins (Bax and Bak) (Gross, et al., 1999). These pro-apoptotic proteins are embedded within the membrane of the mitochondria and when bcl-2 family proteins are absent, the pro-apoptotic proteins trigger apoptosis by disrupting the integrity of the outer mitochondrial membrane. This leads to the release of pro-apoptotic signaling proteins, specifically cytochrome c. The released cytochrome c activates, a cascade of proteins, triggering apoptosis (Kluck, et al., 1997). The extent to which autophagy and apoptosis are intertwined is a heavily researched topic which remains unresolved.

Because of bcl-2's important regulatory role in both apoptosis and autophagy, *BCL2* expression within the cell is highly regulated and, when mutated, causes a disastrous effect within the cell. *BCL2* oncogene is a common form of mutation found in a variety of cancers including, melanoma, breast, prostate, chronic lymphocytic leukemia, and lung cancer (Tron, et al., 1995; Krajewski, et al., 1995 & 1996). This translocation event is associated with chemotherapeutic resistance and poor prognosis for the patient (Debatin, et al., 2002). Due to *BCL2* oncogene expression in a range of different cancers, and its therapeutic resistance, it is a good candidate for siRNA therapy.

This project generated a library of chemically modified siRNAs targeting the *BCL2* oncogene KB cells. By combining 2'-ribose modifications with triazole backbone modifications for the design of siRNAs this project hopes to inform future chemical modification patterns which would improve the therapeutic properties of potential siRNA therapeutics, by improving gene silencing, increasing nuclease resistance, and decreasing the innate immune response.

Chapter 2: Chemical and Physical Experimental Procedures

2.1 Synthesis of Uracil-Triazole-Linked-Uracil Phosphoramidite Dimer

The synthesis of the Uracil Triazole Uracil (**U$_t$U**) phosphoramidite dimer was accomplished following the protocol of Efthymiou & Desaulniers, 2011 (illustrated in Scheme 1). All synthesized compounds were characterized via ^{1}H NMR (Appendix Figure 6).

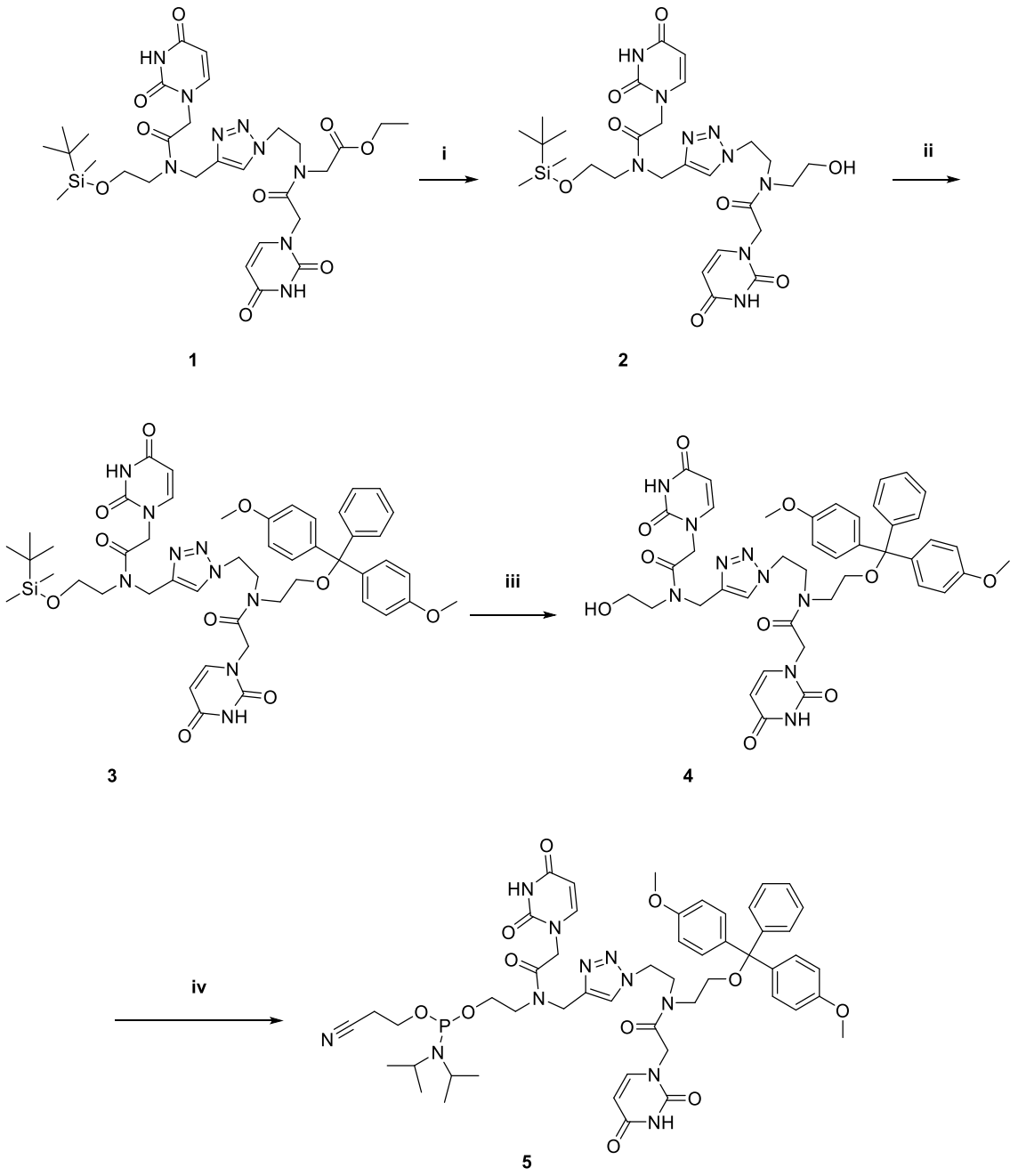

Scheme 1 – Synthesis of the Uracil-Triazole-Uracil Phosphoramidite
(i) 2.5 equiv LiBH4, THF/MeOH (12:1), reflux 2 h, 63% yield of **2**. (ii) 3 equiv DMT-Cl, pyridine, 24 h, 70% yield of **3**. (iii) 3 eq TBAF, THF, 12 h, 61% yield of **4**. (iv) 2 equiv 2-cyanoethyl N,N-diisopropylchlorophosphoramidite, 5.5 equiv DIPEA, 0.5 equiv DMAP, DCM, 4 h, 68% yield of **5**.

***N*-(2-(*tert*-Butyldimethylsilyloxy)ethyl)-uracil-1-yl-*N*-((1-(2-(uracil-1-yl-*N*-(2-hydroxyethyl)acetamido)ethyl)-1H-1,2,3-triazol-4-yl)methyl)acetamide (2)**. Dry THF was added to Compound **1** (500mg, 772 μmol) until fully dissolved under an inert $N_{2(g)}$ atmosphere. $LiBH_4$ (1.02 mmol) was added dropwise and then reaction was refluxed until TLC indicated product formation and consumption of starting material, 2 h. Once the reaction was complete it was quenched with excess MeOH and dried down *in vacuo*. The crude product obtained was then purified using flash chromatography; the product was redissolved in CH_2Cl_2 and eluted through a silica colum using an initial mobile phase of 10% of NH_4OH in a solution of 5% MeOH in CH_2Cl_2, gradually increasing the MeOH concentration gradient to a final mobile phase of 10% NH_4OH in a solution of 15% MeOH in CH_2Cl_2. The purified product, compound **2**, was a white crystaline solid (295 mg, 63%). Compound **2** was a mixture of rotamers with varying signal intesnities; ^{1}H NMR (500 MHz, DMSO-d_6) Compound **2** was a mixture of rotamers with varying signal intesnities; ^{1}H NMR (400 MHz, DMSO-d_6) δ 0.05 (s, 2H), 0.06 (s, 4H), 0.86, 0.97 (2s, 9H), 3.26–3.34 (m, 2H), 3.43–3.74 (m, 7H), 3.82–3.89 (m, 2H), 4.38–4.40 (m, 1H), 4.48 (t, 1.3H, *J*=5.62 Hz), 4.53 (t, 0.7H, *J*=6.25 Hz), 4.55–4.83 (m, 6H), 4.99–5.10 (m, 1H), 5.55–5.58 (m, 2H), 7.31–7.46 (m, 2H), 7.88, 8.05, 8.13, 8.24 (4s, 1H), 11.32 (s, 2H).

***N*-(2-(Bis(4-methoxyphenyl)(phenyl)methoxy)ethyl)-2-(uracil-1-yl)-*N*-(2-(4-((2-(uracil-1-yl)-*N*-(2-((2,3,3-trimethylbutan-2-yl)oxy)ethyl)acetamido)methyl)-1H-1,2,3-triazol-1-yl)ethyl)acetamide (3)**. Compound **2** (175 mg, 0.271 mmol) was dissolved in 10 mL of dry pyridine under an inert $N_{2(g)}$ atmosphere, was added an excess of 4,4-dimethoxytrityl chloride (DMT-Cl) (275 mg, 0.813 mmol) until TLC analysis revealed the product formation and complete consumption of starting material (24 h). After the reaction was complete it was extracted with CH_2Cl_2 and washed with H_2O (2X). The CH_2Cl_2 fractions were collected, pooled, and dried over Na_2SO_4. The extracted crude product was concentrated *in vacuo*. Once concentrated the crude product was dissolved in minimal amounts of CH_2Cl_2/MeOH and purified by flash column chromatography. The

silica column was performed via an eluting gradient of MeOH (5 to 15%) in CH_2Cl_2 to afford the title compound as a white solid (184 mg, 70%). Compound **3** is a mixture of rotamers with varying signal intensities; ^{1}H NMR (400 MHz, $CDCl_3$) δ 0.05 (s, 2H), 0.08 (s, 4H), 0.88, 0.90 (2s, 9H), 2.90– 2.94 (m, 1.5H), 3.08–3.10 (m, 0.5H), 3.21 (t, 1.5H, *J*= 4.69 Hz), 3.27 (t, 0.5H, *J*= 5.08 Hz), 3.32–3.31 (m, 0.2H), 3.37– 3.44 (m, 0.3H), 3.46–3.57 (m, 2.5H), 3.60–3.64 (m, 2H), 3.74– 3.77 (m, 0.75H), 3.79, 3.80 (2s, 7H), 3.82 (t, 1.25H, *J*= 4.7 Hz), 4.50 (t, 1.5H, *J*=5.86 Hz), 4.54 (t, 0.5H, *J*=5.47 Hz), 4.59 (s, 1H), 4.62–4.64 (m, 1H), 4.67 (s, 3H), 4.72 (d, 1H, *J*=7.70 Hz), 5.54–5.57 (m, 1H), 5.64 (d, 0.1H, *J*=1.95 Hz), 5.65 (d, 0.1H, *J*=1.95 Hz), 5.66–5.70 (m, 0.8H), 6.57 (d, 0.1H, *J*=7.82 Hz), 6.67 (d, 0.7H, *J*=7.82 Hz), 6.80–6.84 (m, 4.3H), 7.07–7.09 (m, 0.8H), 7.15–7.21 (m, 7.2H), 7.66, 7.67, 7.74, 7.85 (4s, 1H), 10.32 (s, 2H).

***N*-(2-(Bis(4-methoxyphenyl)(phenyl)methoxy)ethyl)-2-(uracil-1-yl)-*N*-((1-(2-(2-(uracil-1-yl)-*N*-(2-hydroxyethyl)acetamido)ethyl)-1H-1,2,3-triazol-4-yl)methyl)acetamide (4)**. Compound **3** (525 mg, 0.578 mmol) was dissolved in 26 mL of dry THF. TBAF (452 mg, 1.74 mmol) was added and the reaction was stirred for 12 h at room temperature and then extracted with CH_2Cl_2. The organic layer was washed with H_2O and brine (2X). After organic extraction the combined organic fractions were dried over Na_2SO_4, and evaporated under reduced pressure. The crude was dissolved in minimal CH_2Cl_2/MeOH and purified by flash column chromatography, first eluting with 100% CH_2Cl_2 followed by a gradient of MeOH (5 to 15%) in CH_2Cl_2 obtaining compound **4** (295 mg, 61%). Compound **4** is a mixture of rotamers with varying signal intensities; ^{1}H NMR (400 MHz, $CDCl_3$) δ 2.51 (s, 1H), 2.98 (s, 1H), 3.26–3.31 (m, 2H), 3.36–3.40 (m, 3H), 3.54–3.68 (m, 4H), 3.75–3.92 (m, 8H), 4.35–4.88 (m, 8H), 5.51–5.63

(m, 2H), 6.63 (d, 0.2H, *J*= 8.56 Hz), 6.66 (d, 0.3H, *J*= 8.62 Hz), 6.75–6.84 (m, 4H), 7.27–7.41 (m, 8.5H), 7.71, 7.78, 7.85, 8.03 (4s, 1H), 10.33–10.62 (m, 2H).

2-(*N*-(2-(4-((*N*-(2-(Bis(4-methoxyphenyl)(phenyl)methoxy)ethyl)-2-(uracil-1-yl)acetamido)methyl)-1H-1,2,3-triazol-1-yl)ethyl)-2-(uracil-1-yl)acetamido)ethyl(2-cyanoethyl) diisopropylphosphoramidite (5). Compound **4** (125 mg, 0.150 mmol) was dissolved in 5 mL of anhydrous CH_2Cl_2 under an inert $N_{2\ (g)}$ atmosphere. Diisopropylethylamine (105 mg, 0.823 mmol), 4-dimethylaminopyridine (9.1 mg, 75.0 μmol), and 2-cyanoethyl *N*,*N*-diisopropylchlorophosphoramidite (75 mg, 0.300 mmol) were then added to the solution. The reaction was mixed at RT for 4 h and when TLC analysis revealed consumption of starting material and formation of product the reaction was dried *in vacuo* yielding a crude product. The crude was dissolved in minimal 2% triethylamine in hexanes/acetone and purified by flash column chromatography eluting with a gradient of 2% triethylamine in acetone/hexanes (1:1 to 4:1). Once pure compound **5** was obtained, it was a transparent solid (105 mg, 68%). Compound **5** is a mixture of rotamers with varying signal intensities; ^{1}H NMR (400 MHz, $CDCl_3$) δ 1.04–1.19 (m, 12H), 2.62–2.66 (m, 3.25H), 2.94 (t, 1H, *J*= 4.02 Hz), 3.09 (t, 0.78H, *J*= 4.33 Hz), 3.22 (t, 1.20H, J= 4.71 Hz), 3.27 (t, 0.5H, *J*= 4.33 Hz), 3.29– 3.37 (m, 0.25H), 3.54–3.61 (m, 5.5H), 3.70–3.77 (m, 2H), 3.78 (s, 6.25H), 3.81–3.90 (m, 2.25H), 4.51–4.65 (m, 2.5H), 4.72 (s, 2.5H), 4.74–4.77 (m, 1H), 5.52–5.55 (m, 1H), 5.66–5.70 (m, 1H), 6.57 (d, 0.33H, *J*=8.2 Hz), 6.65 (d, 0.66H, J ¼ 8.2 Hz), 6.82–6.86 (m, 4H), 7.27–7.31 (m, 12H), 7.71, 7.76, 7.90, 7.96 (4s, 1H).

2.2 Synthesis of Anti-*BCL2* Oligonucleotides through Solid Support Phosphoramidite Chemistry

All β-cyanoethyl 2'-*O*-TBS protected, 2'-F and 2'-*O*-Me phosphoramidites, reagents and solid supports were purchased from ChemGenes Corporation and Glen Research. All commercial phosphoramidites were dissolved in anhydrous acetonitrile to a concentration of 0.1 M. The chemically synthesized **$\underline{U_tU}$** phosphoramidite was dissolved in 20% tetrahydrofuran in acetonitrile to a concentration of 0.1 M. All sequences were synthesized via solid support phosphoramidite chemistry using the Applied Biosystems 394 DNA/RNA synthesizer. Oligonucleotides were synthesized on 0.2 μM dT solid support except for sequences that were 3'-modified, which were synthesized on 0.2 μM Universal-III solid supports. 1.0 μM synthesis cycles were used and all reactions were performed under an inert N_2 atmosphere maintained at 55 psi. Commercially available phosphoramidites were synthesized using coupling times of 16 minutes, while chemically synthesized **$\underline{UtU}$** coupling time was increased to 30 minutes to ensure proper coupling. Antisense sequences were chemically phosphorylated at the 5'-end by using 2-[2-(4,4'-dimethoxytrityloxy)ethylsulfonyl]ethyl-(2-cyanoethyl)-(*N*,*N*-diisopropyl)-phosphoramidite. Upon completion, columns were removed from the synthesizer, dried under a stream of N_2, sealed and stored at 4°C until purification.

2.3 Purification of Anti-*BCL2* Oligonucleotides

2.3.1 Removal from Solid Support and Deprotection

Oligonucleotides were removed from their solid supports upon exposure to 1.5 ml of EMAM (methylamine 40% wt. in H_2O and methylamine 33% wt. in ethanol, 1:1

(Sigma)). Columns were incubated with EMAM for 1 hour at room temperature with the solution in full contact with the controlled pore glass. The oligonucleotides were then transferred into screw cap microcentrifuge tubes and incubated overnight at room temperature in EMAM to deprotect the nitrogenous bases. The following day, samples were evaporated on a Speedvac evaporator overnight and resuspended in a solution of dimethylsulfoxide (DMSO): 3HF/triethylamine (TEA) (100 µl: 125 µl) (Sigma). The samples were then incubated at 65°C for 2.5 hours to remove the 2'-*O*-TBS protecting groups.

2.3.2 Ethanol Precipitation

The crude oligonucleotides were resuspended in 600 mL of pre-chilled EtOH (chilled via dry ice). 25 µL of 3 M NaOAc (pH 5.2) was then added and solution was mixed via pipetting. This solution was vortexed thoroughly and placed in dry ice for 1 hour. The sample was then centrifuged for 30 minutes at 12000 rpm at 4°C and supernatant was removed. The pelleted oligonucleotide was then resuspended in chilled EtOH. The process was repeated four more times without adding any additional NaOAc. The sample was then dried down using a Speedvac evaporator for 16 hours.

2.3.3 Oligonucleotide Quantification

The concentrated crude oligonucleotide sample was redissolved in 200 µL of DEPC-treated nuclease-free water (Sigma-Aldrich). 1 µL of the RNA sample was added to 999 µL of water in a 1-mL quartz cuvette. The diluted sample was mixed thoroughly via pipetting and the absorbance was measured using a spectrophotometer (Thermo Scientific) at 260 nm. The optical density was calculated by multiplying the absorbance

value calculated by the spectrophotometer by the total volume of the stock oligonucleotide sample (200 μL).

2.3.4 Polyacrylamide Gel Electrophoresis of Oligonucleotides

The polyacrylamide gel was made by mixing 30 mL of 40% acrylamide solution with 6 mL of 10X TBE buffer (pH 8.3), 25.23 g of urea (7M final), and finally topped up to 60 mL with of DEPC-treated nuclease-free water. The solution was vigorously stirred until all of the contents completely dissolved. Once dissolved, polymerization was initiated by adding 80 μL of 25% ammonium persulfate (APS) and 80 μL of tetramethylethylenediamine (TEMED). This final mixture was stirred gently for 30 seconds and immediately loaded into the prepared gel plates. The gel was then left to sit for 45 minutes until it was fully polymerized. Oligonucleotide purity was assessed by loading the gel with 0.5 OD units of oligonucleotide with denaturing loading solution for a total volume of 20 μL. The gel was run using a 0.5X TBE running buffer (25 mL of 10X TBE (pH 8.3) in 475 mL of DEPC-treated nuclease-free water) with the voltage set to 80V and was ran until the bromophenol blue band travelled 75% of the gel's length (~ 16 hours). Upon completion, the gel was stained in a 3X solution of GelRed (Biotium) for 30 minutes while being gently stirred on a shaker. The gel was then visualized via Fluorchem SP (Fisher Scientific) (Appendix Figure 2).

2.3.5 Crush and Soak Purification of Oligonucleotides

All strands that were purified by loading a maximum of 2 OD units of oligonucleotide per well. These strands were not stained were directly assessed under a short-wavelength UV lamp. The bands that showed the slowest migratory rate were physically excised and

placed into a centrifuge tube, which was further placed into a dry ice/EtOH bath for 5 minutes. The gel pieces were then chopped up using a skinny scoopula and re-frozen in a dry ice/EtOH bath. The pieces were suspended in 500 μL of cold gel eluting buffer and chopped up further using a centrifuge pestle as they defrosted in the buffer. The slurry was refrozen in a dry ice/EtOH bath for 15 minutes and left to thaw for another 15 minutes at room temperature. The slurry was then incubated for 48 hours at 37°C on a shaker at 200 rpm. Two days later, the slurry was centrifuged for 30 minutes at 12000 rpm at room temperature and the supernatant was collected in a sterile microcentrifuge tube. The sample was then dried down using a Speedvac evaporator for 16 hours and another ethanol precipitation was performed as described in **Section 2.3.2.**

2.3.6 Desalting of Gel Purified Oligonucleotides

The dried down sample was redissolved in 500 μL of DEPC-treated nuclease-free water and transferred to an MWCO 3000 cellulose centrifugal filter where it was centrifuged at 12000 rpm at 25°C until there was roughly 50 μL of oligonucleotide solution left (~10 minutes). The flow-through was then discarded and 400-500 μL of DEPC-treated nuclease-free water was added to the remaining oligonucleotide solution before centrifuging the sample once again at 12000 rpm. This process was repeated for a total of 3 times. The final 50 μL sample was transferred to a microcentrifuge tube and dried down using a Speedvac evaporator for 16 hours. The purified sample was then resuspended in 100 μL DEPC-treated nuclease-free water of and quantified as described in **Section 2.3.3**.

2.3.7 Annealing Oligonucleotides for Circular Dichroisim and Mel-Temp

Circular dichroisim (CD) spectroscopy and UV-monitored thermal denaturation were performed on a Jasco J-815 CD equipped with temperature control. Equimolar amounts of each RNA (2.4 nmol) were annealed to their complement in 500 µL of a sodium phosphate buffer. The RNA were then incubated at 95°C for 2 minutes and then cooled slowly to room temperature to generate siRNA duplexes used for biological assays.

2.3.8 Annealing Oligonucleotides for Biological Assays

At 10 µM, equimolar amounts of complimentary RNAs were combined and dried down in a Speedvac overnight. The RNAs were then suspended in a binding buffer (75 mM KCl, 50 mM Tris-HCl, 3 mM $MgCl_2$, pH 8.3) and incubated at 95°C for 2 minutes and then cooled slowly to room temperature to generate siRNA duplexes used for biological assays.

2.4 Biophysical Measurements of Anti-*BCL2* Oligonucleotides

2.4.1 Circular Dichroisim Measurement of Anti-*BCL2* Oligonucleotides

CD measurement of each duplex were recorded in quadruplicate from 200-300 nm at 20°C with a screening rate of 10 nm/min and a 0.2 nm data pitch. The average of the four replicates was calculated using Jasco's Spectra Manager version 2 software and adjusted against the baseline measurement of the sodium phosphate buffer.

2.4.2 Thermodynamics of Anti-*BCL2* Oligonucleotides (T_m)

Melting temperatures (T_m) of each sample were measured by setting the UV absorbance to 260 nm and increasing the temperature of the sample from 10 to 95°C at a rate of 0.5°C/min with the absorbance measured at the end of each 0.5°C increment. The absorbance readings were automatically adjusted to the baseline measurement of the sodium phosphate buffer. The T_m values were averaged from three independent experiments and were calculated by using Meltwin version 3.5 software assuming the two-state model.

2.4.3 Preparation of Oligonucleotides for ESI-Q-TOF Mass Spec

All single-stranded RNAs were gradient eluted through a Zorbax Extend C18 HPLC column with a MeOH/H_2O (5:95) solution containing 200 mM hexafluoroisopropyl alcohol and 8.1 mM triethylamine, and finally with 70% methanol. The eluted RNAs were subjected to ESI-MS (ES^-), producing raw spectra of multiply-charged anions and through resolved isotope deconvolution, the molecular weights of the resultant neutral oligonucleotides were confirmed. The final neutral mass of the RNAs were confirmed using this method and were within 2% of predicted mass.

Chapter 3: Biological Experimental Procedures

3.1 Culturing of Cells

3.1.1 Thawing of Frozen Cell Stocks

Cryopreserved KB cells, stored in 1.5 ml of Eagle's Minimum Essential Medium (EMEM) (ATCC) supplemented with 5% DMSO, were removed from CryoPro® liquid nitrogen dewar (VWR) and slowly thawed to 25°C. Cells were reconstituted in 10 ml of EMEM and transferred into a 50 ml polystyrene tissue culture treated incubation flask (Falcon) containing 20 ml of EMEM. Cells were then incubated overnight in a Forma Series II CO_2 Incubator (ThermoScientific) at 37°C under 5% CO_2 atmosphere. Once cells obtained a confluency of 90%, they were passaged normally and transferred into a 250 ml polystyrene tissue culture treated incubation flask (Falcon) containing 25 ml of EMEM supplemented with 10% fetal bovine serum (FBS) (Perbio) and 1% penicillin-streptomycin (Sigma).

3.1.2 Sub-Culturing of KB Cells

$1x10^6$ KB cells were seeded in a 250 ml polystyrene tissue culture treated incubation flask (Falcon) containing 25 ml of EMEM supplemented with 10% (v/v) fetal bovine serum (FBS) (Perbio) and 100 U/ml penicillin and 100 mg/ml streptomycin (Sigma). Cells were incubated in a Forma Series II CO_2 Incubator at 37°C under 5% CO_2 atmosphere until 90% confluency. Once 90% confluency was reached, cells were washed 3 times with 10 ml of phosphate buffered saline (NaCl 137 mM, KCl 2.7 mM, PO_4^{3-} 10 mM, pH 7.4) (PBS). Cells were treated with 3 ml of 0.25% Trypsin (SAFC

Bioscience) to disperse the cells. The cells were then pelleted and resuspended in 5 ml of EMEM for counting. They were then diluted in EMEM to a final concentration of $1x10^6$ cells/ml. This concentration was used for either further sub-culturing or biological assays. Cells were sub-cultured for no more than 10 passages total for biological assays.

3.1.3 Cryopreservation of Cells

KB cells were passaged normally until final resuspension of cells; cells were suspended in EMEM supplemented with 5% DMSO (Sigma) to a concentration of $1x10^7$ cells/ml. A 1 ml aliquot of cells were transferred into 2 ml Fisherbrand cryogenic vials (Fisher) and cooled to 4°C, then frozen at -20°C and finally stored in CryoPro® liquid nitrogen dewar (VWR) until use.

3.2 siRNA Transfection and qPCR Analysis of *BCL2*

3.2.1 siRNA Transfection Procedure for qPCR Analysis

50 µl of KB cells (total of $5x10^4$ cells) were added to each well of a 24-well plate (Falcon®) with 350 µl of growth medium and incubated at 37°C with 5% CO_2. After 24 hours of incubation, cells were treated in triplicate with 1, 10 and 20 nM concentrations of siRNAs using Lipofectamine 2000 (Invitrogen) in 1X Opti-Mem (ATCC). The desired volume of siRNAs was mixed with 25 µl of Opti-Mem in a microcentrifuge tube on ice, and incubated for 5 minutes. 1 µl of Lipofectamine was mixed with 25 µl of Opti-Mem in a microcentrifuge tube and incubated for 5 minutes at room temperature. The contents of the tubes were combined and incubated for 20 minutes at room temperature and transferred into respective wells of the tissue culture treated 24-well plate (Falcon).

3.2.2 RNA Isolation via TRIzol extraction

TRIzol reagent (Ambion) is a selective way to precipitate RNA from DNA from Protein in a sequential manner. After homogenizing the sample with TRIzol Reagent, chloroform was added, and the homogenate was allowed to separate into a clear upper aqueous layer (containing RNA), an interphase, and a red lower organic layer (containing the DNA and proteins) which was discarded and not used for the purposes of this project.

Achieving a cellular concentration of no more than 2.5 x 10^5 cells/well (after a total incubation time of 48 hours) the medium was aspirated and 500 µL of TRIzol reagent was added to each well. The 24-well plate was then placed on a shaker set to high for 15 minutes and then inspected under a microscope to ensure cellular lysis. The contents were then transferred to eppendorf tubes and 150 µL of chloroform was added to each tube. The tubes were then vortexed for several minutes to ensure proper mixing. The tubes were then rested on ice for 30 minutes or until the organic and aqueous layers were fully separated. The samples were then centrifuged at 11500 rpm for 15 minutes at 4°C. The upper aqueous later was carefully extracted and transferred into a new eppendorf tube. 250 µL of 99.99% isopropyl alcohol (Sigma-Aldrich) was then added to each tube, then was mixed via inversion and finally let sit on ice for 2 minutes to settle. The tubes were then centrifuged at 11500 rpm for 10 minutes at 4°C. The supernatant was then discarded leaving the RNA pellet intact. The pellet was then washed with 550 µL of 75% EtOH (diluted with nuclease free water) and then briefly vortexed until the pellet was resuspended. The samples were then centrifuged at 9200 rpm for 5 minutes at 4^{o}C. The EtOH was then removed, leaving the pellet. The samples were then redissolved in 40 µL of nuclease free DEPC treated water and placed in a 55°C water bath for 12 minutes to

aid in dissolving of the pellets. Once fully dissolved the samples were pulse centrifuged, placed on ice and then quantified and qualified outlined in **sections 3.2.3** and **3.2.4**.

3.2.3 RNA Quantification

RNA was quantified (quantity and quality) by measuring absorbance at 230 nm, 260 nm and 280 nm using GENESYS™ 10S UV-Vis Spectrophotometer (Thermo). Concentration of RNA was determined using beer-lamberts law:

$$A = \varepsilon\, c\, l$$

Where A= absorbance at 260 nm, ε = extinction coefficient (which is 0.025 (μg/ml) cm^{-1} for single stranded RNA), c= concentration of sample, and l= path length, which can be arranged to:

$$c = \frac{A}{\varepsilon\, l}$$

And finally RNA concentration was calculated using:

$$Concentration\ of\ ssRNA = \frac{OD_{260\,nm}}{Pathength} \times \varepsilon \times Dilution\ Factor$$

Protein contamination was calculated using absorbance at 280 nm. To estimate nucleic acid purity the absorbance OD 260 nm was divided by absorbance OD 280 nm. If the ratio of OD 260 nm/OD 280 nm was between 1.9 and 2.0 the RNA was used for cDNA synthesis, if lower the RNA was not used for cDNA synthesis. Contamination by phenolate ions, thiocyanates, and other organic compounds from RNA extraction from **section 3.2.1** was assessed at OD 230 nm. Samples with a low 260/230—below 1.8—have a significant presence of organic contaminants that interfere with other downstream processes as PCR inhibitors, therefore only RNA with an OD 260 nm/ OD 230 nm of 2 or higher was used for cDNA synthesis.

3.2.4 Assessment of RNA Integrity

RNA integrity was visualized using a 1% agarose gel in 1X TAE buffer. 1X TAE buffer (40 mM Tris-OH, 20 mM Acetic Acid, pH 7.8) was prepared using 20 mL of 50X TAE buffer in 980 mL of water. 1% Agarose gel was prepared by dissolving 0.3 g of agarose in 30 mL of 1X TEA buffer which was then placed in the microwave on high for 1 minute to completely dissolve the agarose (stopping to stir every 15 seconds). The agarose gel was then placed in the gel cast to solidify for 45 minutes. Once solid the gel was solidified it was placed in the electrophoresis apparatus and filled with 1X TAE buffer. 10 µL of RNA samples (5 µg of RNA total) were then loaded into each well and the gel was ran at 60V for 45 minutes. Once the bands had migrated 80% of the distance of the gel electrophoresis was stopped. The gel was stained in a 3X solution of GelRed (Biotium) for 30 minutes while being gently stirred on a shaker. Finally RNA integrity was visualized via Fluorchem SP (Fisher Scientific) (Appendix Figure 3).

3.2.5 cDNA Synthesis

1 µg of RNA was used for cDNA synthesis using the iScript reverse transcription kit (Biorad). Final volumes of 20 µL per reaction were used for the reverse transcription reactions: 4 µL of iScript advanced reaction mix, 1 µL of iScript advanced reverse transcriptase, 10 µL of water, and 5 µL of RNA sample were combined in a microeppendorf tube on ice. The samples were mixed via pipetting and pulse centrifuged to concentrate. Reverse transcription was performed at 25°C for 5 minutes, 42°C for 30 minutes, and 85°C for 5 minutes using a PX2 thermocycler (Thermo). cDNA samples

were either used immediately or stored at -20°C for real time quantitative polymerase chain reaction (qPCR).

3.2.6 qPCR Analysis of *BCL2*

Relative transcript levels were quantified via qPCR using CFX Connect™ Real-Time PCR Detection System (Biorad). Standard curves were generated for each gene (*BCL2*, 18s rRNA and GAPDH) to evaluate primer efficiency. The qPCR was performed in triplicate using the following conditions: 2 µl of cDNA, and 10 µl of SsoFast EvaGreen Supermix (Biorad) with respective primer concentrations and topped up to a final volume of 20 µl using water (DEPC water was not used during qPCR as it could potentially inhibit the polymerase enzyme). 1 µl of Bcl-2 forward primer: 5'-CTGGTGGGAGCTTGCATCAC -3' and reverse primer: 5'-ACAGCCTGCAGCTTTGTTTC -3' were used for a final concentration of 500 nM. 1.6 µl of GAPDH forward primer: 5'-ACTTTGTGAAGCTCATTTCCTGGTA -3' and reverse primer: 5'- GTGGTTTGAGGGCTCTTACTCCTT -3' were used for a final concentration of 800 nM. 2 µl of 18s forward primer: 5'-CGGCTACCACATCCAAGGAAG- 3' and reverse primer: 5'-CGCTCCCAAGATCCAACTACTAC- 3' for a final concentration of 100 nM. Thermocycler conditions included an initial denaturation and enzyme activation at 95°C for 2 min, followed by 40 cycles of 95°C for 2 seconds, 52°C for 15 seconds, and 72°C for 5 seconds. Fluorescence was measured during the end of each extension phase. After 40 cycles, a melting curve was generated by slowly increasing the temperature from 65°C to 95°C at a rate of 0.1°C/s, while fluorescence was measured at each increment. To ensure no genomic contamination, a control lacking reverse transcriptase was used for

each cDNA sample. No template controls were run for every set of primers. Normalized relative gene expression (ΔΔCq) of Bcl-2 was calculated against both reference genes (GAPDH and 18s) and corrected for primer efficiency using CFX Manager Software (BIORAD).

3.3 Nuclease Stability Assay

At a concentration of 12 µM, 2 µl of siRNAs Bwt, B2, B3, B10, B11, and B12 were incubated with 8 µl of 13.5% fetal bovine serum at 37^{o}C for 0.5, 1, 2, 3, 4, and 5 hours. After incubation, siRNAs were resolved via electrophoresis through the use of a non-denaturing 20% polyacrylamide gel. The polyacrylamide gel was made as described in **section 2.3.4**, but with the absence of urea. This final mixture was stirred gently for 30 seconds and immediately loaded into the prepared gel plates. Once loaded the gel was ran at 60V for 24 hours. After 24 hours the gel was stained using 3X GelRed (Biotium) nucleic acid dye for 30 minutes and then visualized via Fluorchem SP (Fisher Scientific).

3.4 XTT Cellular Proliferation Assay

The XTT cell proliferation assay was first described by Scudiero, et al., 1988 and was used to measure cell growth and drug sensitivity in tumor cell lines. The tetrazolium dye, 2,3-Bis-(2-methoxy-4-nitro-5-sulfophenyl)-2H-tetrazolium-5-carboxanilide (XTT), can be used in cell proliferation, cytotoxicity, and apoptosis assays for adherent and non-adherent cell cultures. XTT salt is reduced by living eukaryotic cells into a brightly colored orange derivative. The XTT derivative created from living cells can be measured at absorbance 475 nm which can be used in a relative manner to determine the cellular proliferation rates. This project uses the XTT assay to determine the cellular proliferation

rates of cells treated with anti-*BCL2* siRNAs, untreated control groups and a non-target siRNA negative control groups.

3.4.1 Optimization of Proliferation Assay

Before the XTT assay could be conducted the number of cells and incubations times needed to be optimized to determine the highest fidelity results possible. In order to determine the optimal number of cells to seed 2.5x serial dilution of cells were plated in triplicate in tissue culture treated 96-well plate (Falcon) from 1.0 x 10^5 cells/well to 65 cells/well. 200 µL of each cell dilution in triplicate or 200 µL of media only was plated into each well and incubated at 37°C with 5% CO_2 for 48 hours. After 48 hours of incubation, each well was treated with 50 µl of XTT, activated by 2% *N*-methyl dibenzopyrazine methyl sulfate and incubated for 2 hours at 37°C with 5% CO_2. After 2 hours of incubation, absorbance was measured at 475 nm and 660 nm using an xMark™ Microplate Absorbance Spectrophotometer (Biorad). Specific absorbance was calculated via: A_{475} nm (experimental)–A_{475} nm (Blank)–A_{660} nm (experimental) and a standard curve was created to determine the optimal amount of cells to plate for the XTT assay.

3.4.2 siRNA Transfection and Procedure for XTT Assay

Once the optimal number of cells was determined 50 µL of KB cells (2.5 x 10^3 KB cells/well) were seeded into each well of a tissue culture treated 96-well plate (Falcon) with 150 µl of growth media and incubated at 37°C with 5% CO_2 for 24 hours. After 24 hours of incubation, cells were transfected in triplicate with siRNA 1 through 29 at three concentrations (1, 10 and 20 nM) using Lipofectamine 2000 in 1X Opti-Mem according to the manufacturer's protocol. Cells were then incubated for 24 hours at 37°C with 5%

CO_2. After 24 hours of incubation, cells were treated with 50 µl of XTT, activated by 2% N-methyl dibenzopyrazine methyl sulfate and incubated for 2 hours at 37°C with 5% CO_2. After 2 hours of incubation, absorbance was measured at 475 nm and 660 nm using an xMark™ Microplate Absorbance Spectrophotometer (Biorad). Specific absorbance was calculated via: A_{475} nm (experimental)–A_{475} nm (Blank)–A_{660} nm (experimental) and results were normalized to an untreated control.

3.4.3 XTT Time Course Procedure

Cellular proliferation was determined using XTT Cell Proliferation Assay Kit (ATCC®) for siRNAs: Bwt, B2, B3, B4, B5, B6, B10, B11, B12, and NC. Cells were seeded at concentrations required to reach 90% confluency at each end point (1, 2, 3 and 4 days post-transfection). After 24 hours of incubation, cells were transfected in triplicate with 20 nM of respective siRNAs using Lipofectamine 2000 in 1X Opti-Mem according to the manufacturer's protocol. Cells were incubated at 37°C with 5% CO_2. Cells were transfected again following the same procedure every 48 hours. At each end point, 50 µl of XTT was added to siRNA-treated cells, activated by 2% *N*-methyl dibenzopyrazine methyl sulfate and incubated for 2 hours at 37°C with 5% CO_2. After 2 hours of incubation, absorbance was measured at 475 nm and 660 nm using an xMark™ Microplate Absorbance Spectrophotometer (Biorad). Specific absorbance was calculated via A_{475} nm (experimental)–A_{475} nm (Blank)–A_{660} nm (experimental) and results were normalized to an untreated control.

3.5 Human Interferon Alpha ELISA Assay

3.5.1 Isolation of Human Peripheral Blood Mononuclear Cells

After ethical approval from the University Of Ontario Institute Of Technology's Research Ethics Board, human blood was obtained from consenting normal healthy donors (University of Ontario Institute of Technology, Oshawa, Ontario) (Appendix Figure 1). Human blood (9 volumes; 30 mL) was collected in 50 ml syringes prefilled with 3.2% (w/v) trisodium citrate as an anti-coagulation agent and were immediately diluted with 30 mL of balanced salt solution (D-glucose 0.1%, $CaCl_2$ 0.05 mM, $MgCl_2$ 0.98 mM, KCl 5.4 mM, and TRIS 0.145 M). Peripheral blood mononuclear cells (PBMCs) were prepared by density gradient centrifugation using Ficoll separating solution (GE Healthcare). Into 50 mL centrifuge tubes (Falcon), pre-filled with 3ml of Ficoll, 4ml of blood was carefully layered on-top of the Ficoll. The centrifuge tubes were then centrifuged at 400 g for 40 minutes at room temperature. The buffy coat layer from each centrifuge tube was then isolated and pooled into a clean 50 mL centrifuge tube. Three volumes of balanced salt solution was added to the tube and it was mixed gently via inversion before centrifugation at 100 g for 10 minutes at room temperature. The supernatant was removed and the PBMC pellet was resuspended in an equal volume of balanced salt solution. The sample was then centrifuged at 100 g for 10 minutes at room temperature and the supernatant was discarded. The PBMC pellet was then suspended in 5 mL of RPMI 1640 (ATCC) supplemented with 10% (v/v) FBS, 1 mM L-glutamine. Isolated PBMC cells were counted in a haemocytometer. 4.0×10^5 cells were seeded in a 96-well plate containing 200 µl RPMI 1640 (ATCC) supplemented with 10% (v/v) FBS, 1 mM L-glutamine, 100 U/ml penicillin and 100 mg/ml streptomycin.

3.5.2 Transfection of PBMCs and ELISA Preparation

4.0×10^5 cells were seeded in a tissue culture treated 96-well plate containing 200 µl RPMI 1640 (ATCC) supplemented with 10% (v/v) FBS, 1 mM L-glutamine, 100 U/ml penicillin and 100 mg/ml streptomycin for a total volume of 150 µl per well. Once seeded into the 96-well plate the PBMC cells were immediately stimulated in triplicate using 20 nM of siRNAs: Bwt, B2, B3, B4, B5, B6, B10, B11, B12, and NC, following the transfection procedures in **section 3.4.2**. 24 hours post siRNA transfection, culture plates were centrifuged at 400 g for 10 minutes at 4°C and the supernatant was collected. The supernatant was kept on ice and directly processed with Verikine ELISA kits (PBL).

3.5.2 Human interferon-α ELISA Procedure

Human interferon-α (IFN-α) levels were measured according to the manufacturer's protocol (PBL) using purified IFN- α standard to construct standard curves and supernatant from the PBMCs to test the unknown levels of IFN-α. The PBMCs supernatant was diluted 1:1 with supplied diluent from the kit. To each well of the ELISA plate 100 µL of either IFN-α or supernatant was added (in technical duplicates), the plate was then covered and incubated at room temperature for an hour. The wells were then washed once with the supplied wash buffer solution. Once the wells were washed 100 µL of the antibody solution was added to each well, the plate was then covered and incubated for an hour. After one hour the plate was emptied and each well was washed three times with the supplied wash buffer solution. After the wash 100 µL of the HRP solution was added to each well, which was then covered and incubated for one hour. After one hour of incubation the plate was washed four times with the supplied wash buffer solution and

100 μL of the TMB solution was added to each well, and then incubated in the dark for 15 minutes. After 15minutes stop solution was added to each well and absorbance was measured at 450 nm using xMark™ Microplate Absorbance Spectrophotometer (Biorad). A standard curve was constructed using the four parameter logistic (4-PL) curve fit and experimental concentrations of IFN- α were calculated using the generated curve (Appendix Figure 4).

Chapter 4: Results and Discussion

4.1 Sequences of siRNAs Generated

The sequences of the siRNAs generated for this project are listed in table below (Table 1). The modification patterns were variations upon a theme. The optimal placement of the **U_tU** modification was determined by the research of Efthymiou & Desaulniers (2012). When placed within an siRNA the **U_tU** modification retained the best gene silencing ability when placed near the 3'-end or 3'-overhang of the sense strand. However, in this study, an exogenous luciferase assay gene was used. To assess a more clinically relevant endogenous system, this study aimed at generating siRNAs containing a combination of modifications that target BCL2.

As such, in this work the 2'-F and 2'-*O*-Me modifications were placed at varying locations within the sense and anti-sense strands. The 2'-ribose modifications within the sense strand had one of two modification patterns, either clustered around the 3'-end of the sense strand, or found throughout the entirety of the sense strand. On the anti-sense strand the 2'-modifications were either on the pyrimidine bases near the 5'-end or clustered around the 3'- end of the strand. The other pattern for 2'-ribose modifications was their placement on pyrimidines within the antisense strand. The placement of these chemical modifications were informed by the thermodynamic asymmetry principal of siRNA strand selection: the strand that is most likely to be taken up by the RISC complex is the least thermodynamically stable 5'- end (Kawamata & Tomari, 2010). Therefore the 2'-*O*-Me and 2'-F modifications—which are thermodnyamically stabalizing modifications (Sabahi, et al., 2001; Wang & Kool, 1995) —were placed around the 3'-end of the sense strand to stabalize the 5'-end of the anti-sense strand, so that it is more

likely to be taken up by RISC. Efthymiou & Desaulniers (2012) determined that the **U_tU** modification was destabilizing and was therefore placed near the 3'-end or on the 3'-overhang of the sense strand.

Table 1 – Nucleotide sequences of all anti-BLC2 siRNAs generated.

Anti-*BCL2* siRNA	Nucleotide Sequence	Anti-*BCL2* siRNA	Nucleotide Sequence
Bwt	5'-GCCUUCUUUGAGUUCGGUGtt -3' 3'-ttCGGAAGAAACUCAAGCCAC-5'	B15	5'-GCCUUCUUUGAGUUCGGUG**U_tU**-3' 3'-ttCGGAAGAAACUCAAGCCAC-5'
B2	5'-GCCUUCUUUGAG**U_tU**CGGUGtt-3' 3'-ttCGGAAGAAACUCAAGCCAC-5'	B16	5'-GCCUUCUUUGAGUUCGGUGtt -3' 3'-ttCGGAAGAAACUCAAGCCAC-5'
B3	5'-GCCUUCUUUGAGUUCGGUG**U_tU**-3' 3'-ttCGGAAGAAACUCAAGCCAC-5'	B17	5'-GCCUUCUUUGAG**U_tU**CGGUGtt-3' 3'-ttCGGAAGAAACUCAAGCCAC-5'
B4	5'-GCCUUCUUUGAGUUCGGUGtt -3' 3'-ttCGGAAGAAACUCAAGCCAC-5'	B18	5'-GCCUUCUUUGAGUUCGGUG**U_tU**-3' 3'-ttCGGAAGAAACUCAAGCCAC-5'
B5	5'-GCCUUCUUUGAG**U_tU**CGGUGtt-3' 3'-ttCGGAAGAAACUCAAGCCAC-5'	B19	5'-GCCUUCUUUGAGUUCGGUGtt -3' 3'-ttCGGAAGAAACUCAAGCCAC-5'
B6	5'-GCCUUCUUUGAGUUCGGUG**U_tU**-3' 3'-ttCGGAAGAAACUCAAGCCAC-5'	B20	5'-GCCUUCUUUGAG**U_tU**CGGUGtt-3' 3'-ttCGGAAGAAACUCAAGCCAC-5'
B7	5'-GCCUUCUUUGAGUUCGGUGtt -3' 3'-ttCGGAAGAAACUCAAGCCAC-5'	B21	5'-GCCUUCUUUGAGUUCGGUG**U_tU**-3' 3' -ttCGGAAGAAACUCAAGCCAC-5'
B8	5'-GCCUUCUUUGAG**U_tU**CGGUGtt-3' 3'-ttCGGAAGAAACUCAAGCCAC-5'	B22	5'-GCCUUCUUUGAGUUCGGUGtt -3' 3'-ttCGGAAGAAACUCAAGCCAC-5'
B9	5'-GCCUUCUUUGAGUUCGGUG**U_tU**-3' 3'-ttCGGAAGAAACUCAAGCCAC-5'	B23	5'-GCCUUCUUUGAG**U_tU**CGGUGtt-3' 3'-ttCGGAAGAAACUCAAGCCAC-5'
B10	5'-GCCUUCUUUGAGUUCGGUGtt -3' 3'-ttCGGAAGAAACUCAAGCCAC-5'	B24	5'-GCCUUCUUUGAGUUCGGUG**U_tU**-3' 3'-ttCGGAAGAAACUCAAGCCAC-5'
B11	5'-GCCUUCUUUGAG**U_tU**CGGUGtt-3' 3'-ttCGGAAGAAACUCAAGCCAC-5'	B25	5'-GCCUUCUUUGAGUUCGGUGtt -3' 3'-ttCGGAAGAAACUCAAGCCAC-5'
B12	5'-GCCUUCUUUGAGUUCGGUG**U_tU**-3' 3'-ttCGGAAGAAACUCAAGCCAC-5'	B26	5'-GCCUUCUUUGAG**U_tU**CGGUGtt-3' 3'-ttCGGAAGAAACUCAAGCCAC-5'
B13	5'-GCCUUCUUUGAGUUCGGUGtt-3' 3'-ttCGGAAGAAACUCAAGCCAC-5'	B27	5'-GCCUUCUUUGAGUUCGGUG**U_tU**-3' 3'-ttCGGAAGAAACUCAAGCCAC-5'
B14	5'-GCCUUCUUUGAG**U_tU**CGGUGtt-3' 3'-ttCGGAAGAAACUCAAGCCAC-5'	NC	5'-CUUACGCUGAGUACUUCGAtt-3' 3'-ttGAAUGCGACUCAUGAAGCU-5'

Wild-type and Modified Anti-BCL2 siRNAs
***U_tU**= Uracil Triazole Uracil. Red= 2'-O-Me. Green= 2'-F. NC= Negative Control (Anti-Luciferase siRNA).*
The top strand corresponds to the sense strand; the bottom strand corresponds to the antisense strand.
In all duplexes, the 5'-end of the antisense strand contains a 5'-phosphate group.

Several of the siRNAs were used for several experiments beyond the qPCR screen, they are outlined in Table 2 below.

Table 2 – Nucleotide sequences of best candidate siRNAs

Anti-*BCL2* siRNA	**Nucleotide Sequence**
Bwt	5'-GCCUUCUUUGAGUUCGGUGtt -3' 3'-ttCGGAAGAAACUCAAGCCAC-5'
B2	5'-GCCUUCUUUGAG**U$_t$U**CGGUGtt-3' 3'-ttCGGAAGAAACUCAAGCCAC-5'
B3	5'-GCCUUCUUUGAGUUCGGUG**U$_t$U**-3' 3'-ttCGGAAGAAACUCAAGCCAC-5'
B4	5'-GCCUUCUUUGAGUUCGGUGtt -3' 3'-ttCGGAAGAAACUCAAGCCAC-5'
B5	5'-GCCUUCUUUGAG**U$_t$U**CGGUGtt-3' 3'-ttCGGAAGAAACUCAAGCCAC-5'
B6	5'-GCCUUCUUUGAGUUCGGUG**U$_t$U**-3' 3'-ttCGGAAGAAACUCAAGCCAC-5'
B7	5'-GCCUUCUUUGAGUUCGGUGtt -3' 3'-ttCGGAAGAAACUCAAGCCAC-5'
B8	5'-GCCUUCUUUGAG**U$_t$U**CGGUGtt-3' 3'-ttCGGAAGAAACUCAAGCCAC-5'
B9	5'-GCCUUCUUUGAGUUCGGUG**U$_t$U**-3' 3'-ttCGGAAGAAACUCAAGCCAC-5'
B10	5'-GCCUUCUUUGAGUUCGGUGtt -3' 3'-ttCGGAAGAAACUCAAGCCAC-5'
B11	5'-GCCUUCUUUGAG**U$_t$U**CGGUGtt-3' 3'-ttCGGAAGAAACUCAAGCCAC-5'
B12	5'-GCCUUCUUUGAGUUCGGUG**U$_t$U**-3' 3'-ttCGGAAGAAACUCAAGCCAC-5'

*Wild-type and Modified Anti-BCL2 siRNAs **U$_t$U**= Uracil Triazole Uracil. Red= 2'-O-Me. Green= 2'-F. NC= Negative Control (Anti-Luciferase siRNA). The top strand corresponds to the sense strand; the bottom strand corresponds to the antisense strand. In all duplexes, the 5'-end of the antisense strand contains a 5'-phosphate group.*

4.2 Circular Dichroisim

Circular dichroisim was performed for all siRNAs generated to investigate the secondary structure and what effect, if any, the chemical modifications had on the secondary structure of the siRNAs. All the siRNAs showed characteristic peaks of A-form helix; they all showed a positive spike in the CD band at 260 nm, a negative spike CD band at 210 nm, and a very shallow dip between 290-300 nm (Ranjbar, 2009). The CD spectra are broken up into groups to better see the trends.

The first group being: Bwt, B2-6, B10-12, and B16-18. This group of siRNAs contained 2'-modifications on the 3'-end of the sense strand with and without the **$\underline{U_tU}$** modification near the 3'-end of the sense strand or the 3'-overhang of the sense strand (Figure 7).

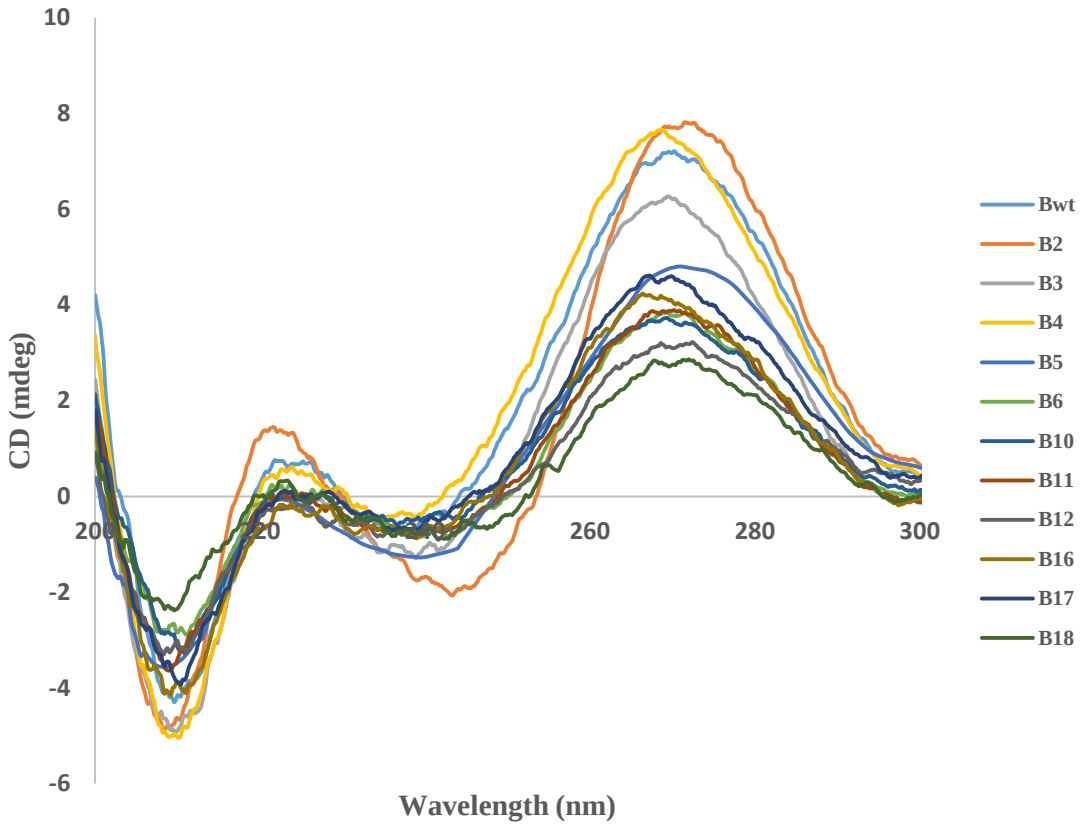

Figure 7 - The RNA duplex conformation of anti-BCL2 siRNAs, containing ***U$_t$U*** *modifications on the sense strand and 2'-ribose modifications located about the 3'-end of the sense strand, displayed through circular dichroism spectroscopy.*
Wild-type and modified anti-BCL2 siRNAs (~2.4 nmol/duplex) were suspended in 500 µL of a sodium phosphate buffer (90 mM NaCl, 10 mM Na2HPO4, 1 mM EDTA, pH 7) and the solution was scanned from 200–300 nm at 20°C. All scans were performed in quadruplicate and averaged using version 2 of Jasco's Spectra Manager software.

The second group (B7-9, and B13-15) had full 2'-modification on the sense strand in conjunction with the **U$_t$U** modification. (Figure 8).

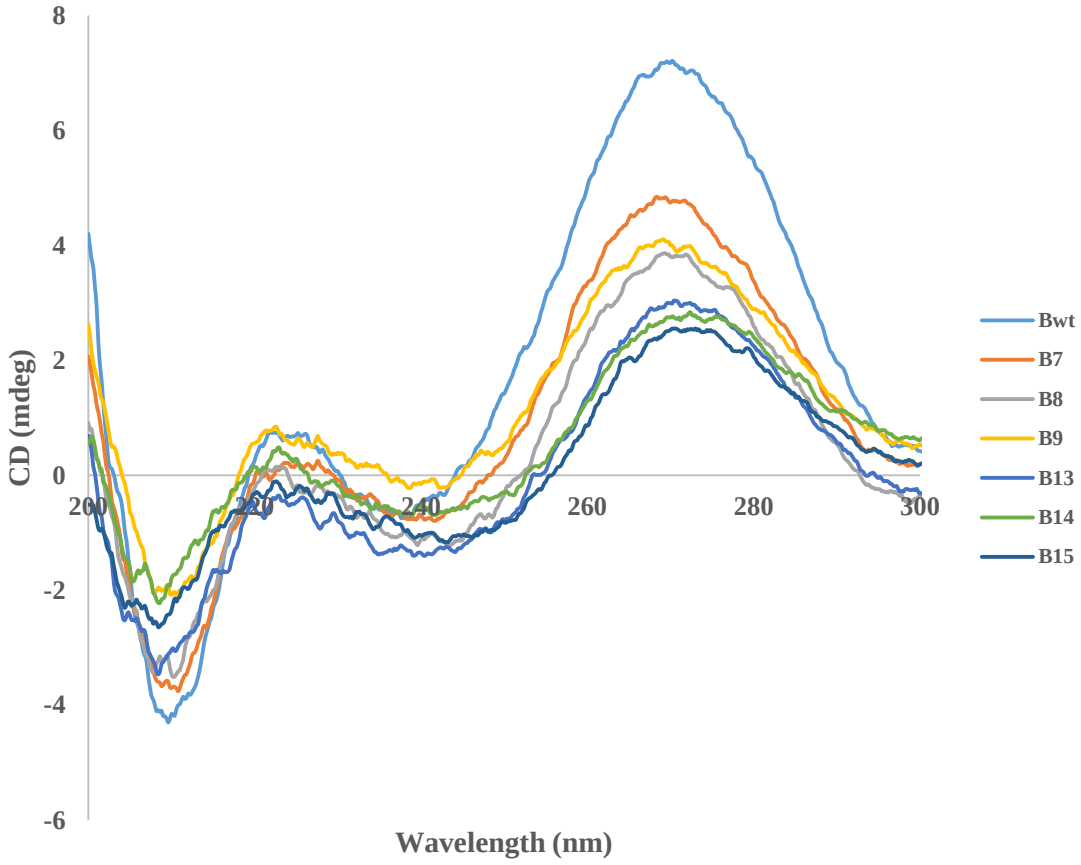

Figure 8 - The RNA duplex conformation of anti-BCL2 siRNAs, containing ***U$_t$U*** *modifications on the sense strand and 2'-ribose modifications located throughout the entire sense strand, displayed through circular dichroism spectroscopy. Wild-type and modified anti-BCL2 siRNAs (~2.4 nmol/duplex) were suspended in 500 µL of a sodium phosphate buffer (90 mM NaCl, 10 mM Na2HPO4, 1 mM EDTA, pH 7) and the solution was scanned from 200–300 nm at 20°C. All scans were performed in quadruplicate and averaged using version 2 of Jasco's Spectra Manager software.*

The final group (B19-27) were sequences which contained 2'-modification of the sense and anti-sense strands in conjunction with the **U$_t$U** modification (Figure 9).

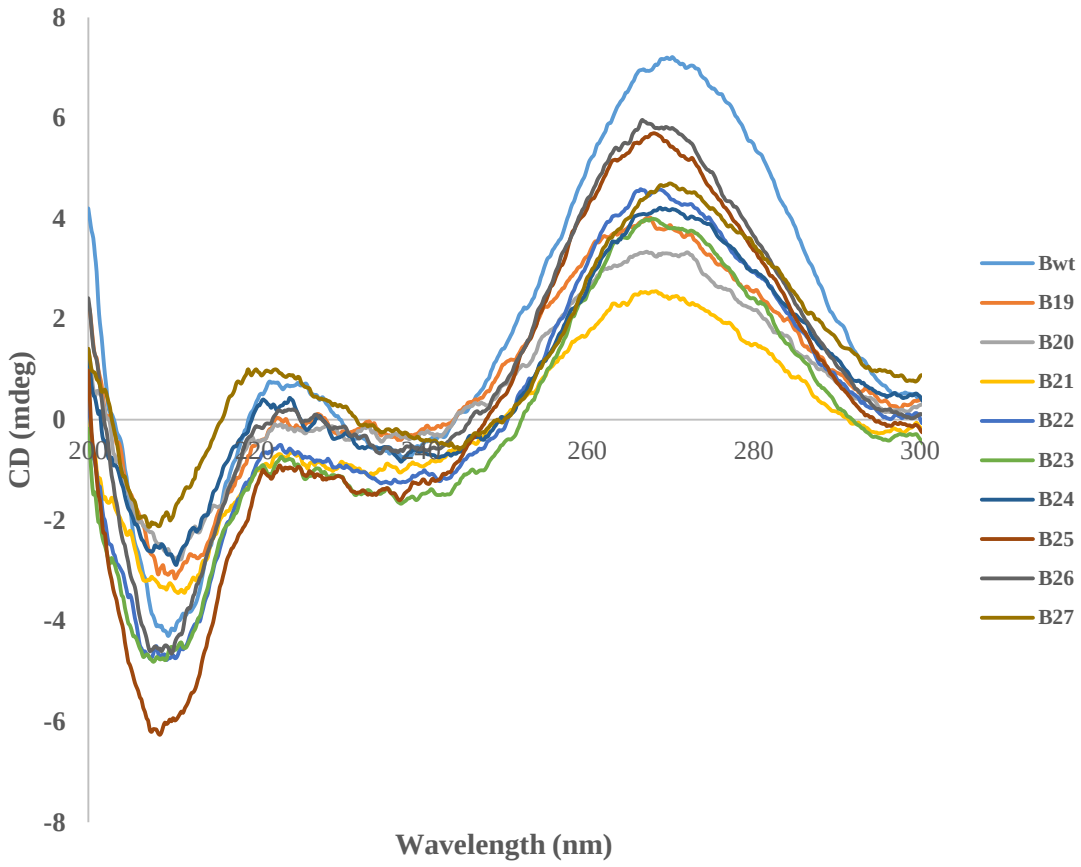

Figure 9 - The RNA duplex conformation of anti-BCL2 siRNAs, containing ***U$_t$U*** *modifications on the sense strand and 2'-ribose modifications located throughout the sense strand and anti-sense strand, displayed through circular dichroism spectroscopy.*
Wild-type and modified anti-BCL2 siRNAs (~2.4 nmol/duplex) were suspended in 500 µL of a sodium phosphate buffer (90 mM NaCl, 10 mM Na2HPO4, 1 mM EDTA, pH 7) and the solution was scanned from 200–300 nm at 20°C. All scans were performed in quadruplicate and averaged using version 2 of Jasco's Spectra Manager software.

Finally, Figure 10 displays all of the chemically modified siRNAs generated for this project.

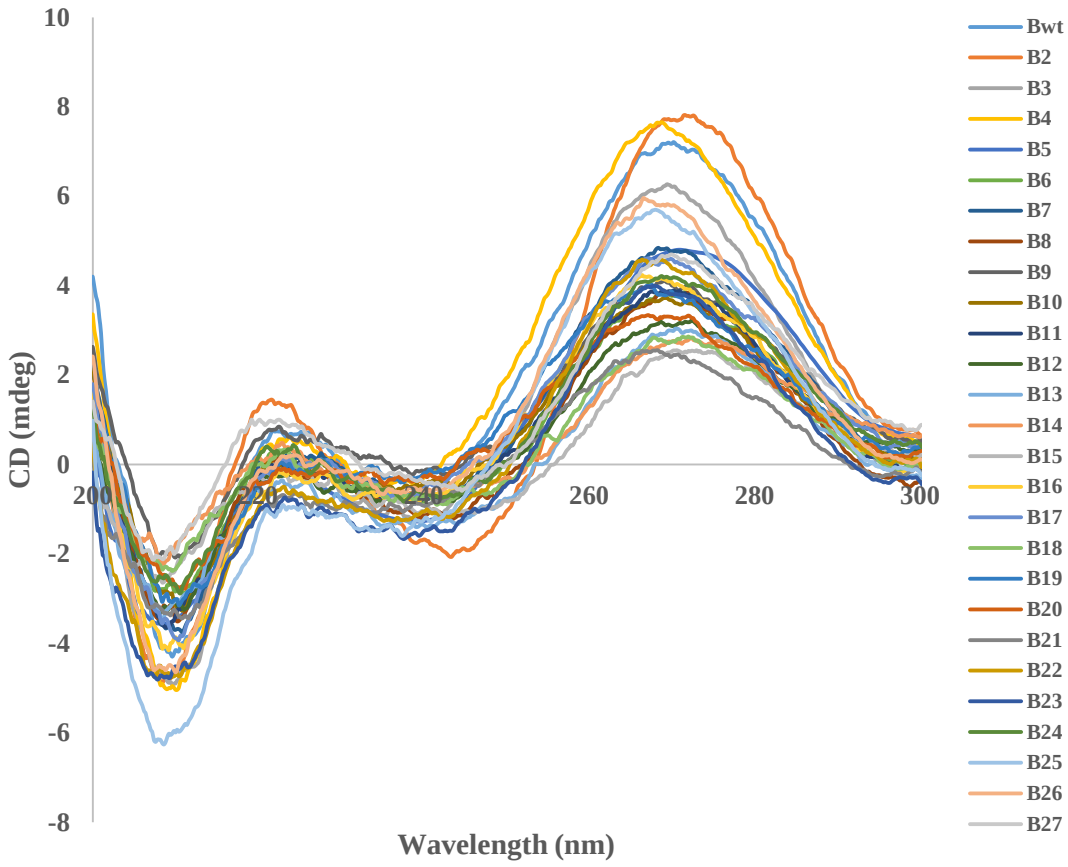

Figure 10 - The RNA duplex conformation of all anti-BCL2 siRNAs displayed through circular dichroism spectroscopy. Wild-type and modified anti-BCL2 siRNAs (~2.4 nmol/duplex) were suspended in 500 µL of a sodium phosphate buffer (90 mM NaCl, 10 mM Na2HPO4, 1 mM EDTA, pH 7) and the solution was scanned from 200–300 nm at 20°C. All scans were performed in quadruplicate and averaged using version 2 of Jasco's Spectra Manager software.

All of the siRNA generated are confirmed to be in the A-form as opposed to the other common conformations, B-form and Z-form. The most common conformation of DNA is B-form helixes. These B-form duplexes are characterized by a positive long wavelength band or bands at about 260–280 nm and a large negative band around 245 nm (Kypr, et al., 2009). Another, less common, conformation is Z-form. Z-form closely resembles an inversion of the B-form conformation; it contains a negative band at about 290 nm, a positive band around 260 nm and another characteristic, extremely deep negative band at short wavelength (~205 nm) (Kypr, et al., 2009). CD has confirmed that all siRNAs

generated for this project retain their A-form helical conformation and the chemical modifications did not greatly deviate the secondary structure of the duplexes. Because they retain their A-form conformation the chemically modified siRNAs generated should be compatible within the RNAi pathway (Ranjbar, 2009) (Chiu & Rana, 2002) (Kypr, et al., 2009).

4.3 Thermodynamics of siRNA (T_m)

The thermodynamic properties of the siRNAs were assessed by measuring the specific melting temperature of the siRNA duplexes. The melting temperature (T_m) of double stranded nucleotides is defined as the temperature at which 50% of all molecules of a given DNA sequence are hybridized into a double strand, and 50% are present as single strands. The T_m of oligonucleotides is affected by two main factors, external factors (such as salt concentration, length of sequence, and concentration of the sample) and internal factors such as base pair composition and secondary structures. The T_ms and the ΔT_ms of the anti-*BCL2* siRNA duplexes (Table 3).

Table 3- The melting temperature and change in melting temperature vs. Bwt of all anti-BCL2 siRNAs.

Anti-*BCL2* siRNA	**T_m** (°C)	**ΔT_m** (°C)
Bwt	75.5	0.0
B2	72.3	-3.1
B3	75.6	0.2
B4	76.4	1.0
B5	76.1	0.7
B6	76.6	1.2
B7	78.3	2.9
B8	76.5	1.0
B9	78.5	3.0
B10	78.3	2.9
B11	76.5	1.0
B12	78.5	3.0
B13	76.7	1.3
B14	75.8	0.3
B15	76.9	1.4
B16	79.3	3.9
B17	79.1	3.7
B18	79.5	4.1
B19	77.2	1.8
B20	76.9	1.5
B21	78.0	2.5
B22	83.1	7.6
B23	81.9	6.5
B24	83.4	8.0
B25	81.8	6.3
B26	80.6	5.1
B27	81.9	6.4

The siRNAs (~2.4 nmol/duplex) were suspended in 500 µL of a sodium phosphate buffer (90 mM NaCl, 10 mM Na2HPO4, 1 mM EDTA, pH 7) and Tm's were measured in triplicate at 260 nm, from 10-95°C. The temperature was increased at a rate of 0.5°C/min and the absorbance was measured at the end of every 0.5°C increment. The Tm's of three independent experiments were averaged and calculated using Meltwin version 3.5 software assuming the two-state model.

The T_m the unmodified wild-type (Bwt) siRNA was 75.5°C, which was the predicted value calculated using the Oligoanalyzer tool (nearest-neighbor two-state model). B2, which had an internal **$\underline{U_tU}$** modification, showed a decreased T_m of 72.3°C (ΔT_m of -3.1°C). B3, which had a **$\underline{U_tU}$** overhang, showed a very slight increase of T_m of 75.6°C

(ΔT_m of 0.2°C). These results are consistent with those of Efthymiou & Desaulniers, 2011; when **$\underline{U_tU}$** was placed internally the T_m decreased and when **$\underline{U_tU}$** was placed in an overhang position the T_m was either slightly increased or slightly decreased (negligibly affcting the thermodynamics of the duplex). The 2'-ribose modifications used in this project—2'-*O*-Me and 2'-F—are known to be stabalizing modifications which increase the thermodynamic stability of the duplex (Sabahi, et al., 2001; Wang & Kool, 1995). When 2'-*O*-Me was partially incorperated throughout the sense strand (B4) the T_m of the duplex increased to 76.4°C (ΔT_m of 1.0°C). When the 2'-F modification was partially incorperated throughout the sense strand (B10) the T_m of the duplex increased to 76.7°C (ΔT_m of 1.3°C). When a mixed sequence of 2'-F and 2'-*O*-Me bases were partially incorporated within the sense strand of the duplex the T_m increased to 77.2°C (ΔT_m of 1.8°C). When 2'-*O*-Me and 2'-F modifications were placed throughout the entirety of the sense strand (B7 and B13) the T_m of the duplexes increase to 78.3°C and 79.3°C, respectively (ΔT_m of 2.9°C and 3.9°C). When the sense and anti-sense strands had 2'-ribose modification the T_m of the duplex increased even more; B19-27 all had 2'-ribose modifications on the sense and anti-sense strands and showed the highest thermodynamic stability. When 2'-F modifications were partially incorporated into the sense and anti-sense strand (B19) the T_m of the duplex had a sharp increased to 83.1°C (ΔT_m of 7.6°C). When 2'-F were incorporated into the sense strand and a mixture of 2'-*O*-Me and 2'-F were incorporated into the anti-sense strand (B22) the T_m increased to 81.8°C (ΔT_m of 6.3°C). Finally when a mixed sequence of 2'-O-Me and 2'-F were incorporated into the sense and anti-sense strands (B25) the T_m increased to 83.9°C (ΔT_m of 8.4°C). When **$\underline{U_tU}$** was placed internally with any of the 2'-ribose modification patterns (B5, B8, B11,

B14, B17, B20, B23, and B26) it had a thermodynamically destabilizing effect, lowering the T_m of the all the duplexes without an internal **$\underline{U_tU}$** modification (with an average ΔT_m of -1.4°C vs equivalent duplexes without internal **$\underline{U_tU}$**). These results confirm that internal **$\underline{U_tU}$** placement is thermodynamically destabilizing and may aid in strand selection when designing chemically modified siRNAs. When **$\underline{U_tU}$** was placed at the overhang position it had a negligible effect on the thermodynamics of the duplex with an average ΔT_m of 0.2°C vs equivalent duplexes without a **$\underline{U_tU}$** overhang. Overall the thermodynamics of the siRNAs were as predicted, which should translate into better gene knockdown results and potentially better strand selection by RISC (Kawamata & Tomari, 2010).

4.4 Masses of Synthesized Oligonucleotides

To ensure all chemical modifications were successfully incorporated into the synthetic oligonucleotides the masses of each oligonucleotide was determined using electrospray ionizing quantitative time-of-flight mass spectrometry (ESI Q-TOF). All oligonucleotides were within predicted mass and thus molecular identity was confirmed (Table 4).

Table 4 - The predicted and recorded masses of chemically modified oligonucleotides using quantitative time-of-flight spectrometry

Oligonucleotide	Predicted Mass	Observed Mass	Oligonucleotide Sequence
1	6618.84	6618.83	5'- GCCUUCUUUGAGUUCGGUGtt -3'
2	6586.05	6586.02	5'- GCCUUCUUUGAG**U_tU**CGGUGtt -3'
3	6604.02	6604.00	5'- GCCUUCUUUGAGUUCGGUG**U_tU** -3'
4	6725.96	6725.97	5'- GCCUUCUUUGAGUUCGGUGtt -3'
5	6712.29	6712.14	5'- GCCUUCUUUGAG**U_tU**CGGUGtt -3'
6	6744.29	6744.05	5'- GCCUUCUUUGAGUUCGGUG**U_tU** -3'
7	6841.37	6841.08	5'- GCCUUCUUUGAGUUCGGUGtt -3'
8	6851.23	6851.27	5'- GCCUUCUUUGAG**U_tU**CGGUGtt -3'
9	6856.50	6856.17	5'- GCCUUCUUUGAGUUCGGUG**U_tU** -3'
10	6629.81	6629.80	5'- GCCUUCUUUGAGUUCGGUGtt -3'
11	6616.01	6616.04	5'- GCCUUCUUUGAG**U_tU**CGGUGtt -3'
12	6603.93	6603.82	5'- GCCUUCUUUGAGUUCGGUG**U_tU** -3'
13	6652.79	6652.77	5'- GCCUUCUUUGAGUUCGGUGtt -3'
14	6783.88	6784.83	5'- GCCUUCUUUGAG**U_tU**CGGUGtt -3'
15	6683.940	6684.11	5'- GCCUUCUUUGAGUUCGGUG**U_tU** -3'
16	6685.87	6685.86	5'- GCCUUCUUUGAGUUCGGUGtt -3'
17	6678.99	6678.17	5'- GCCUUCUUUGAG**U_tU**CGGUGtt -3'
18	6672.07	6672.83	5'- GCCUUCUUUGAGUUCGGUG**U_tU** -3'
23	6697.18	6697.01	5'-ph-CACCGAACUCAAAGAAGGCtt-3'
24	6792.01	6791.94	5'-ph-CACCGAACUCAAAGAAGGCtt-3'
25	6771.08	6771.06	5'-ph-CACCGAACUCAAAGAAGGCtt-3'

ESI Q-TOF were recorded in a negative electrospray mode after HPLC elution using two mobile phases; MeOH/H_2O 5:95 (v/v) with 200 mM hexafluoroisopropyl alcohol and 8.1 mM triethylamine, and 70% MeOH. ***U_tU*** *= Uracil Triazole Uracil. Green= 2'-F Modification. Red= 2'-O-Me Modification. ph= 5'-phosphate.*

4.5 Nuclease Stability Assay

It has been previously reported that **U_tU** and 2'-*O*-Me modifications incur nuclease stability when compared to unmodified siRNAs (Efthymiou, et al., 2012; Egil, et al., 2005; Allerson, et al., 2005). To test the serum nuclease stability unmodified and modified siRNAs (Bwt, B2, B3, B4, B5, and B6) were incubated in fetal bovine serum (FBS) for up to five hours to analyze the truncated products in a time-dependent manner using polyacrylamide gel electrophoresis (Figure 11). For this study 2'-F modifications

were not assessed because literature has shown that they provide little to no nuclease stability protection over unmodified siRNAs (Manoharan, 1999).

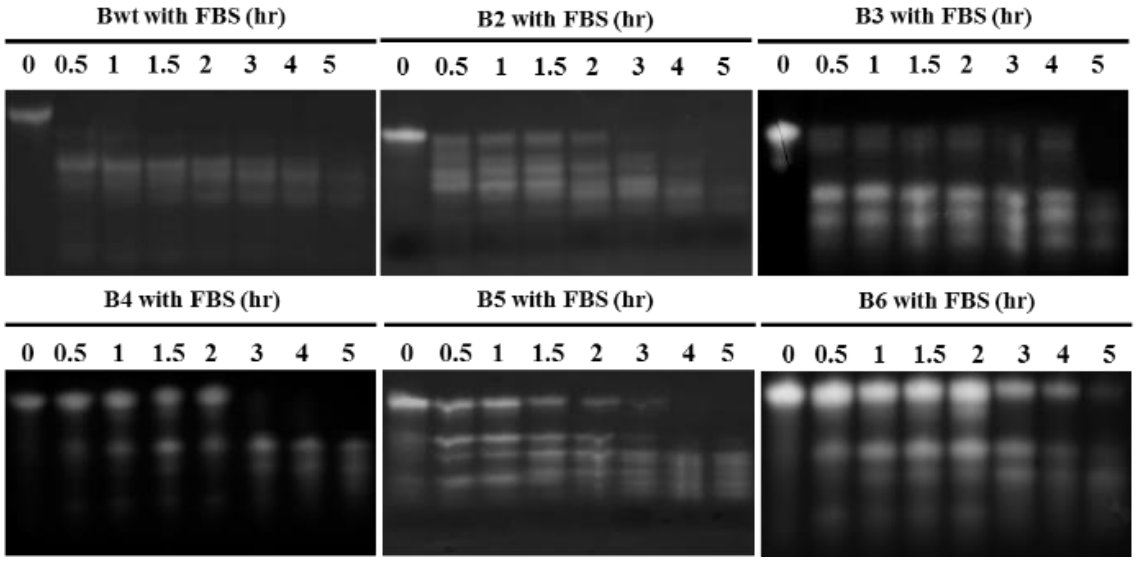

Figure 11 - Nuclease stability assay of select anti-BCL2 siRNAs.
20% Non-denaturing polyacrylamide gel with degradation products of siRNAs after incubation with 13.5% fetal bovine serum at 37.5°C from 0 hours to 5 hours.

Unmodified siRNA (Bwt) degraded almost immediately, with little to no siRNA present within 0.5 hours of incubation in the presence of nucleases. When the **U_tU** modification was incorporated internally (B2), the full siRNA duplex persisted for up to 2 hours, and when placed at an overhang position (B3), the duplex was persistent for up to 4 hours. 2'-*O*-Me modifications clustered around the sense strand (B4) increased nuclease stability, allowing the siRNA duplex to last for 2 hours in the presence of nucleases. When the 2'-*O*-Me modification was combined with an internal **U_tU** modification (B5), the duplex lasted up to 3 hours. When the 2'-*O*-Me modification was combined with the **U_tU** overhang (B6), the siRNA duplex was still present after 5 hours of incubation in the presence of nucleases. When the 2'-*O*-Me modification was combined with the **U_tU** backbone modification, nuclease resistance was greatly increased. Any change to the

native chemical structure caused a significant increase in nuclease stability, especially when the **$\underline{U_tU}$** backbone and 2'-*O*-Me modifications were combined.

4.6 qPCR Assessment of Anti-*BCL2* siRNAs

4.6.1 Gene silencing ability of Anti-*BCL2* siRNAs

After biophysical properties of the library of anti-*BCL2* siRNAs were measured they were then assessed for their ability to knock-down *BCL2* mRNA *in vitro* in KB cell lines (these cells were kindly donated by DLVR Therapeutics). Cell were transfected at three concentrations (1nM, 10nM and 20nM), with anti-*BCL2* siRNAs. 24 hours post transfection RNA was isolated then converted to cDNA. The cDNA was then used to evaluate gene expression using qPCR; expression was normalized to an untreated control using reference genes 18s rRNA and glyceraldehyde 3-phosphate dehydrogenase (GAPDH). An untreated control group was transfected with an empty lipofectamine 2000 transfection reagent and a negative control group was transfected with an anti-luciferase siRNA and not target any endogenous gene. Results of the initial qPCR screen are outlined below (Figure 12).

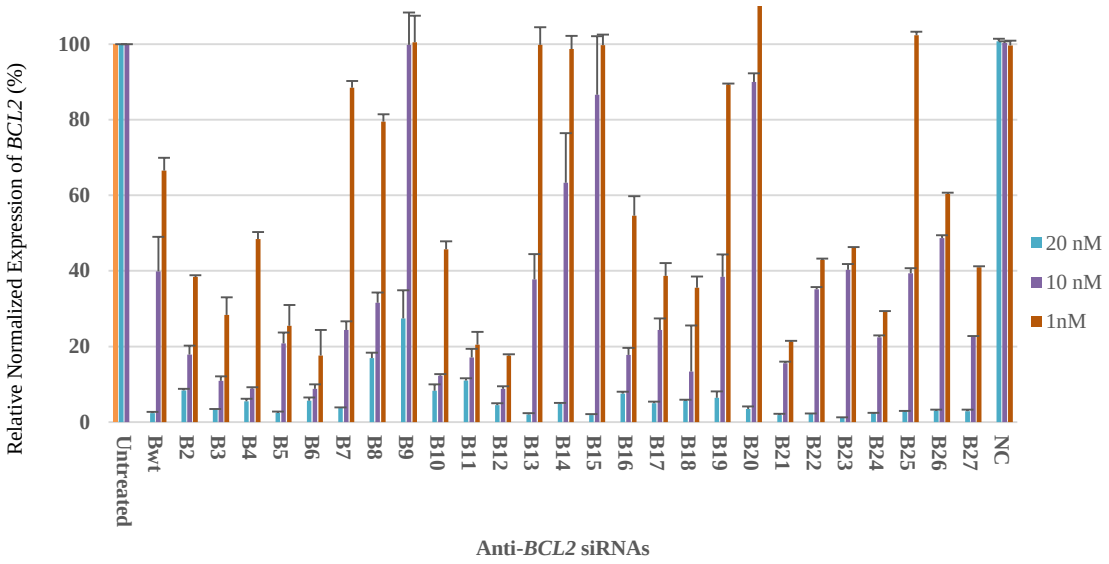

Figure 12 - Relative gene expression of BCL2 in KB cells using the best candidate anti-BCL2 siRNAs.
Relative expression was measured in in KB cells 24 hours post anti-BCL2 siRNA transfections at 1 nM, 10 nM and 20 nM. Gene expression was measured using qPCR and expression was normalized to an untreated control using reference genes 18s rRNA and glyceraldehyde 3-phosphate dehydrogenase (GAPDH). Untreated control was transfected with an empty lipofectamine 2000 transfection reagent. NC was a negative control which did not target any endogenous gene.

The initial qPCR screen showed very promising and expected results. Chemical modification of the siRNA constructs did not compromise gene silencing ability for most anti-*BCL2* siRNAs. Most anti-*BCL2* siRNAs showed effective dose-dependent knockdown of *BCL*2. The siRNAs that did not knock-down *BCL2* were siRNAs which were heavily modified with 2'-ribose modifications (B7, B8, B9, B13, B14, and B15). Literature has shown when heavily modifying siRNA with 2'-ribose modifications the siRNA loses its ability to silence the target mRNA (Elbashir, et al., 2001). More recent studies however, have shown that when blunt-ending the construct, rather than using 3'-overhangs, siRNAs retain their activity when heavily modified with 2'-ribose modifications (Kraynack & Baker, 2006). This strategy could be employed for future siRNA design when 2'-ribose modifications are incorporated. Another group of siRNAs which did not perform very well were siRNAs which contained modification on the sense

and the anti-sense strands (B19, B20, and B25). This observation has been reported previously and could be due to difficulty loading the modified RNA into the RISC complex (Kraynack & Baker, 2006).

Several of the chemically modified siRNAs exhibited enhanced activity compared to unmodified wild-type siRNA (Bwt) at concentrations at 10 nM and below (Figure 13).

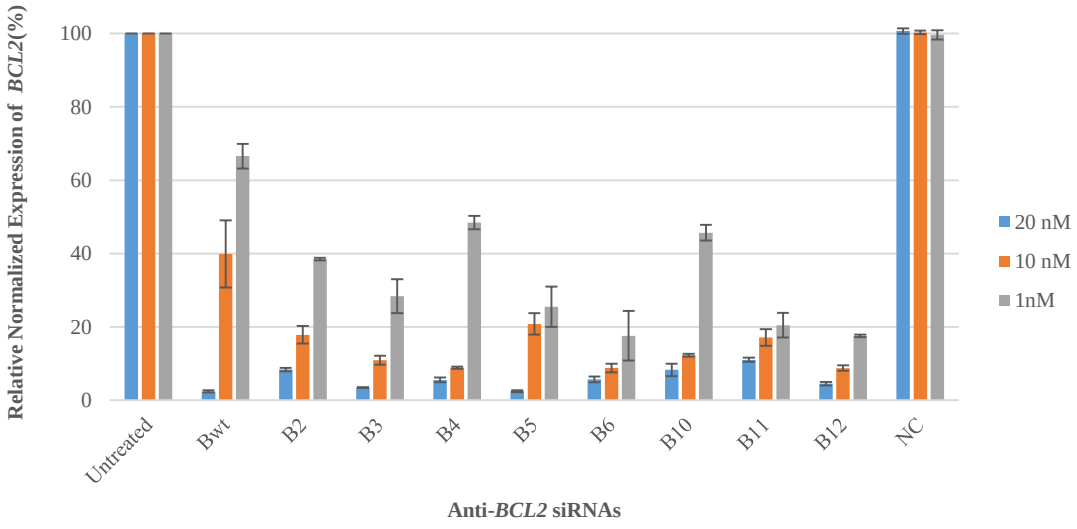

Figure 13 - Relative gene expression of BCL2 in KB cells using the best candidate anti-BCL2 siRNAs. Transfections of anti-BCL2 siRNAs at concentrations of 1 nM, 10 nM and 20 nM and gene expression was assessed 24 after transfection. Gene expression was measured using qPCR and expression was normalized to an untreated control using reference genes 18s rRNA and glyceraldehyde 3-phosphate dehydrogenase (GAPDH). Untreated control was transfected with an empty lipofectamine 2000 transfection reagent. NC was a negative control which did not target any endogenous gene.

From the initial screen of the siRNA library, 8 siRNAs were chosen for further investigation because of their dose dependent knockdown of *BCL2* and enhanced activity over Bwt (B2, B3, B4, B5, B6, B10, B11 and B12). siRNAs which contained **U_tU** modifications combined with 2'-ribose modifications clustered around the 5'-end of the sense strand (B2, B5, and B11) showed enhanced gene silencing ability compared to Bwt at all concentrations. When **U_tU** was placed in an overhang position (B3, B6, and

B12), whether in conjunction with 2'-ribose modifications or not, the siRNAs showed the greatest silencing ability over all concentrations while retaining a dose dependent response. These results are similar to the results of Efthymiou, et al. 2012, when **$\underline{U_tU}$** was placed in a 3'-overhang position or near the 3'-end of a sense strand gene silencing was similar or better than wild-type siRNA. This could be explained by the thermodynamic asymetry principal, which states that RISC is more likely to take up the strand which has the least thermodynamically stable 5'-end (Kawamata & Tomari, 2010). Therefore, by placing a destabiliing modification (**U_tU**) around the 3'-end of the sense strand and stabalizing modifications (2'-*O*-Me and 2'-F) at the 5'-end of the sense strand the anti-sense (desired) strand is taken up by RISC. This could be the reason for the enhanced activity we see for these 8 siRNAs. These siRNAs were able to effictivly knock-down *BCL2* at theraputic concentrations and are thus promising candidates for anti-cancer treatment.

4.7 Anti-BCL2 XTT Cellular Proliferation Results

4.7.1 Optimization of XTT Assay

Before cellular proliferation assays could be carried out, the procedure needed to be optimized for the cell line of use, KB cells. To determine the optimal number of cells used to seed with a 2.5X dilution series was set up starting with 100,000 cells/well down to a final concentration of 0 cells/well. The results were plotted in sigma-plot (Figure 14).

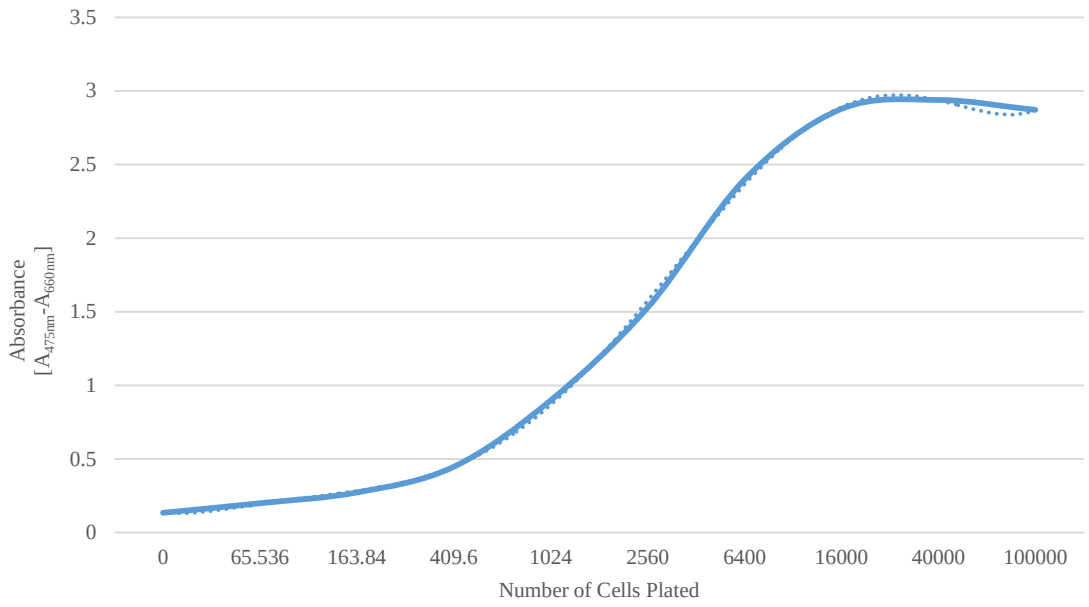

Figure 14 - : Optimization of XTT cellular proliferation assay.
KB cells were plated starting with a concentration of 100000 cells/well in a 2.5X dilution series down to 0 cells/well. Cells were incubated for 48 hours and then processed using XTT assay kit. Absorbance vs. cells plated was plotted and a sigmoidal regression was performed to determine the line of best fit to calculate the point of inflection to determine the optimal number of cells to plate for 48 hour experiments.

After the results were plotted a standard curve was calculated using sigmoidal regression, generating the equation:

$$f(x) = \frac{2.80}{1 + e^{\left(\frac{x-2400}{1170}\right)}}$$

Resulting with an R^2 value of 0.9997. The point of inflection was calculated to be 2400 and thus the optimal number of cells to seed for the siRNA screen experiment was 2400 cells per well. Upon microscopic inspection 2400 cells per well ended up being the number of cells needed to reach confluency after 48 hours 1000 cells per well were sub-confluent and 6400 cells per well were overgrown. Thus, moving forward with further experimentation with the time course assay (**Section 4.7.3**) the number of cells used for each end point was the number of cells needed to reach confluency at each end point.

4.7.2 Cellular Proliferation Screen with Anti-*BCL2* siRNAs

BCL2 oncogene is responsible for the overproduction of the bcl2 protein, which is a key regulatory protein in cellular apoptosis. The bcl-2 protein prevents pro-apoptotic factors from triggering type I and type II cell death, and thus overexpression of *BCL2* prevents cells from undergoing apoptosis (Tsujimoto, et al., 1985), therefore knocking out *BCL2* should cause a decrease in cellular proliferation. An XTT cellular proliferation kit (ATCC) was used to determine proliferation rates of KB cells treated with anti-*BCL2* siRNA in comparison to untreated cells 24 hours post siRNA transfection (Figure 15).

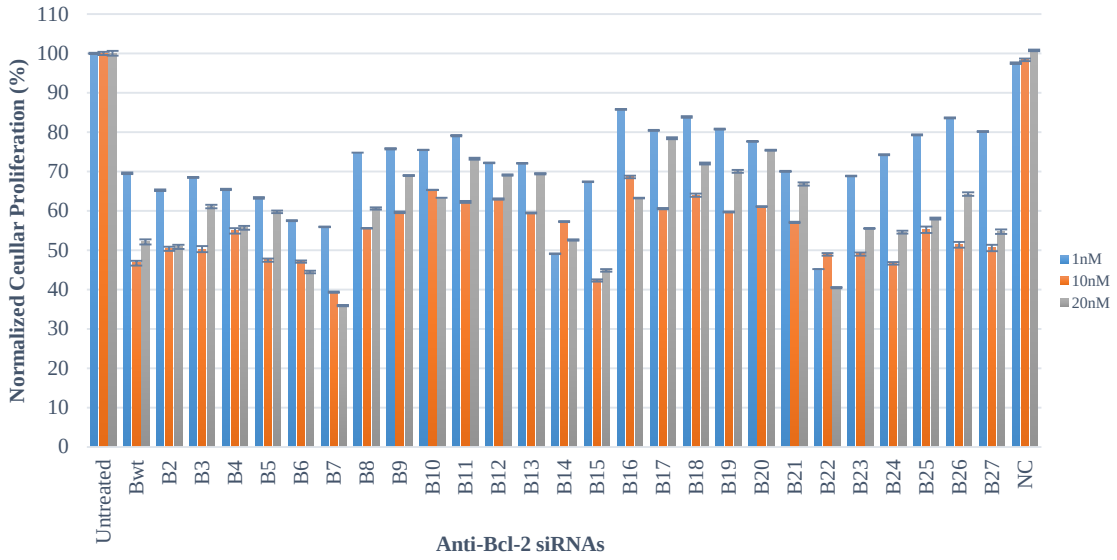

Figure 15 – XTT Cellular Proliferation siRNA screen.
KB cells were plated starting with a concentration of 100000 cells/well. 24 hours later cells were transfected with 1, 10 and 20 nM of anti-BCL2 siRNAs. 48 hours post-transfection cellular proliferation was determined via XTT cellular proliferation assay. Results were normalized to untreated cells and expressed as a percentage of cellular proliferation. A siRNA—which does not target any endogenous gene—was used as a negative control.

The anti-*BCL2* siRNAs were able to decrease cellular proliferation by 10% or more at all concentrations when compared to untreated cells. To ensure that the decreased cellular proliferation was not due to toxicity from the siRNAs a negative control was used. This negative control siRNA targeted luciferase, which is not an endogenous gene. The

negative control showed the same cellular proliferation rate as the untreated control indicating that the siRNAs were not inherently toxic to the cells. Therefore, the decrease in proliferation rates are not due to the presence of dsRNA alone and are most likely associated with *BCL2* knockdown due to the anti-*BCL2* siRNAs.

4.7.3 Time Course Cellular Proliferation Screen with Best Candidate Anti-*BCL2* siRNAs

From the qPCR screen, the best candidate siRNAs were used to determine cellular proliferation rates from continual knockdown over the course of four days using the 8 best candidate anti-BCL2 siRNAs (transfection every 48-hours with 20nM siRNA). Figure 16 illustrates that mRNA levels are still depleted after 48-hours.

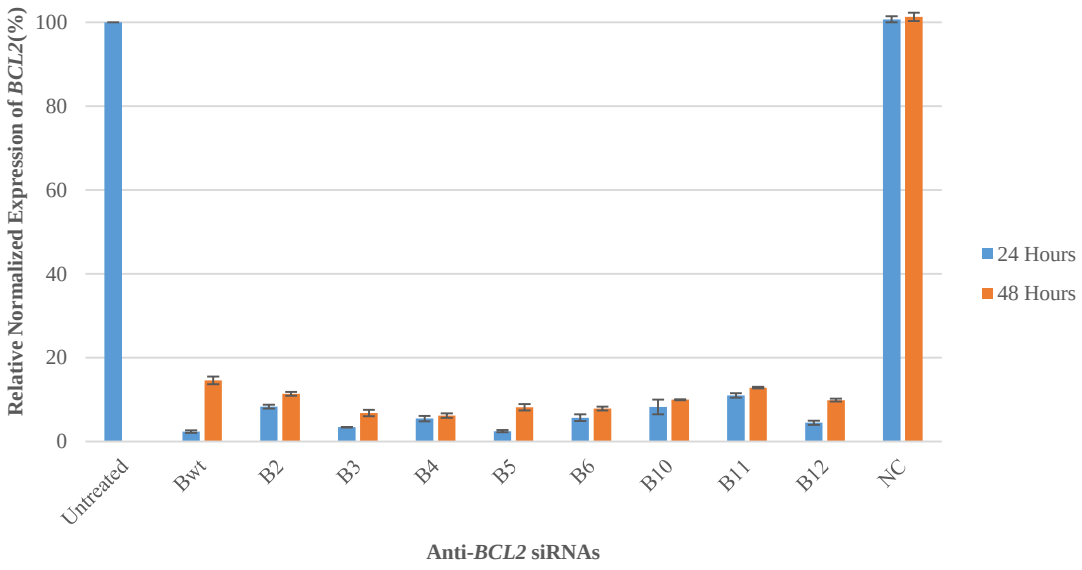

Figure 16 – Time Course Relative gene expression of BCL2 in KB cells using the best candidate anti-BCL2 siRNAs. Transfections of anti-BCL2 siRNAs at 20 nM and gene expression was assessed 24 and 48 hours after transfection. Gene expression was measured using qPCR and expression was normalized to an untreated control using reference genes 18s rRNA and glyceraldehyde 3-phosphate dehydrogenase (GAPDH). Untreated control was transfected with an empty lipofectamine 2000 transfection reagent. NC was a negative control which did not target any endogenous gene.

All of the best candidate siRNAs were able to decrease cellular proliferation within 24 hours by at least 30% when compared to untreated controls (Figure 17).

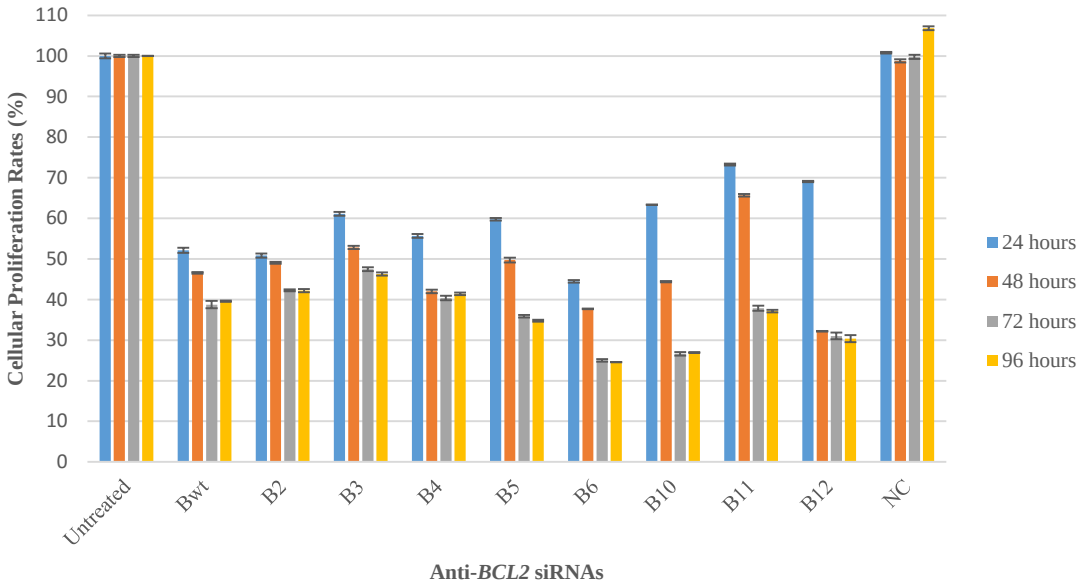

Figure 17 - Time course cellular proliferation results of best candidate anti-BCL2 siRNAs.
KB cells were plated at various concentrations (to reach confluency at each end point and transfected at 24, 48, and 72 hours with 20 nM of anti-BCL2 siRNAs. At each end point cellular proliferation was determined via XTT cellular proliferation assay. Results were normalized to untreated cells and expressed as a percentage of cellular proliferation. A siRNA—which does not target any endogenous gene—was used as a negative control.

Cellular proliferation continued to decrease after 48, and 72 hours. By 96 hours, cellular proliferation rates stabilized at their lowest rate when compared to the untreated control. Continual knockout of *BCL2* caused a 50-60% decrease in cellular proliferation after 96 hours compared to the untreated control. These results show that by depleting oncogene *BCL2*, cellular proliferation rates decrease, validating the potential of siRNAs as a therapeutic.

4.8 Human Interferon Alpha ELISA Assay Results

In vivo, double-stranded RNAs stimulate innate immunity by triggering the type I interferon response (Marques & Williams, 2005). *In vitro*, the immune response is highly dependent on the specific cell line used, and many cell lines do not possess the receptors necessary to respond to siRNAs, whereas using human peripheral mononuclear cells

(PBMC) isolated from whole human blood is a fast and reliable *in vitro* approach to predict *in vivo* response (Zamanian-Daryoush, et al., 2008). Therefore, after obtaining ethical approval, human PBMCs were isolated from whole blood donated by healthy volunteers after obtaining written consent. PBMCs were stimulated using 20 nM of anti-BCL2 siRNAs complexed with lipofectamine 2000. After 24 hours, human interferon alpha (IFN-α) levels were measured using a VeriKine ELISA kit (PBL Assay Science) according to the manufacturer's protocol (Figure 18).

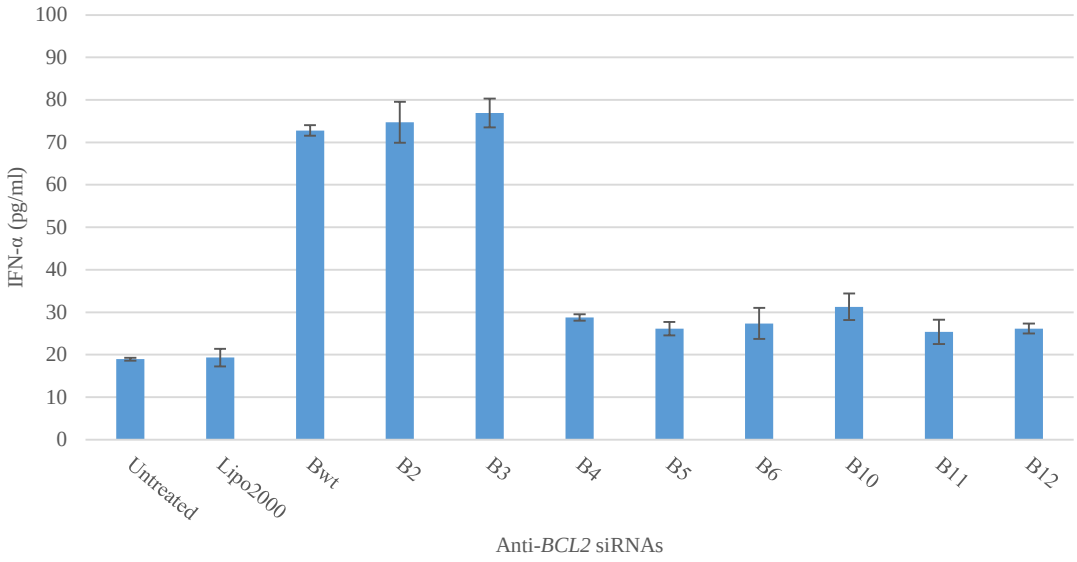

Figure 18 - Human interferon alpha production in response to anti-BCL2 siRNAs.
*Human PBMC*s were stimulated with 20 nM of anti-BCL2 siRNAs supplemented with Lipofectamine 2000. IFN-α was measured in the supernatant 24 hours post-transfection by ELISA. Results were calculated based upon a high-sensitivity standard curve (Appendix Figure 4).

PBMCs challenged with unmodified siRNA as well as **U$_t$U** modified siRNAs (Bwt, B2, and B3) induced IFN-α production (72.8, 74.4, and 76.9 pg ml^{-1} respectively), whereas siRNAs containing 2'-ribose modifications (B4, B5, B6, B10, B11 and B12) showed a decrease in immune response similar to untreated controls (28.8, 26.1, 27.3, 31.2, 25.4, and 26.1 pg ml^{-1} respectively). This data suggests that the **U$_t$U** modification alone does

not alter immune response in comparison to unmodified siRNA (Bwt). However, when the **U_tU** modification was combined with 2'-ribose modifications the innate immune response was diminished as indicated by a decrease in IFN-α production from PBMCs (Statistical Significance $P<0.001$ using student t-test). It is well established that 2'-ribose modifications evade immune detection (Valenzuela, et al., 2015), but backbone modifications (including the **U_tU** modification) are almost unknown with respect to their effect on immune response. One backbone modification, the phosphothioate backbone modification, is not considered an immunostimulatory modification but does not reduce immune response as the 2'-ribose modifications do (Verthelyiemail & Zeuner, 2003) much in the same way the **U_tU** modification did not affect the amount of IFN-α production. What is promising, however, is that the **U_tU** modification can be combined with 2'-ribose modifications to overcome immune activation.

4.9 Summary of Results

All of the anti-*BCL2* siRNAs generated showed effective dose-dependent gene knockdown at clinically relevant concentrations, with several siRNAs showing results similar or better than the wild-type anti-*BCL2* siRNA. The chemically modified siRNAs showed increased stability in the presence of serum nucleases; the greatest stability being siRNAs containing 2'-*O*-Me in conjunction with the **U_tU** modification. By targeting a clinically relevant oncogene, *BCL2*, cellular proliferation rates were diminished when siRNAs depleted *BCL2*. This diminished proliferation rate continued as long as the siRNAs were knocking down *BCL2*. This result indicated that by knocking down an anti-apoptosis oncogene, normal apoptosis can occur, and proliferation rates decrease. Finally, the anti-*BCL2* siRNAs were assessed for their ability to diminish primary interferon

response in human PBMC isolates. 2'-Ribose modifications were able to diminish immune detection whereas the **$\underline{U_tU}$** alone did not alter the immune response in comparison to wild-type siRNA, but when **$\underline{U_tU}$** was combined with 2'-modifications the immune evasion was similar to that of 2'-modifications alone. Overall, **$\underline{U_tU}$** can be combined with 2'-ribose modifications to improve the therapeutic properties of siRNAs without compromising its ability to knockdown target genes. This work has been published in the Royal Society of Chemistry Journal: Medicinal Chemistry Communications (Hagen, et al., 2015) and is included in the appendix (**Error! Reference source not found.**).

Chapter 5: Conclusions and Future Directions

5.1 Conclusions

siRNA oligonucleotides containing commercially available 2′-ribose modifications (2′-*O*-Me/2′-F) can be combined with a novel triazole-linked backbone modification in siRNA design and these siRNAs are amendable within the RNAi pathway. The qPCR screens show that these chemical modifications have effective gene-silencing activity either independently or in combination. Although, these results show that there is a limit to the amount of modification that can be incorporated before RNAi activity diminishes; when the sense and anti-sense strands were heavily modified, gene silencing activity was severely diminished. The optimal placement of modifications seems to follow the thermodynamic asymmetry rule of siRNA design (Kawamata & Tomari, 2010), the least thermodynamically stable 5'- end of the siRNA is taken up by RISC. Therefore, the most effective modification patterns were when stabilizing modifications (2'-ribose) were placed around the 5'-end of the sense strand, and a destabilizing modification (**U_tU**) was placed around the 3'- end of the sense strand. Effective gene silencing is not the only, nor the main factor when designing siRNAs. There are several practical challenges to siRNA design which can be overcome by chemical modification. Beyond gene knockdown assessment of nuclease stability, immune response and phenotypic effect (cellular proliferation assay) were also investigated.

After assessment of gene knockdown nuclease stability was investigated, as both modifications have shown serum nuclease stability over unmodified siRNAs. The mechanism of siRNA degradation via nucleases proceeds by transesterification, so most

chemical modifications which replace the hydroxyl at the 2′-position provide some protection from degradation in a position-specific manner. Likewise, backbone modifications also make RNA a less labile substrate for nucleases. As expected, the chemically modified siRNAs show excellent biological stability with high nuclease resistance, whereas unmodified siRNAs are readily degraded by serum nucleases. Nuclease stability was additive when combining triazole-linked backbone modifications with 2′-ribose modifications, especially when the triazole modification was placed at the overhang position. This enhanced nuclease stability is a desirable property when designing therapeutic siRNAs, and the chemical modification patterns employed in this study could be used to inform future siRNA design.

Another major limitation of the pharmaceutical application of siRNAs is the innate immune response. The innate immune system has a variety of receptors which recognize and respond to small nucleic acids, triggering cytokine and interferon release (Marques & Williams, 2005). Both 2′-O-Me and 2′-F modifications block immune response *in vitro* and *in vivo* (Fucini, et al., 2012), whereas the triazole-linked nucleic acid had not been tested for immune response. Our results show that triazole-linked backbone modifications illicit a similar immune response as unmodified siRNAs, and are detected by the innate immune system. When the triazole-linked backbone modification is combined with 2′-ribose modified siRNAs, the immune response is diminished to a similar level as induced by siRNAs containing only 2′-ribose modifications. Many studies have shown that 2'-*O*-Me and 2'-F modifications directly decrease innate immune response and decrease IFN-α production (Collingwood, et al., 2008; Judge, et al., 2006; Judge & MacLaclan, 2008). 2'-modified siRNAs have shown to be a TLR antagonist *in vitro* and *in vivo*. Robbins and

collouges (2007), have shown that 2'-*O*-Me RNA directly inhibits cytokine induction by directly antagonizing TLR-7 in a non-sequence dependant manor, and postulate that 2'-F modifications should behave the same. Therefore, simply by placing a few 2'-ribose modifications within a siRNA, immune response will be greatly diminished when compared to native siRNAs. This should help inform future siRNA modification patterns; by placing a few 2'-ribose modifications within a siRNA, immune activation can be diminished.

Finally, the utility of these siRNAs were assessed by targeting a clinically relevant oncogene, *BCL2*, which is implicated in a diverse range of chemotherapeutic resistant cancers (Reed, 1995). Not only were the siRNAs successful in knocking down BCL2 expression *in vitro*, but were also able to decrease cellular proliferation rates. These results mirror those of oblimersen sodium (Genasense), a *BCL2* antisense oligonucleotide. In preclinical trials, Genasense depleted *BCL2* mRNA which correlated to increased apoptosis and decreased cellular proliferation *in vitro* (Herbst & Frankel, 2004; Kang & Reynolds, 2009). A more recent study of anti-*BCL2* siRNAs (Lin, *et al*. 2012) generated anti-*BCL2* siRNAs, containing 2'-ribose modifications. The siRNAs were assessed by their ability to induce tumor cell apoptosis in KB cell xenograft tumor-bearing mice. They reported significant tumor apoptosis and significant tumor size reduction when mice were treated with ani-*BCL2* siRNAs. Although, not measuring the same metric, increased apoptosis and decreased cellular proliferation are indicative of the same result: when bcl2, an important apoptotic regulator, is depleted tumorigenic cells no longer proliferate out of control and undergo apoptosis. Although, for anticancer therapy, knockdown of the *BCL2* gene is not sufficient to achieve complete antitumor activity.

Beyond bcl2, there is a variety of regulatory proteins and genes which regulate the apoptosis state of the cell, let alone all of the other regulatory proteins and genes present. But, by combining of *BLC2* gene knockdown with traditional chemotherapy therapeutic, efficacy can be enhanced in multidrug-resistant cancer cells (Saad, et al., 2008; George, et al., 2009; Chen, et al., 2009; Meng, et al., 2010; Pandyra, et al., 2007). Overall, by combining 2′-ribose modifications with a novel triazole-linked backbone modification, we have generated siRNAs with chemical modification patterns which have enhanced nuclease stability and decreased immune activity without compromising the potency of the duplex as a trigger of RNAi.

Overall, by combining 2'-ribose modifications with the triazole-linked backbone modification several therapeutic barriers can be overcome, including, potent gene knockdown, nuclease stability, and innate immune response. The result of this project can help inform future chemical modification patterns amendable with siRNA design with the hopes of developing a siRNA therapeutic.

5.2 Future Prospects

This project have several avenues left to explore, including determining the true potency of these siRNAs, determining the exact molecular effects these modifications have within the RNAi pathway, improving the therapeutic features of these siRNAs by combining more modifications, and finally by bridging the results of this study to inform the design of novel dicer substrate siRNAs.

The first avenue of investigation to follow up this study would be to determine the IC_{50} values of the best candidate siRNAs. IC_{50} is a common method used by researchers and is

defined in siRNA research as concentration where the targeted mRNA is reduced by 50%. This method was developed early on in siRNA research as a way to directly compare siRNAs with anti-sense oligonucleotides, and is now used as the standard for measuring siRNA potency (Far & Sczakiel, 2003; Miyagishi, et al., 2003; Alagia, et al., 2015; Peel, et al., 2015). Thus the results of generating IC_{50} curves would help us understand the potency of the siRNAs. This would be an easy experiment to conduct; a dose-response curve would be constructed by transfecting cell cultures with concentrations of siRNA at a concentration which completely knocks down mRNA to a concentration that no longer affects mRNA levels within the cells. This would be a good follow up study because all of the best candidate siRNAs have similar knockdown values at the concentrations tested in the project, so by determining the IC_{50} values the potency of the siRNAs can be determined as well as understanding the subtle effects of the chemical modifications within the siRNAs.

A large challenge facing siRNA therapeutics, not addressed in this study, is the inability of siRNAs to readily cross the cellular membrane. This is due to the polyanionic nature of the phosphodiester backbone, causing the siRNA to be negatively charged and thus unable to pass across the fatty lipid bilayer. Recently, our research group has reported the conjugation of cholesterol to a uracil based triazole backbone and which was placed within the internal region of an siRNA (Peel, et al., 2015) (Figure 19). This was the first time that a nonionic linkage unit derivatized with a base-modified hydrophobic group has been placed within a siRNA. Several other examples of base-modified siRNAs have been explored; however, they have been utilized within the context of a sugar linked to a natural phosphodiester backbone.

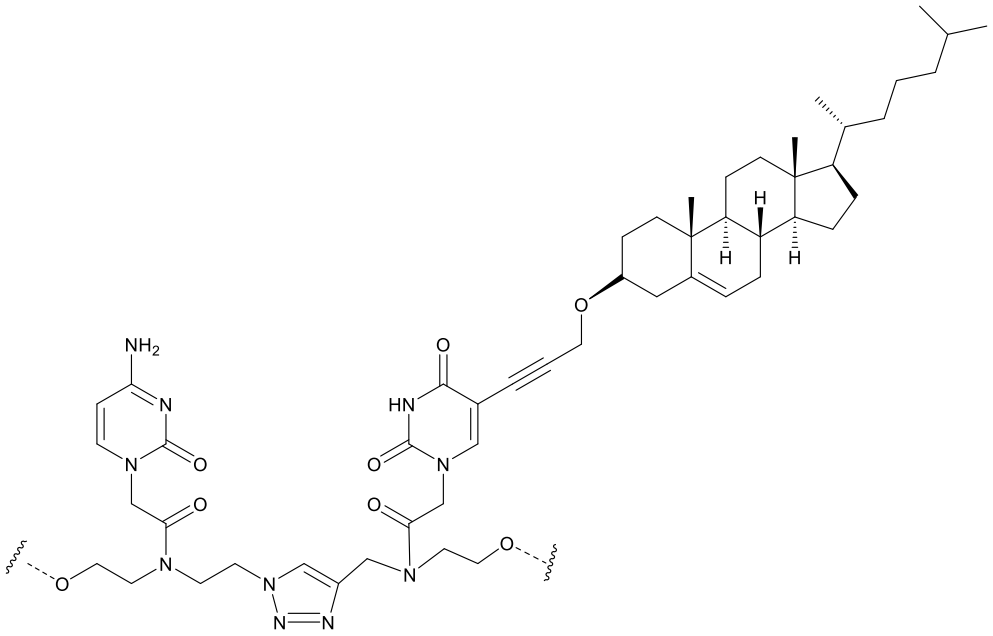

*Figure 19 – Chemical structure of cytosine-triazole linked-uracil cholesterol (**$\underline{C_tU}^{CH}$**).*

We investigated if the conjugation to a lipophilic molecule, such as cholesterol, would aid in transfection without the need of a carrier (such as lipofectamine). Without a carrier the **$\underline{C_tU}^{CH}$** had knockdown comparable to that with a carrier, indicating that it did aid in crossing the cellular membrane. The **$\underline{C_tU}^{CH}$** modification was not combined with any other modification. The results of this thesis project indicate that by combining the **$\underline{C_tU}^{CH}$** modification with 2'-ribose modifications thermodynamics could be fine-tuned and immune stimulation can be diminished, as the triazole modification alone does not alter immune response. Thus, future siRNA design could incorporate triazole modifications (with lipophilic conjugation) in conjunction with 2'-ribose modifications to improve all aspects of siRNA therapy: enhanced nuclease stability, thermodynamic modulation, decreased immune activation, and greater cell permeability.

Beyond testing the therapeutic applications of these chemically modified siRNAs it would be of interest to further investigate the molecular behaviour of these siRNAs within the RNAi pathway. The performance of the siRNAs was tested in a downstream way; measuring mRNA levels after gene knockdown using qPCR. It would be wise to test performance of native siRNAs vs modified siRNAs in strand selection assays, RISC assembly assays, and Argonaute loading assays to determine the true nature of the enhanced properties of these siRNAs within the RNAi pathway. This could help shed some light on the underlying mechanisms as to why the chemically modified siRNAs have a greater effect than native siRNAs.

A strand selection assay is two dual luciferase assays done in tandem using psiCHECK vectors (Promega). The first plasmid would contain the genetic information corresponding to the sense strand of the siRNA while the other plasmid contains sequence corresponding to the anti-sense strand. This is a crude method to quantify strand selection *in vitro* and this assay would confirm the strand selection bias which the chemical modifications impart upon the siRNAs. The results would indicate whether the thermodynamic asymmetry principal does indeed hold true for strand selection bias using the specific chemical modification pattern employed.

The RISC assembly assay and Argonaute loading assay would determine if the chemical modifications have any impact upon RISC formation *in vitro* and help de-convolute what really affects siRNA potency. There are conflicting reports as to what constitutes canonical RNAi, some groups report that Dicer is disposable for proper strand selection/RISC assembly and argonaute is only important for strand selection and RISC assembly, and determines the potency of the siRNA (Yoda, et al., 2010; Betancur &

Tomari, 2012; Ye, et al., 2011); whereas other groups believe that dicer is invaluable for proper RISC assembly and strand selection, and thus determines potency (Sakurai, et al., 2011; Wang, et al., 2011; Noland, et al., 2011). The latter theory is called the hand-off mechanism and it is believed that siRNAs which go through dicer and form a pre-RISC complex before argonaute and RISC form are more potent effectors of RNAi. Liu, et al. (2012) developed a step by step method to investigate RISC and argonaute loading. This method would be used to determine how dicer is involved in RISC loading in the presence of chemically modified siRNAs. The assay itself consists of incubating cell cultures with radiolabelled siRNAs and running native gel electrophoresis mobility shift assays to monitor the assembly components of the RISC complex. This is done *in vitro* cell cultures expressing differentially epitope labelled and overexpressed RISC proteins. This assay is now used by several labs when researching the molecular nature of RNAi and the potency of siRNAs (Liu, et al., 2012; Snead, et al., 2012; Yoda, et al., 2010).

Another avenue worth exploring is chemical modifications within dicer substrate siRNAs. Dicer substrate siRNAs are a recent but very promising development in siRNA design. First described by Kim, et al. (2005), dicer substrate siRNAs (DsiRNAs) are siRNAs which are slightly longer than tradiational synthetic siRNAs. These DsiRNAs are first processed by dicer and then loaded into RISC in contrast to siRNAs which bypass dicer. Through refinment, DsiRNAs have proven to be up to 100-times more potent and longer lasting gene knockdown when compared to siRNAs without any chemical modifications, also showing decresed immune activation in compairason to native siRNAs, completely diminishing the primary immune response (Snead, et al., 2012). There has been much commercial interest in DsiRNAs, as several nucleic acid research

companies have developed DsiRNA products (Bio-Rad and IDT) as well as several pharmacutical developing DsiRNAs (Tekmira, Alnylam, ISIS, and Dicerna), all racing to develop the first DsiRNA theraputic.

Although DsiRNAs are being havily investigated there has only been one published paper regarding chemical modifications within DsiRNAs (Collingwood, et al., 2008), and is an area wide open for future research. In their 2008 paper, they generated a small library of DsiRNAs containing only 2'-*O*-Me and 2'-F modifications, in positions known to improve properties of siRNAs. This is an opportunity to apply chemical modification patterns compatable with siRNAs and apply them to DsiRNAS to help improve upon the theraputic limitations of siRNAs and further optamize DsiRNAs. One interesting avenue to explore would be the dicer cleavage region itself, this region was completely avoided in the Collingwood (2008) paper due to the fear of dicer not cleaving the DsiRNA into a mature siRNA product. I would like to design DsiRNA with cleavable and non-cleable chemical modifications within and around the dicer cleavage region. This provides an exciting opportunity to explore the molecular function of the RNAi pathway, as it has been shown that siRNAs containing non-cleavable modifications around the argonaute cleavage region will still continue RNAi and supress mRNAs (Efthymiou, et al., 2012). By placing chemical modifications within the dicer cleavage region our understanding of the RNAi pathway could be further refined.

There are many exciting opporunities worth further investaion. Including, determining potency by calculating IC_{50} values, investigating the exact molecular effects within the RNAi pathway, improving the therapeutic features of these siRNAs by combining more

modifications, and finally by using these results to inform the design of novel dicer substrate siRNAs.

References

Addepalli, H., 2010. Modulation of thermal stability can enhance the potency of siRNA. *Nucleic Acids Res,* Volume 38, pp. 7320-7331.

Akar, U., 2008. Silencing of Bcl-2 expression by small interfering RNA induces autophagic cell death in MCF-7 breast cancer cells. *Autophagy,* Volume 4, pp. 669-679.

Akira, S. & Takeda, K., 2004. Toll-like receptor signalling. *Nat Rev Immunol,* Volume 4, pp. 499-511.

Alagia, A., Terrazas, M. & Eritja, R., 2015. Modulation of the RNA interference activity using central mismatched siRNAs and acyclic threoninol nucleic acids (aTNA) units. *Molecules,* Volume 20, pp. 7602-7619.

Al-Khalili, L., Cartee, G. & Krook, A., 2003. RNA interference-mediated reduction in GLUT1 inhibits serum-induced glucose transport in primary human skeletal muscle cells. *Biochem Biophys Res Commun,* Volume 307, pp. 127-132.

Allerson, C. R., 2005. Fully 2'-modified oligonucleotide duplexes with improved *in vitro* potency and stability compared to unmodified small interfering RNA. *J Med Chem,* Volume 48, pp. 901-904.

Altona, C. & Sundaralingam, M., 1972. Conformational analysis of the sugar ring in nucleosides and nucleotides. New description using the concept of pseudorotation. *J Am Chem Soc,* Volume 94, pp. 8205-8212.

Ambardekar, V., 2011. The modification of siRNA with 3′ cholesterol to increase nuclease protection and suppression of native mRNA by select siRNA polyplexes. *Biomaterials,* Volume 32, pp. 1404-1411.

Athyros, V., 2008. Antisense technology for the prevention or the treatment of cardiovascular disease: the next blockbuster. *Expert Opin Investig Drugs,* Volume 17, pp. 969-972.

Balachandran, S., 2000. Essential role for the dsRNA-dependent protein kinase PKR in innate immunity to viral infection. *Immunity,* Volume 13, pp. 129-141.

Baltimore, D., 1970. Viral RNA-dependent DNA polymerase: RNA-dependent DNA polymerase in virions of RNA tumour viruses. *Nature,* Volume 226, pp. 1209-1211.

Bennett, F. & Swayze, E. E., 2010. RNA targeting therapeutics: molecular mechanisms of antisense oligonucleotides as a therapeutic platform. *Ann Rev Pharm Tox,* Volume 50, pp. 259-293.

Berezikov, E., 2011. Evolution of microRNA diversity and regulation. *Nat Rev Genet,* Volume 12, pp. 846-860.

Berns, K., 2004. A large-scale RNAi screen in human cells identifies new components of the p53 pathway. *Nature,* Volume 428, pp. 431-437.

Betancur, J. & Tomari, Y., 2012. Dicer is despensable for asymmetric RISC loading in mammals. *RNA,* Volume 18, pp. 24-30.

Birmingham, A., 2006. 3'-UTR seed matches, but not overall identity, are associated with RNAi off-targets. *Nat Methods,* Volume 3, pp. 199-204.

Blackburn, G., Gait, M. & Loakes, D., 2006. *DNA and RNA structure in Nucleic Acids in Chemistry and Biology*. 1 ed. Cambridge: RSC.

Bone, R., 1992. Definitions for sepsis and organ failure and guidelines for the use of innovative therapies in sepsis. The ACCP/SCCM Consensus Conference Committee. American College of Chest Physicians/Society of Critical Care Medicine. *Chest,* Volume 101, pp. 1644-1655.

Braun, J., Huntzinger, E. & Izaurralde, E., 2013. The role of GW182 proteins in miRNA-mediated gene silencing. *Adv Exp Med Biol,* Volume 768, pp. 147-163.

Brummelkamp, T. & Bernards, R., 2003. New tools for functional mammalian cancer genetics. *Nat Rev Cancer,* Volume 3, pp. 781-789.

Cerutti, H. & Casas-Mollano, J., 2006. On the origin and functions of RNA-mediated silencing: from protists to man. *Curr Genet,* Volume 50, p. 81–99..

Chen, A., 2009. Co-delivery of doxorubicin and Bcl-2 siRNA by mesoporous silica nanoparticles enhances the efficacy of chemotherapy in multidrug-resistant cancer cells. *Small,* Volume 5, pp. 2673-2677.

Chiu, Y. & Rana, T., 2002. RNAi in human cells: basic structural and functional features of small interfering RNA. *Mol Cell,* Volume 10, pp. 549-561.

Chounga, S., 2006. Chemical modification of siRNAs to improve serum stability without loss of efficacy. *Biochem Biophys Res Commun,* Volume 342, p. 919–927.

Collingwood, M., 2008. Chemical modification patterns compatible with high potency dicer-substrate small interfering RNAs. *Oligonucleotides,* Volume 18, p. 187–199.

Cory, S. & Adams, J., 2002. The Bcl2 family: regulators of the cellular life-or-death switch. *Nat Rev Cancer,* Volume 2, pp. 647-656.

Crick, F., 1970. The central dogma of molecular biology. *Nature,* Volume 227, pp. 561-563.

Debatin, K., Poncet, D., 2002. Chemotherapy: targeting the mitochondrial cell death pathway. *Oncogene,* Volume 21, p. 8786–8803.

Deleavey, G. & Damha, M., 2012. Designing chemically modified oligonucleotides for targeted gene silencing. *Chem Biol,* Volume 24, pp. 937-954.

Demidov, V., 1994. Stability of peptide nucleic acids in human serum and cellular extracts. *Biochem Pharmacol,* Volume 48, pp. 1310-1313.

Diebold, S., 2006. Nucleic acid agonists for toll-like receptor 7 are defined by the presence of uridine ribonucleotides. *Eur J Immunol,* Volume 36, pp. 3256-3267.

Doi, N., 2003. Short-interfering-RNA-mediated gene silencing in mammalian cells requires Dicer and eIF2C translation initiation factors. *Curr Biol,* Volume 13, pp. 41-46.

Eckstein, F., 2002. Developments in RNA chemistry, a personal view. *Biochimi,* Volume 84, pp. 841-848.

Efthymiou, T. C. & Desaulniers, J.-P., 2011. Synthesis and properties of oligonucleotides that contain a triazole-linked nucleic acid dimer. *J Heterocycl Chem,* Volume 48, pp. 533-539.

Efthymiou, T. C., Peel, B., Huyng, V., Orentario, J., & Desaulniers, J-P., 2012. Efficient synthesis and cell-based silencing activity of siRNAs that contain triazole backbone linkages. *Bioorg Med Chem Lett,* Volume 15, pp. 1722-1726.

Efthymiou, T., Peel, B., Huynh, V. & Desaulniers, J., 2012. Evaluation of siRNAs that contain internal variable-length spacer linkages. *Bioorg Med Chem Lett,* Volume 22, pp. 5590-5594.

Egholm, M., 1993. PNA hybridizes to complementary oligonucleotides obeying the Watson-Crick hydrogen-bonding rules. *Nature,* Volume 365, pp. 566-568.

Egil, M., 2005. Probing the influence of stereoelectronic effects on the biophysical properties of oligonucleotides: comprehensive analysis of the RNA affinity, nuclease resistance, and crystal structure of ten 2‘-O-ribonucleic acid modifications. *Biochem,* Volume 44, pp. 9045-9057.

Elbashir, S., Lendeckel, W. & Tuschl, T., 2001. RNA interference is mediated by 21- and 22-nucleotide RNAs. *Genes & Dev,* Volume 15, pp. 188-200.

Elbashir, S. M., 2001. Functional anatomy of siRNAs for mediating efficient RNAi in *Drosophila melanogaster* embryo lysate. *EMBO J,* Volume 20, pp. 6877-6888.

Fabian, M. & Sonenberg, N., 2010. Regulation of mRNA translation and stability by miRNAs. *Annu Rev Biochem,* Volume 19, pp. 351-379.

Faehnle, C., 2013. The making of a slicer: activation of human Argonaute-1. *Cell Rep,* Volume 27, pp. 1901-1909.

Far, R.-K. & Sczakiel, G., 2003. The activity of siRNA in mammalian cells is related to structural target accessibility: a comparison with antisense oligonucleotides. *Nucleic Acids Res,* Volume 31, pp. 4417-4424.

Feng, G., Chong, K., Kumar, A. & Williams, B., 1992. Identification of double-stranded RNA-binding domains in the interferon-induced double-stranded RNA-activated p68 kinase. *Proc Natl Acad Sci,* Volume 89, pp. 5447-5451.

Fire, A., & Mello, C., 1998. Potent and specific genetic interference by double-stranded RNA in *Caenorhabditis elegans*. *Nature,* Volume 391, pp. 806-811.

Fucini, R., 2012. Adenosine modification may be preferred for reducing siRNA immune stimulation. *Nucleic Acid Therapy,* Volume 22, pp. 205-210.

García, M., Meurs, E. & Esteban, M., 2007. The dsRNA protein kinase PKR: virus and cell control. *Biochimie,* Volume 89, pp. 799-811.

Geary, R., Henry, S. & Grillone, L., 2002. Fomivirsen: clinical pharmacology and potential drug interactions. *Clin Pharmacokinet,* Volume 41, pp. 255-260.

Geary, R., Yu, R. & Levin, A., 2001. Pharmacokinetics of phosphorothioate antisense oligodeoxynucleotides. *Curr Opin Investig Drugs,* Volume 2, pp. 562-573.

George, J., Banik, N. & Ray, S., 2009. Bcl-2 siRNA augments taxol mediated apoptotic death in human glioblastoma U138MG and U251MG cells. *Neurochem Res,* Volume 34, pp. 66-78.

Griffith, M., 2013. Mining the druggable genome. *Nat Methods,* Volume 10, pp. 1209-1210.

Gross, A., McDonnell, J. & Korsmeyer, S., 1999. BCL-2 family members and the mitochondria in apoptosis. *Genes & Dev,* Volume 13, pp. 1899-1911.

Guo, S. & Kemphues, K., 1995. par-1, a gene required for establishing polarity in *C. elegans* embryos, encodes a putative Ser/Thr kinase that is asymmetrically distributed. *Cell,* Volume 81, pp. 611-620.

Hagen, G., Peel, B. J., Samis, J. & Desaulniers, J.-P., 2015. Synthesis and *in vitro* assessment of chemically modified siRNAs targeting BCL2 that contain 2′-ribose and triazole-linked backbone modifications. *Med Chem Comm,* Volume **6**, pp. 1210-1215.

Hair, P., Cameron, F. & McKeage, K., 2013. Mipomersen sodium: first global approval. *Drugs,* pp. 487-493.

Hall, A., 2004. RNA interference using boranophosphate siRNAs: structure-activity relationships. *Nucleic Acids Res,* Volume 32, pp. 5991-6000.

Hamilton, A. & Baulcombe, D., 1999. A species of small antisense RNA in posttranscriptional gene silencing in plants. *Science,* Volume 286, pp. 950-952.

Hanahan, D. & Weinberg, R., 2011. Hallmarks of cancer: the next generation. *Cell,* Volume 144, pp. 646-674.

Hanahan, D. & Weinberg, R. A., 2000. The hallmarks of cancer. *Cell,* Volume 100, pp. 57-70.

Hannon, G., 2002. RNA Interference. *Nature,* Volume 418, pp. 244-251.

Haupenthal, J., 2006. Inhibition of RNAse A family enzymes prevents degradation and loss of silencing activity of siRNAs in serum. *Biochem Pharmacol,* pp. 702-710.

Herbst, R. & Frankel, S., 2004. Oblimersen sodium (Genasense bcl-2 antisense oligonucleotide): a rational therapeutic to enhance apoptosis in therapy of lung cancer. *Clin Cancer Res,* Volume 10, pp. 42-45.

Herdewijn, P., 2000. Heterocyclic modifications of oligonucleotides and antisense technology. *Antisense Nucleic Acid Drug Dev,* Volume 10, pp. 297-310.

Hong, J., 2010. Comprehensive analysis of sequence-specific stability of siRNA. *FASEB J,* Volume 24, pp. 4844-4855.

Hornung, V., 2005. Sequence-specific potent induction of IFN-alpha by short interfering RNA in plasmacytoid dendritic cells through TLR7. *Nat Med,* Volume 11, pp. 263-270.

Hudson, T., 2013. Genome variation and personalized cancer medicine. *J Intern Med,* Volume 274, pp. 440-450.

Hughes, J., Rees, S., Kalindjian, S. & Philpott, K., 2011. Principles of early drug discovery. *Br J Pharmacol,* Volume 162, p. 1239–1249.

Jackson, A., 2006. Widespread siRNA "off-target" transcript silencing mediated by seed region sequence complementarity. *RNA,* Volume 12, p. 1179–1187.

Judge, A., Bola, G., Lee, A. & MacLachlan, I., 2006. Design of noninflammatory synthetic siRNA mediating potent gene silencing *in vivo*. *Mol Ther,* Volume 13, pp. 494-505.

Judge, A. & MacLaclan, I., 2008. Overcoming the innate immune response to siRNAs. *Hum Gene Ther,* Volume 19, pp. 111-124.

Juliano, R., 1999. Antisense pharmacodynamics: critical issues in the transport and delivery of antisense oligonucleotides. *Pharm Res,* Volume 16, pp. 494-502.

Juliano, R., Bauman, J., Kang, H. & Ming, X., 2009. Biological barriers to therapy with antisense and siRNA oligonucleotides. *Mol Pharm,* Volume 6, pp. 696-695.

Kang, H. & Reynolds, P., 2009. Bcl-2 inhibitors: targeting mitochondrial apoptotic pathways in cancer therapy. *Clin Cancer Res,* Volume 15, pp. 11-26.

Kawai, T. & Akira, S., 2006. Innate immune recognition of viral infection. *Nat Immunol,* Volume 7, pp. 131-137.

Kawai, T. & Akira, S., 2011. Toll-like receptors and their crosstalk with other innate receptors in infection and immunity. *Immunity,* Volume 27, pp. 637-650.

Kawai, T., 2005. IPS-1, an adaptor triggering RIG-I- and Mda5-mediated type I interferon induction. *Nat Immunol,* Volume 6, pp. 981-988.

Kawamata, T. & Tomari, Y., 2010. Making RISC. *Trends Biochem Sci,* Volume 35, pp. 368-376.

Kennerdell, J. & Carthew, R., 1998. Use of dsRNA-mediated genetic interference to demonstrate that frizzled and frizzled 2 act in the wingless pathway. *Cell,* Volume 95, pp. 1017-1026.

Kim, D., 2005. Synthetic dsRNA Dicer substrates enhance RNAi potency and efficacy. *Nat Biotech,* Volume 23, pp. 222-226.

Kluck, R., Bossy-Wetzel, E., Green, D. & Newmeyer, D., 1997. The release of cytochrome c from mitochondria: a primary site for Bcl-2 regulation. *Science,* Volume 275, pp. 1132-1136.

Koonin, E., Gorbalenya, A. & Chumakov, K., 1989. Tentative identification of RNA-dependent RNA polymerases of dsRNA viruses and their relationship to positive strand RNA viral polymerases. *FEBS,* Volume 252, pp. 42-46.

Krajewski, S., 1995. Reduced expression of proapoptotic gene BAX is associated with poor response rates to combination chemotherapy and shorter survival in women with metastatic breast adenocarcinoma. *Cancer Res,* Volume 55, pp. 4471-4478.

Krajewski, S., Chatten, J., Hanada, M. & Reed, J., 1996. Immunohistochemical analysis of the Bcl-2 oncoprotein in human neuroblastomas. Comparisons with tumor cell differentiation and N-Myc protein. *Lab Invest,* Volume 72, pp. 42-54.

Kraynack, B. F. & Baker, B., 2006. Small interfering RNAs containing full 2′-O-methylribonucleotide-modified sense strands display Argonaute2/eIF2C2-dependent activity. *RNA,* Volume 12, pp. 163-176.

Krieg, A., 1995. CpG motif within bacterial DNA was responsible for the immunostimulatory effects and developed synthetic CpG ODN. *Nature,* Volume 374, pp. 546-549.

Kypr, J., Kejnovská, I., Renčiuk, D. & Vorlíčková, M., 2009. Circular dichroism and conformational polymorphism of DNA. *Nucleic Acids Res,* Volume 37, pp. 1713-1725.

Lee, E. & Muller, W., 2010. Oncogenes and tumor suppressor genes. *Perspect Biol,* Volume 2, pp. 1-20.

Li, K., Lin, S., Brunicardi, F. & Seu, P., 2003. Use of RNA interference to target cyclin E-overexpressing hepatocellular carcinoma. *Cancer Res,* Volume 63, pp. 3593-3597.

Li, L.-C., 2006. Small dsRNAs induce transcriptional activation in human cells. *PNAS,* Volume 103, p. 17337–17342.

Lin, Q., 2012. Efficient systemic delivery of siRNA by using high-density lipoprotein-mimicking peptide lipid nanoparticles. *Nanomedicine,* Volume 7, pp. 1813-1825.

Liu, X., Jin, D., McManus, M. & Mourelatos, Z., 2012. Precursor microRNA-programmed silencing complex assembly pathways in mammals. *Mol Cell,* Volume 46, pp. 507-517.

Lund, E. & Dahlberg, J., 2006. Substrate selectivity of exprotin 5 and dicer in the biogenesis of microRNAs. *Quant Biol,* Volume 71, pp. 59-66.

MacFarlane, L.-A. & Murphy, P., 2010. MicroRNA: Biogenesis, function and role. *Curr Genomics,* Volume 11, pp. 537-560.

Majlessi, M., Nelson, N. & Becker, M., 1998. Advantages of 2'-O-methyl oligoribonucleotide probes for detecting RNA targets. *Nucleic Acids Res,* Volume 26, pp. 2224-2229.

Manoharan, M., 1999. 2'-carbohydrate modifications in antisense oligonucleotide therapy: importance of conformation, configuration and conjugation. *Biochem Biophys Acta,* Volume 1489, pp. 117-130.

Marques, J., 2006. A structural basis for discriminating between self and nonself double-stranded RNAs in mammalian cells. *Nat Biotechnol,* Volume 24, pp. 559-565.

Marques, J. & Williams, B., 2005. Activation of the mammalian immune system by siRNAs. *Nat Bio Tech,* Volume 23, pp. 1399-1405.

Martinez, J. & Tuschl, T., 2004. RISC is a 5′ phosphomonoester-producing RNA endonuclease. *Genes Dev,* Volume 18, pp. 975-980.

Meister, G., 2004. Human argonaute2 mediates RNA cleavage targeted by miRNAs and siRNAs. *Mol Cell,* Volume 15, pp. 185-197.

Meng, H., 2010. Engineered design of mesoporous silica nanoparticles to deliver doxorubicin and P-glycoprotein siRNA to overcome drug resistance in a cancer cell line. *ACS Nano,* Volume 4, pp. 4539-4550.

Mescalchin, A., 2007. Cellular uptake and intracellular release are major obstacles to the therapeutic application of siRNA: novel options by phosphorothioate-stimulated delivery. *Expert Opin Biol Ther,* Volume 7, pp. 1531-1538.

Meselson, M. & Stahl, F., 1958. Replication of DNA in *E. coli*. *PNAS,* Volume 44, pp. 671-682.

Miyagishi, M., Hayashi, M. & Taira, K., 2003. Comparison of the suppressive effects of antisense oligonucleotides and siRNAs directed against the same targets in mammalian cells. *Antisense Nucleic A,* Volume 13, pp. 1-7.

Napoli, C., Lemieux, C., 1990. Introduction of a chimeric chalcone synthase gene into petunia results in reversible co-suppression of homologous genes in trans. *Plant Cell,* Volume 2, pp. 279-289.

Nishina, K., 2008. Efficient *in vivo* delivery of siRNA to the liver by conjugation of alpha-tocopherol. *Mol Ther,* Volume 16, pp. 734-740.

Noland, C., Ma, E. & Doudna, J., 2011. siRNA respositioning for guide strand selection by human Dicer complexes. *Mol Cell,* Volume 43, pp. 110-121.

Ozinsky, A., 2000. The repertoire for pattern recognition of pathogens by the innate immune system is defined by cooperation between toll-like receptors. *PNAS,* Volume 97, pp. 13766-13771.

Pandyra, A., Berg, R., Vincent, M. & Koropatnick, J., 2007. Combination silencer RNA (siRNA) targeting Bcl-2 antagonizes siRNA against thymidylate synthase in human tumor cell lines. *J Pharmacol Exper Therap,* Volume 322, pp. 123-132.

Patel, L., Parker, B., Yang, D. & Zhang, W., 2013. Translational genomics in cancer research: converting profiles into personalized cancer medicine. *Cancer Biol Med,* Volume 10, pp. 214-220.

Pattingre, S., 2005. Bcl-2 antiapoptotic proteins inhibit Beclin 1-dependent autophagy. *Cell,* Volume 122, pp. 927-939.

Paula, D., Vitória, M., Bentley, L. & Mahato, R., 2007. Hydrophobization and bioconjugation for enhanced siRNA delivery and targeting. *RNA,* Volume 13, pp. 431-456.

Peacock, H., Kannan, A., Beal, P. & Burrows, C., 2011. Chemical modification of siRNA bases to probe and enhance RNA interference. *J Org Chem,* Volume 76, pp. 7295-7300.

Peel, B., Hagen, G., Krishnamurthy, K. & Desaulniers, J.-P., 2015. Conjugation and evaluation of small hydrophobic molecules to triazole linked siRNAs. *Med Chem Lett,* Volume 6, pp. 117-122.

Pellestor, F. & Paulasova, P., 2004. The peptide nucleic acids (PNAs), powerful tools for molecular genetics and cytogenetics. *Eur J Hum Genet,* Volume 12, pp. 694-700.

Pensato, S., Saviano, M. & Romanelli, A., 2007. New peptide nucleic acid analogues: synthesis and applications. *Expert Opin Biol Ther,* Volume 7, pp. 1219-1232.

Pichlmair, A., 2006. RIG-I-mediated antiviral responses to single-stranded RNA bearing 5'-phosphates. *Science,* Volume 314, pp. 997-1001.

Prakash, T., 2011. An overview of sugar-modified oligonucleotides for antisense therapeutics. *Chem Biodivers,* Volume 8, pp. 1616-1641.

Prakash, T., 2005. Positional effect of chemical modifications on short interference RNA activity in mammalian cells. *J Med Chem,* Volume 48, pp. 4247-4253.

Raines, R., 1998. Ribonueclease A. *Chem Rev,* Volume 98, pp. 1045-1066.

Ranjbar, B., 2009. Circular dichroism techniques: biomolecular and nanostructural Analyses. *Chem Biol Drug Des,* Volume 74, pp. 101-120.

Reed, J., 1995. Bcl-2 family proteins: regulators of chemoresistance in cancer. *Toxicol Lett,* Volume 82, pp. 155-158.

Robbins, M., 2007. 2′-O-methyl-modified RNAs act as TLR7 antagonists. *Mol Ther,* Volume 15, p. 1663–1669.

Robbins, M., Judge, A. & MacLachlan, I., 2009. siRNA and innate immunity. *Oligonucleotides,* Volume 19, pp. 89-101.

Romano, N. & Macino, G., 1992. Quelling: transient inactivation of gene expression in *Neurospora crassa* by transformation with homologous sequences. *Mol Microbiol,* Volume 6, pp. 3343-3353.

Saad, M., Garbuzenko, O. & Minko, T., 2008. Co-delivery of siRNA and an anticancer drug for treatment of multidrug-resistant cancer. *Nanomedicine,* Volume 3, pp. 761-776.

Sabahi, A., 2001. Hybridization of 2'-ribose modified mixed-sequence oligonucleotides: thermodynamic and kinetic studies. *Nucleic Acids Res,* Volume 29, pp. 2163-2170.

Sakurai, K., 2011. A role for human Dicer in pre-RISC loading of siRNAs. *Nucleic Acids Res,* Volume 39, pp. 1510-1525.

Schwarz, D., 2003. Asymmetry in the assembly of the RNAi Enzyme Complex. *Cell,* Volume 115, pp. 199-208.

Scudiero, D., 1988. Evaluation of a soluble tetrazolium/formazan assay for cell growth and drug sensitivity in culture using human and other tumor cell lines. *Cancer Research,* Volume 48, pp. 4827-4833.

Snead, N., 2012. Molecular basis for improved gene silencing by Dicer substrate interfering RNA compared with other siRNA variants. *Nucleic Acids Res,* Volume 41, pp. 6209-6221.

Stein, C., 2010. Efficient gene silencing by delivery of locked nucleic acid antisense oligonucleotides, unassisted by transfection reagents. *Nucleic Acids Res,* Volume 38, pp. e3: 1-8.

Stephenson, M. & Zamecnik, P. C., 1978. Inhibition of Rous sarcoma viral RNA translation by a specific oligodeoxyribonucleotide. *PNAS,* Volume 75, pp. 285-288.

Suntharalingam, G., 2006. Cytokine storm in a phase 1 trial of the anti-CD28 monoclonal antibody TGN1412. *N Engl J Med,* Volume 355, pp. 1018-1028.

Takeda, K. & Akira, S., 2005. Toll-like receptors in innate immunity. *Int Immunol,* Volume 17, pp. 1-14.

Teijaro, J., 2014. Mapping the innate signaling cascade essential for cytokine storm during influenza virus infection. *PNAS,* Volume 111, pp. 3799-3804.

Temin, H. & Mizutani, S., 1970. Viral RNA-dependent DNA Polymerase: RNA-dependent DNA Polymerase in Virions of Rous Sarcoma Virus. *Nature,* Volume 226, pp. 1211-1213.

Tron, V., 1995. Immunohistochemical analysis of Bcl-2 protein regulation in cutaneous melanoma. *Am J Pathology,* Volume 146, pp. 643-650.

Tsujimoto, Y., Cossman, J., Jaffe, E. & Croce, C., 1985. Involvement of the bcl-2 gene in human follicular lymphoma. *Science,* Volume 228, pp. 1440-1443.

Tsujimoto, Y., 1984. Cloning of the chromosome breakpoint of neoplastic B cells with the t(14;18) chromosome translocation. *Science,* Volume 226, pp. 1097-1099.

Turner, J. J., 2007. MALDI-TOF mass spectral analysis of siRNA degradation in serum confirms an RNAse A-like activity. *Mol Biosyst,* Volume 3, pp. 43-50.

Ui-Tei, K., 2008. Thermodynamic stability and Watson–Crick base pairing in the seed duplex are major determinants of the efficiency of the siRNA-based off-target effect. *Nucleic Acids Res,* Volume 36, pp. 7100-7109.

Valenzuela, R., 2015. Base modification strategies to modulate immune stimulation by an siRNA. *Chembiochem,* Volume 16, pp. 262-267.

Verthelyiemail, D. & Zeuner, R., 2003. Differential signaling by CpG DNA in DCs and B cells: not just TLR9. *Trends Immuno,* Volume 24, pp. 519-522.

Volkov, A., 2009. Selective protection of nuclease-sensitive sites in siRNA prolongs silencing effect. *Oligonucleotides,* Volume 19, pp. 191-202.

Wang, H., 2011. Structural insights into RNA processing by the human RISC-loading complex. *Nat Struct Mol Biol,* Volume 16, pp. 1148-1153.

Wang, Q., 2003. A stepwise huisgen cycloaddition process: copper(I)-catalyzed regioselective “ligation” of azides and terminal alkynes. *JACS,* Volume 125, pp. 3192-3193.

Wang, S. & Kool, E. T., 1995. Relative stabilities of triple helices composed of combinations of DNA, RNA, and 2'-O-methyl-RNA backbones. *Nucleic Acids Res,* Volume 23, pp. 1157-1164.

Watanabe, T., Geary, R. & Levin, A., 2006. Plasma protein binding of an antisense oligonucleotide targeting human ICAM-1 (ISIS 2302). *Oligonucleotides,* Volume 16, pp. 169-180.

Watson, J. D. & Crick, F. H. C., 1953. A structure for deoxyribose nucleic acid. *Nature,* Volume 171, pp. 737-738.

Weinberg, R., 1991. Tumor suppressor genes. *Nature,* Volume 254, pp. 1138-1146.

Wilhelmsson, M., 2010. Fluorescent nucleic acid base analogues. *Q Rev Biophys,* Volume 43, pp. 159-183.

Wilson, C. W. & Doudna, J., 2013. The molecular mechanisms of RNA interference. *Annu Rev Biophys,* Volume 42, pp. 217-239.

Wolfrum, C., 2007. Mechanisms and optimization of *in vivo* delivery of lipophilic siRNAs. *Nat Biotechnol,* Volume 25, pp. 1149-1157.

Wu, P., 2004. Efficiency and fidelity in a click-chemistry route to triazole dendrimers by the copper(I)-catalyzed ligation of azides and alkynes. *Angewandte Chem,* Volume 43, pp. 3928-3932.

Wu, S., Lopez-Berestein, G., Calin, G. & Sood, A., 2014. Targeting the undruggable: advances and obstacles in current RNAi therapy. *Sci Transl Med,* Volume 6, pp. 240-247.

Wu, Y., 2014. 2’-F and 2'-OMe-phosphorodithioate modified siRNAs show increased loading into the RISC complex and enhanced anti-tumour activity. *Nat Commun,* Volume 12, pp. 34-59.

Yakovchuk, P., Protozanova, E. & Frank-Kamenetskii, M., 2006. Base-stacking and base-pairing contributions into thermal stability of the DNA double helix. *Nucelic Acids Res*, Volume 32, pp. 564-574..

Ye, X., 2011. Structure of C3PO and mechanism of human RISC activation. *Nat Struct Mol Biol*, Volume 18, p. 650–657.

Yoda, M., 2010. ATP-dependent human RISC assembly pathways. *Nat Struct Mol Biol*, Volume 17, pp. 17-23.

Zamanian-Daryoush, M., 2008. Determinants of cytokine induction by small interfering RNA in human peripheral blood mononuclear cells. *J Interferon Cytokine Res*, Volume 28, pp. 221-233.

Zamecnik, P. & Stephenson, M. L., 1978. Inhibition of Rous sarcoma virus replication and cell transformation by a specific oligodeoxynucleotide. *PNAS*, Volume 75, pp. 280-284.

Zhang, J., Zhuang, S., Tong, C. & Liu, W., 2013. Probing the molecular interaction of triazole fungicides with human serum albumin by multispectroscopic techniques and molecular modeling. *J Agric Food Chem*, Volume 61, pp. 7203-7211.

Appendix

UNIVERSITY OF ONTARIO INSTITUTE OF TECHNOLOGY

RESEARCH ETHICS BOARD
OFFICE OF RESEARCH SERVICES

Date: February 3rd, 2015

To: Gordon Hagen (Student PI) and John Samis (Supervisor)

From: Bill Goodman, REB Chair

REB File #: 14-068

Project Title: Synthesis and in vitro assessment of chemically modified siRNAs containing 2'-ribose modifications and triazole linked backbone modifications

DECISION: APPROVED

CURRENT EXPIRY: February 1st, 2016

NOTE: Notwithstanding this approval, you are required to obtain/submit, to UOIT's Research Ethics Board, any relevant approvals/permissions required, prior to commencement of this project.

The University of Ontario, Institute of Technology Research Ethics Board (REB) has reviewed and approved the above research proposal. This application has been reviewed to ensure compliance with the Tri-Council Policy Statement: Ethical Conduct for Research Involving Humans (TCPS2 (2014)) and the UOIT Research Ethics Policy and Procedures.

Please note that the (REB) requires that you adhere to the protocol as last reviewed and approved by the REB. Always quote your REB file number on all future correspondence.

CONTINUING REVIEW REQUIREMENTS:

- **Renewal Request Form:** All approved projects are subject to an **annual** renewal process. Projects must be renewed or closed by the expiry date indicated above ("Current Expiry"). **Projects that are not renewed within 30 days of the expiry date will be automatically suspended by the REB; and projects that are not renewed within 60 days of the expiry date will be automatically closed by the REB.** Once your file has been formally closed, a new submission will be required to open a new file.
- **Change Request Form:** any changes or modifications (i.e. adding a Co-PI or a change in methodology) must be approved by the REB through the completion of a change request form before implemented.
- **Adverse or unexpected Events Form:** events must be reported to the REB within 72 hours after the event occurred with an indication of how these events affect (in the view of the Principal Investigator) the safety of the participants and the continuation of the protocol. (I.e. un-anticipated or un-mitigated physical, social or psychological harm to a participant).
- **Research Project Completion Form:** must be completed when the research study has completed.

All Forms can be found at http://research.uoit.ca/faculty/policies-procedures-forms.php.

REB Chair	Ethics and Compliance Officer
Dr. Bill Goodman, FBIT bill.goodman@uoit.ca	compliance@uoit.ca

University of Ontario, Institute of Technology
2000 Simcoe Street North, Oshawa ON, L1H 7K4
PHONE: (905) 721-8668, ext. 3693
Version: Jan. 2015

Appendix Figure 1 - Research Ethics Board approval form.

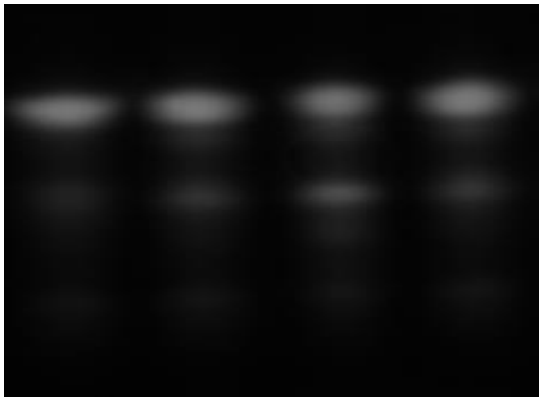

Appendix Figure 2 - Sample picture of a standard oligonucleotide test gel.
20% denaturing polyacrylamide gel was run in 0.5X TBE buffer. The gel was loaded with 0.5 OD units of oligonucleotide with denaturing loading solution for a total volume of 20 µL, the gel was ran for 16 hours at 80V. The gel was stained in a 3X solution of GelRed (Biotium) for 30 minutes while being gently stirred on a shaker. Finally RNA integrity was visualized via Fluorchem SP (Fisher Scientific). This gel displays pure and degraded oligonucleotides and most lanes needed further gel purification before use.

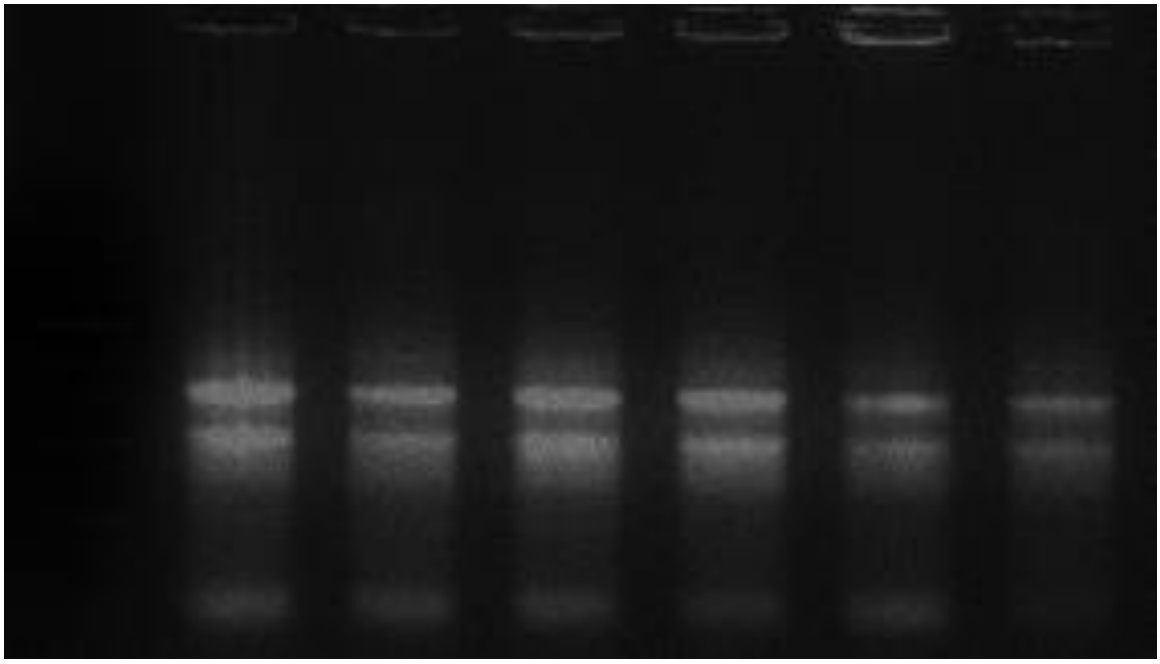

Appendix Figure 3 - Sample picture of a successful RNA preparation.
RNA was extracted using TRIzol reagent and visualized by running 5 µg of total RNA in a 1X agarose gel electrophoresis (60V for 45 minutes). The gel was stained in a 3X solution of GelRed (Biotium) for 30 minutes while being gently stirred on a shaker. Finally RNA integrity was visualized via Fluorchem SP (Fisher Scientific). Top band corresponds to mammalian 28s rRNA, middle band corresponds to mammalian 18s rRNA, lowest band corresponds to small RNA (mRNA, tRNA, etc.).

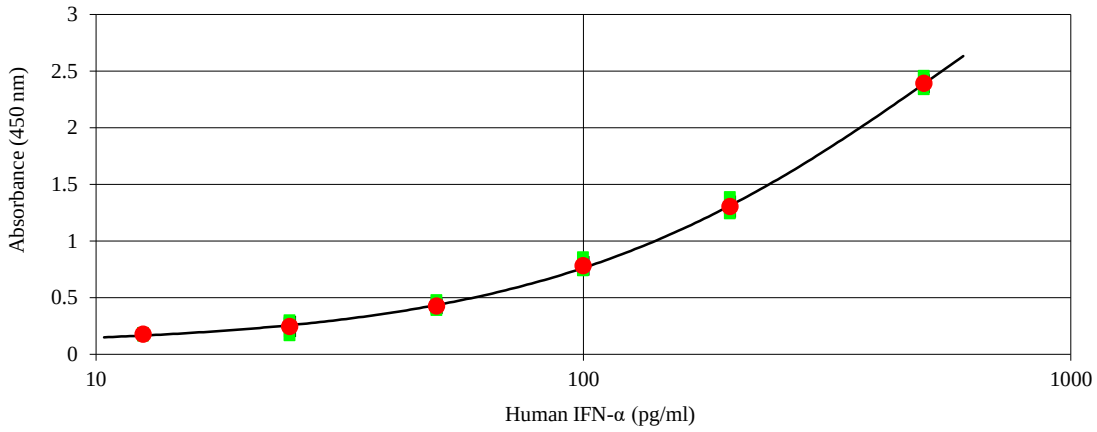

Appendix Figure 4 - High sensitivity standard curve of human IFN-α.
Assay range 12.5 – 500 pg/ml. Standard curve constructed by plotting the optical densities (OD) of standards using 4-parameter fit for the standard curve (Blanks were subtracted from the standards). R^2=1 and Err= 0.011.

MedChemComm

CONCISE ARTICLE

Cite this: Med. Chem. Commun., 2015, 6, 1210

Synthesis and *in vitro* assessment of chemically modified siRNAs targeting *BCL2* that contain 2′-ribose and triazole-linked backbone modifications†

Gordon Hagen,[a] Brandon J. Peel,[a] John Samis[b] and Jean-Paul Desaulniers*[a]

Received 10th April 2015,
Accepted 15th May 2015

DOI: 10.1039/c5md00147a

www.rsc.org/medchemcomm

Short-interfering RNAs (siRNAs) are naturally occurring biomolecules used for post-transcriptional gene regulation, and therefore hold promise as a future therapeutic by silencing gene expression of overexpressed deleterious genes. However, there are many inherent problems with the native RNA structure. This project investigates the ability of a library of chemically modified siRNAs to target the therapeutically relevant oncogene, *BCL2*, by combining 2′-ribose sugar modifications with a novel triazole-linked backbone modification, previously described by our group. Solid support phosphoramidite chemistry was used to incorporate chemical modifications at various positions within anti-*BCL2* siRNAs. *In vitro* effects were evaluated through qPCR, cell viability, nuclease stability, and an ELISA assay. Our results indicate that these unique modifications are well tolerated within RNAi and show enhanced activity and stability over natural siRNAs, while also improving upon inherent issues of toxicity and immunological activity.

Short-interfering RNAs (siRNAs) are a class of biomolecules characterized by their ability to silence gene expression at the translational level through the RNA interference (RNAi) pathway.[1,2] RNAi is an innate cellular pathway that involves short double-stranded RNA molecules bound to the RNA-induced-silencing-complex (RISC). RISC unwinds and dissociates the sense RNA strand and retains the antisense RNA strand to create an 'active-RISC-RNA-complex.' This active complex binds to a complementary mRNA transcript in a sequence-dependent manner, and through the action of Argonaute 2, catalytically degrades the mRNA.[3] siRNAs hold promise as a future therapeutic, as many diseases are characterized by aberrant gene expression.[4,5] SiRNAs are widely used as a research tool, probing molecular function by suppressing gene expression, but have yet to be utilized as a therapeutic due to several limitations. One major limitation of siRNAs is the susceptibility to degradation by endogenous nucleases, which causes siRNAs to have a very short half-life and decreased potency *in vivo*.[6] Another major limitation of siRNA therapeutics is the propensity to illicit an innate immune response causing pro-inflammatory cytokines to be released, leading to a systemic immune response.[7] SiRNAs are also prone to cause off-target effects, leading to suppression of non-target mRNA sequences.[8] Finally, siRNAs have difficulty being internalized by cells, thus making their bioavailability a challenge. These limitations are often due to the native structure of RNA which is recognized by endogenous proteins. However, through the use of chemical modifications, many of these pharmacological shortcomings and limitations can be modulated.[9]

Some of the most common chemical modifications used in oligonucleotide design are 2′-ribose modifications. These modifications involve replacing the natural 2′-hydroxyl group with another functional group, such as a 2′-*O*-methyl (2′-*O*-Me) and/or 2′-fluoro (2′-F).[10] 2′-ribose modifications are becoming more common in oligonucleotide design, and their building block phosphoramidites are commercially available for solid-phase oligonucleotide synthesis.[10] When these modifications are used within siRNA macromolecules in biological experiments, data has demonstrated an increase in the nuclease stability of RNA duplexes,[11] a decrease in the immune response,[12] and an increase in the thermodynamic stability of the siRNA duplex.[13] Backbone modifications, which replace the native phosphodiester linkage, are another less common chemical modification employed in oligonucleotide synthesis to overcome therapeutic barriers.[14] One such example is the non-ionic triazole-linked nucleic acid dimer, previously described by our research group.[15–17] When this

[a] *Faculty of Science, University of Ontario Institute of Technology, Oshawa, ON. L1H 7K4, Canada. E-mail: Jean-Paul.Desaulniers@uoit.ca*

[b] *Faculty of Health Science, University of Ontario Institute of Technology, Oshawa, ON. L1H 7K4, Canada*

† Electronic supplementary information (ESI) available: Full list of siRNAs synthesised and assessed as well as detailed experimental materials and methods can be found in the electronic supplementary information. See DOI: 10.1039/c5md00147a

Appendix Figure 5 – MedChemComm Publication 2015.

backbone modification was incorporated into an siRNA, gene-silencing data illustrated dose-dependent knockdown of an exogenous gene *in vitro* and improved serum nuclease resistance when compared to an unmodified siRNA.[16] Oligonucleotide therapeutics which are commercially available contain multiple types of chemical modifications within their structure, but currently no universally acceptable chemical modification design exists for siRNAs, despite some significant advances in the field.[18]

The triazole-linked backbone modification developed by our laboratory has yet to be investigated for immune stimulation or for its use in gene-silencing clinically relevant endogenous genes. The gene in this study that we examine is *BCL2*. *BCL2* encodes the bcl2 protein, which is an important regulator of type I and II programmed cell death (apoptosis and autophagy, respectively).[19–21] This gene can become mutated into an oncogene through a translocation event which causes overexpression of *BCL2*, thus leading to decreased cell death and increased cellular proliferation.[19–21] *BCL2* is associated with several clinical cancer types and is implicated in chemotherapeutic resistance, thus making *BCL2* a good therapeutic target for siRNA design.[22]

This paper aims to generate chemically-modified siRNAs that target the clinically relevant oncogene, *BCL2*, *in vitro*. These siRNAs contain a uracil-triazole-uracil backbone modification in conjunction with 2′-ribose modifications to determine if therapeutic limitations of nuclease susceptibility and immune activation can be modulated in an attempt to further siRNA therapeutic design.

A library of anti-*BCL2* siRNAs were generated using solid support phosphoramidite chemistry (see Table S1 in the ESI†). The library of siRNAs contains a combination of 2′-ribose modifications in conjunction with a uracil-triazole-uracil backbone (U_tU) modification (Fig. 1). All chemically-modified siRNAs generated retain standard A-type helical conformation, as confirmed by circular dichroism (see Fig. S4 in the ESI†). Both negative and positive circular dichroism bands at approximately 210 nm and 265 nm, respectively, are observed.

We have previously described optimal placement of U_tU modifications within siRNAs,[16] thus U_tU modifications were placed at either the 3′-overhang position or within the 3′-region of the sense strand. The 2′-ribose modifications were placed in siRNA duplexes either with or without U_tU modifications. The 2′-ribose modifications were placed at various positions on the sense strand; they were placed around the 3′-end region or throughout the entirety of the strand. Alternatively, the 2′-ribose modifications were placed on the pyrimidyl-linked ribose sugars throughout the antisense strand. The ability of each siRNA to knockdown *BCL2* mRNA was assessed at three concentrations (20 nM, 10 nM and 1 nM), 24 hours post-transfection in KB cells by measuring normalized expression levels using qPCR. Gene-silencing data from the chemically modified siRNAs show effective dose-dependent down-regulation of *BCL2* at all concentrations (see Fig. S1 in the ESI†). Several of the chemically-modified siRNAs exhibit enhanced activity compared to unmodified wild-type siRNA (Bwt) at concentrations of 10 nM and below. From the initial screen of the siRNA library, eight siRNAs were chosen for further investigation because of enhanced dose-dependent knockdown of *BCL2* compared to Bwt (Table 1).

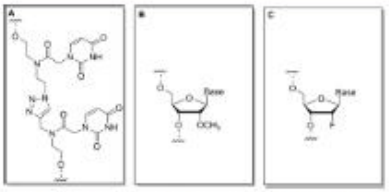

Fig. 1 Structures of chemical modifications used in the synthesis of anti-*BCL2* siRNAs. A) Uracil-triazole-uracil dimer (U_tU). B) Ribose 2′-*O*-methyl (2′-*O*-Me) nucleoside; C) ribose 2′-fluoro (2′-F) nucleoside.

Table 1 Sequences of selected anti-*BCL2* siRNAs[a]

RNA	siRNA duplex
Bwt	5′-GCCUUCUUUGAGUUCGGUGtt-3′ 3′-ttCGGAAGAAACUCAAGCCAC-5′
B2	5′-GCCUUCUUUGAGU$_t$U$_t$UCGGUGtt-3′ 3′-ttCGGAAGAAACUCAAGCCAC-5′
B3	5′-GCCUUCUUUGAGUUCGGUGU$_t$U$_t$-3′ 3′-ttCGGAAGAAACUCAAGCCAC-5′
B4	5′-GCCUUCUUUGAGUUCGGUGtt-3′ 3′-ttCGGAAGAAACUCAAGCCAC-5′
B5	5′-GCCUUCUUUGAGU$_t$U$_t$CGGUGtt-3′ 3′-ttCGGAAGAAACUCAAGCCAC-5′
B6	5′-GCCUUCUUUGAGUUCGGUGU$_t$U$_t$-3′ 3′-ttCGGAAGAAACUCAAGCCAC-5′
B10	5′-GCCUUCUUUGAGUUCGGUGtt-3′ 3′-ttCGGAAGAAACUCAAGCCAC-5′
B11	5′-GCCUUCUUUGAGU$_t$U$_t$CGGUGtt-3′ 3′-ttCGGAAGAAACUCAAGCCAC-5′
B12	5′-GCCUUCUUUGAGUUCGGUGU$_t$U$_t$-3′ 3′-ttCGGAAGAAACUCAAGCCAC-5′
NC	5′-CUUACGCUGAGUACUUCGAtt-3′ 3′-ttGAAUGCGACUCAUGAAGCU-5′

[a] UtU corresponds to the uracil-triazole-uracil modification; Ç or Ụ corresponds to the 2′-*O*-Me modification; Ç or Ụ corresponds to the 2′-F modification. NC is a negative control siRNA and corresponds to a sequence which does not target endogenous mRNA. The top strand corresponds to the sense strand; the bottom strand corresponds to the antisense strand. In all duplexes, the 5′-end of the bottom antisense strand contains a 5′-phosphate group.

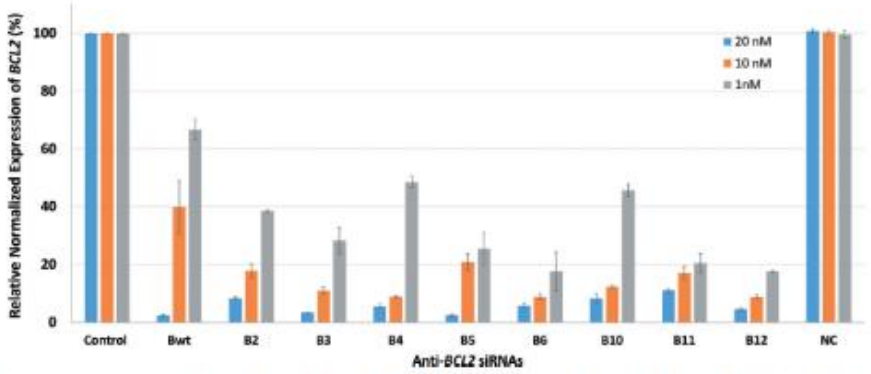

Fig. 2 Relative gene expression of *BCL2* in KB cells 24 hours post anti-*BCL2* siRNA transfections at 1 nM, 10 nM and 20 nM. Gene expression was measured using qPCR and expression was normalized to an untreated control using reference genes 18s rRNA and glyceraldehyde 3-phosphate dehydrogenase (GAPDH).

When U_fU modifications were combined with 2′-ribose modifications clustered around the 3′-end of the sense strand, gene silencing ability was enhanced compared to Bwt at concentrations above 1 nM (Fig. 2). When the U_fU modification was placed in an overhang position (B3, B6, and B12), whether in conjunction with 2′-ribose modifications or not, the siRNAs showed the greatest silencing ability at all concentrations while retaining a dose-dependent response. This data indicates that the chemical modification patterns chosen for this study are amendable within the RNAi pathway, and have excellent gene silencing ability.

After mRNA knockdown was assessed, it was relevant to investigate the biological stability of these siRNAs in the presence of nuclease enzymes. Independently, it has been previously reported that both U_fU and 2′-ribose modifications incur nuclease stability when compared to unmodified siRNAs.[11,16] Unmodified and modified siRNAs were incubated in fetal bovine serum (FBS) for up to five hours to analyze the truncated products in a time-dependent manner using polyacrylamide gel electrophoresis (Fig. 3).

Unmodified siRNA (Bwt) degraded almost immediately, with little to no siRNA present within 0.5 hours of incubation in the presence of nucleases. When the U_fU modification was incorporated internally within the siRNA (B2), the full siRNA duplex persisted for up to 2 hours, and when placed at an overhang position (B3), the duplex was persistent for up to 4 hours. 2′-*O*-Me modifications clustered at the 3′-region of the sense strand (B4) increased nuclease stability, allowing the siRNA duplex to last for 2 hours in the presence of nucleases. When the 2′-*O*-Me modification was combined with an internal U_fU modification (B5), the duplex lasted up to 3 hours. When the 2′-*O*-Me modification was combined with the U_fU overhang (B6), the siRNA duplex was still present after 3 hours of incubation in the presence of nucleases. When the

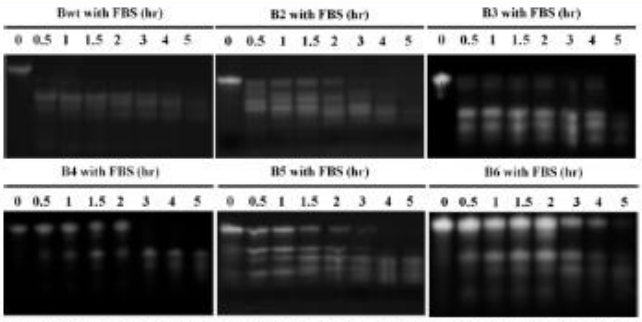

Fig. 3 Nuclease stability assay. 20% non-denaturing polyacrylamide gel with degradation products of siRNAs Bwt and B2–B6 after incubation with 13.5% fetal bovine serum at 37.5 °C from 0 hours to 5 hours.

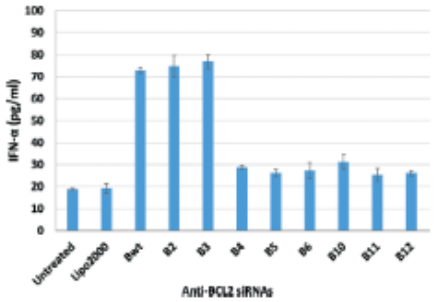

Fig. 4 Human interferon alpha production in response to anti-*BCL2* siRNAs. PBMCs were stimulated with 20 nM of anti-*BCL2* siRNAs supplemented with Lipofectamine 2000. IFN-α was measured in the supernatant 24 hours post-transfection by ELISA.

2′-*O*-Me modification was combined with the U_tU backbone modification, nuclease resistance was greatly increased. Any change to the native chemical structure caused a significant increase in nuclease stability, especially when backbone and ribose modifications were combined.

In vivo, double-stranded RNAs stimulate innate immunity by triggering the type I interferon response.[7] *In vitro*, the immune response is highly dependent on the specific cell line used, and many cell lines do not possess the receptors necessary to respond to siRNAs, whereas using human peripheral mononuclear cells (PBMC) isolated from whole human blood serves as a fast and reliable *in vitro* approach to predict *in vivo* response.[23] Therefore, after obtaining ethical approval, human PBMCs were isolated from whole blood donated by healthy volunteers after obtaining written consent. PBMCs were stimulated using 20 nM of anti-*BCL2* siRNAs complexed with lipofectamine 2000. After 24 hours, human interferon alpha (IFN-α) levels were measured using a VeriKine ELISA kit (PBL Assay Science) according to the manufacturer's protocol (Fig. 4).

PBMCs challenged with unmodified siRNA as well as triazole modified siRNAs (Bwt, B2, and B3) induced IFN-α production (72.8, 74.4, and 76.9 pg ml^{-1} respectively), whereas siRNAs containing 2′-ribose modifications (B4, B5, B6, B10, B11 and B12) showed a decrease in immune response similar to untreated controls (28.8, 26.1, 27.3, 31.2, 25.4, and 26.1 pg ml^{-1} respectively). This data suggests that the U_tU modification alone does not alter immune response in comparison to unmodified siRNA (Bwt). However, when the U_tU modification was combined with 2′-ribose modifications the innate immune response was diminished as indicated by a decrease in IFN-α production from PBMCs.

The siRNAs in this study target a clinically relevant oncogene, *BCL2*. *BCL2* oncogene is responsible for the overproduction of the bcl2 protein, which is a key regulatory protein in cellular apoptosis. Bcl2 prevents pro-apoptotic factors from triggering type I and type II cell death, and thus overexpression of *BCL2* prevents cells from undergoing apoptosis.[19–21] KB cells are known to overexpress the *BCL2* oncogene. Therefore, decreasing *BCL2* expression, *via* RNAi should cause a decrease in cellular proliferation. An XTT cellular proliferation kit (ATCC) was used to determine proliferation rates of KB cells treated with anti-*BCL2* siRNA in comparison to untreated cells 24 hours post siRNA transfection (see Fig. S3 in the ESI†). The anti-*BCL2* siRNAs were able to decrease cellular proliferation by 20% or more at all concentrations when compared to untreated cells. To ensure that the decreased cellular proliferation was not due to toxicity from the siRNAs, a negative control was used, which did not target an endogenous gene; the negative control exhibited the same cellular proliferation rate as the untreated control. From the qPCR screen, the best candidate siRNAs (Table 1) were used to determine cellular proliferation rates from continual knockdown over the course of four days (see Fig. S2 in the ESI†). All of the best candidate siRNAs were able to decrease cellular proliferation within 24 hours by at least 30% when compared to untreated controls (Fig. 5).

Cellular proliferation continued to decrease after 48 and 72 hours. By 96 hours, cellular proliferation rates stabilized

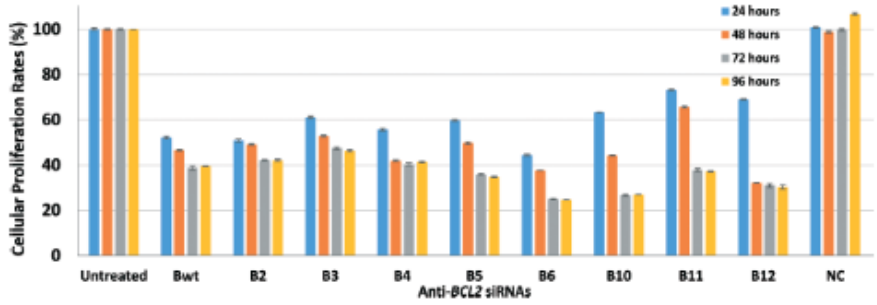

Fig. 5 Time course cellular proliferation assay. Relative cellular proliferation rates of KB cells treated with 20 nM of anti-*BCL2* siRNAs compared to untreated KB cells. Cellular proliferation rates were measured using XTT reagent at 24, 48, 72 and 96 hours.

at their lowest rate when compared to the untreated control. Continual knock-down of *BCL2* caused a 50–60% decrease in cellular proliferation after 96 hours compared to the untreated control.

Conclusions

siRNA oligonucleotides containing commercially available 2′-ribose modifications (2′-*O*-Me/2′-F) can be combined with a novel triazole-linked backbone modification in siRNA design and these siRNAs are amendable within the RNAi pathway. The qPCR *BCL2* screens show that these modifications have enhanced gene-silencing activity either independently or in conjunction within the same siRNA. As expected, the chemically modified siRNAs also show excellent biological stability with high nuclease resistance, whereas unmodified siRNAs are readily degraded by serum nucleases.[6,11,16] Nuclease stability was additive when combining triazole-linked backbone modifications with 2′-ribose modifications, especially when the triazole modification was placed at the overhang position. This enhanced biological stability is desirable for pharmaceutical applications.

Another major limitation of the pharmaceutical application of siRNAs is the innate immune response. The innate immune system has a variety of receptors which recognize and respond to small nucleic acids, triggering cytokine and interferon release.[7] Both 2′-*O*-Me and 2′-F modifications block immune response *in vitro* and *in vivo*,[24] whereas the triazole-linked nucleic acid has not been tested for immune response. Our results show that triazole-linked backbone modifications illicit a similar immune response as unmodified siRNAs, and are detected by the innate immune system. When the triazole-linked backbone modification is combined with 2′-ribose modified siRNAs, the immune response is diminished to a similar level as induced by siRNAs containing only 2′-ribose modifications. Overall, this shows that the triazole-linked nucleic acid can be combined with commercially available 2′-ribose modifications to evade immune response while still maintaining RNAi efficacy.

Furthermore, the utility of these siRNAs were assessed by targeting a clinically relevant oncogene, *BCL2*, which is implicated in a diverse range of cancers.[22] Not only were the siRNAs successful in knocking down *BCL2* expression *in vitro*, but were also able to decrease cellular proliferation rates. These results mirror those of oblimersen sodium (Genasense), a *BCL2* antisense oligonucleotide. In preclinical trials, Genasense depleted *BCL2* mRNA which correlated to increased apoptosis and decreased cellular proliferation *in vitro*.[25,26]

Overall, by combining 2′-ribose modifications with a novel triazole-linked backbone modification, we have generated siRNAs with chemical modification patterns which have enhanced nuclease stability and decreased immune activity without compromising the potency of the duplex as a trigger of RNAi.

Acknowledgements

We acknowledge the National Sciences and Engineering Research Council (NSERC) and the Canada Foundation for Innovation (CFI) for funding.

Notes and references

1 C. Napoli, C. Lemieux and G. Jorgensen, *Plant Cell*, 1990, **2**, 279.
2 A. Fire, S. Xu, M. K. Montgomery, S. A. Kostas, S. E. Driver and C. C. Mello, *Nature*, 1998, **391**, 806–811.
3 R. C. Wilson and J. A. Doudna, *Annu. Rev. Biophys.*, 2013, **42**, 17.
4 D. Hanahan and R. Weinberg, *Cell*, 2011, **144**, 646.
5 V. Emilsson, G. Thorleifsson, B. Zhang, A. S. Leonardson, F. Zink, J. Zhu, S. Carlson, A. Helgason, G. B. Walters, S. Gunnarsdottir, M. Mouy, V. Steinthorsdottir, G. H. Eiriksdottir, G. Bjornsdottir, I. Reynisdottir, D. Gudbjartsson, A. Helgadottir, A. Jonasdottir, U. Styrkarsdottir, S. Gretarsdottir, K. P. Magnusson, H. Stefansson, R. Fossdal, K. Kristjansson, H. G. Gislason, T. Stefansson, B. G. Leifsson, U. Thorsteinsdottir, J. R. Lamb, J. R. Gulcher, M. L. Reitman, A. Kong, E. E. Schadt and K. Stefansson, *Nature*, 2008, **452**, 423.
6 J.-R. Bertrand, M. Pottier, A. Vekris, P. Opolon, A. Maksimenko and C. Malvy, *Biochem. Biophys. Res. Commun.*, 2002, **296**, 1000.
7 J. T. Marques and B. Williams, *Nat. Biotechnol.*, 2005, **23**, 1399.
8 A. L. Jackson and P. S. Linsley, *Nat. Rev. Drug Discovery*, 2010, **9**, 57–67.
9 A. Gallas, C. Alexander, M. Davies, S. Puri and S. Allen, *Chem. Soc. Rev.*, 2013, **42**, 7983.
10 D. Corey, *J. Clin. Invest.*, 2007, **117**, 3615.
11 M. Egli, G. Minasov, V. Tereshko, P. S. Pallan, M. Teplova, G. B. Inamati, E. A. Lesnik, S. R. Owens, B. S. Ross, T. P. Prakash and M. Manoharan, *Biochemistry*, 2005, **44**, 9045.
12 A. D. Judge, G. Bola, A. C. H. Lee and I. Maclachlan, *Mol. Ther.*, 2005, **13**, 494.
13 A. Sabahi, J. Guidry, G. B. Inamati, M. Manoharan and P. Wittung-Stafshede, *Nucleic Acids Res.*, 2001, **29**, 2163.
14 G. Deleavery and M. J. Damha, *ChemBioEng Rev.*, 2012, **19**, 937–954.
15 T. Efthymiou and J.-P. Desaulniers, *J. Heterocycl. Chem.*, 2011, **48**, 333.
16 T. Efthymiou, V. Huynh, J. Oentoro, B. Peel and J.-P. Desaulniers, *Bioorg. Med. Chem. Lett.*, 2012, **22**, 1722.
17 B. J. Peel, G. Hagen, K. Krishnamurthy and J.-P. Desaulniers, *ACS Med. Chem. Lett.*, 2015, **6**, 117.
18 G. Ozcan, B. Ozpolat, R. L. Coleman, A. K. Sood and G. Lopez-Berestein, *Adv. Drug Delivery Rev.*, 2015, DOI: 10.1016/j.addr.2015.01.007.
19 M. Cleary, S. Smith and J. Sklar, *Cell*, 1986, **47**, 19.
20 Y. Tsujimoto, J. Cossman, E. Jaffe and C. M. Croce, *Science*, 1985, **228**, 1440.

21 G. Kroemer, *Nat. Med.*, 1997, **3**, 614.
22 J. C. Reed, *Toxicol. Lett.*, 1995, **82–83**, 155.
23 M. Zamanian-Daryoush, J. T. Marques, M. P. Gantier, M. A. Behlke, M. John, P. Rayman, J. Finke and B. R. Williams, *J. Interferon Cytokine Res.*, 2008, **28**, 221.
24 R. V. Fucini, H. J. Haringsma, P. Deng, W. M. Flanagan and A. T. Willingham, *Nucleic Acid Ther.*, 2012, **22**, 205.
25 R. Herbst and S. Frankel, *Clin. Cancer Res.*, 2004, **10**, 42.
26 M. H. Kang and P. Reynolds, *Clin. Cancer Res.*, 2009, **15**, 1126.

Appendix Figure 6- ^{1}H NMR of Synthesized Compounds.

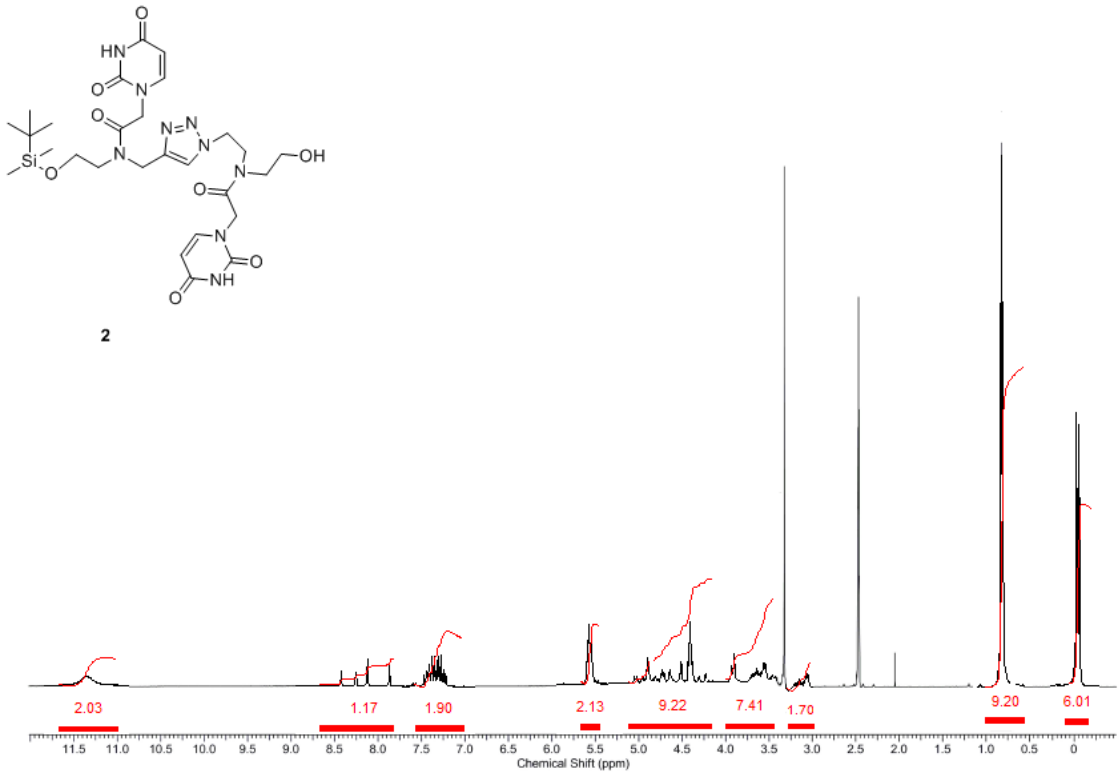

*Proton NMR Spectrum of Compound **(2)**. ^{1}H-NMR spectrum observed in DMSO-d_6 at 400 MHz.*

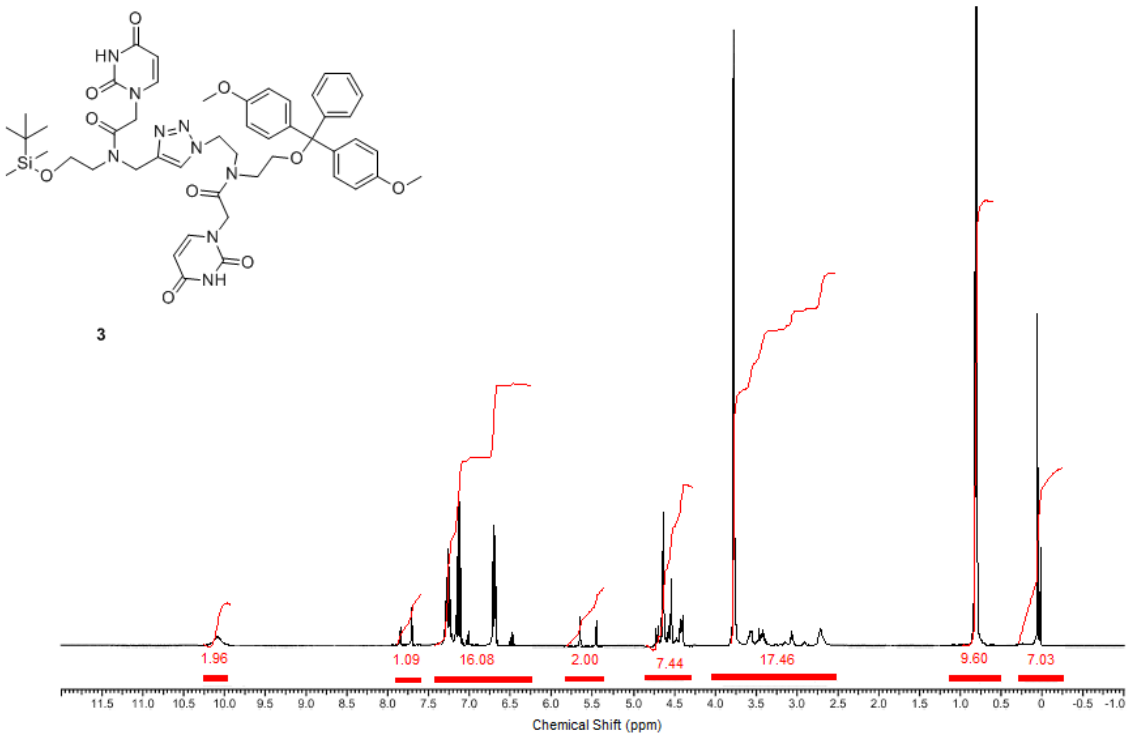

*Proton NMR Spectrum of Compound **(3)**. ^{1}H-NMR spectrum observed in $CDCl_3$ at 400 MHz.*

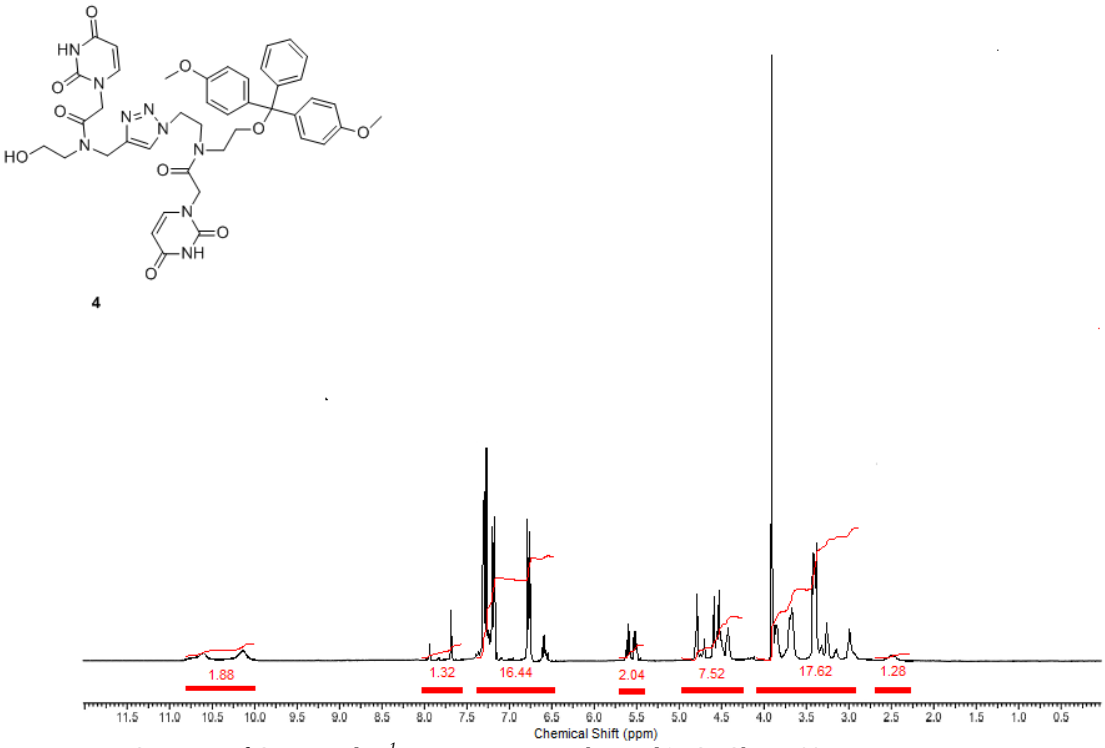

*Proton NMR Spectrum of Compound **4**. ^{1}H-NMR spectrum observed in $CDCl_3$ at 400 MHz.*

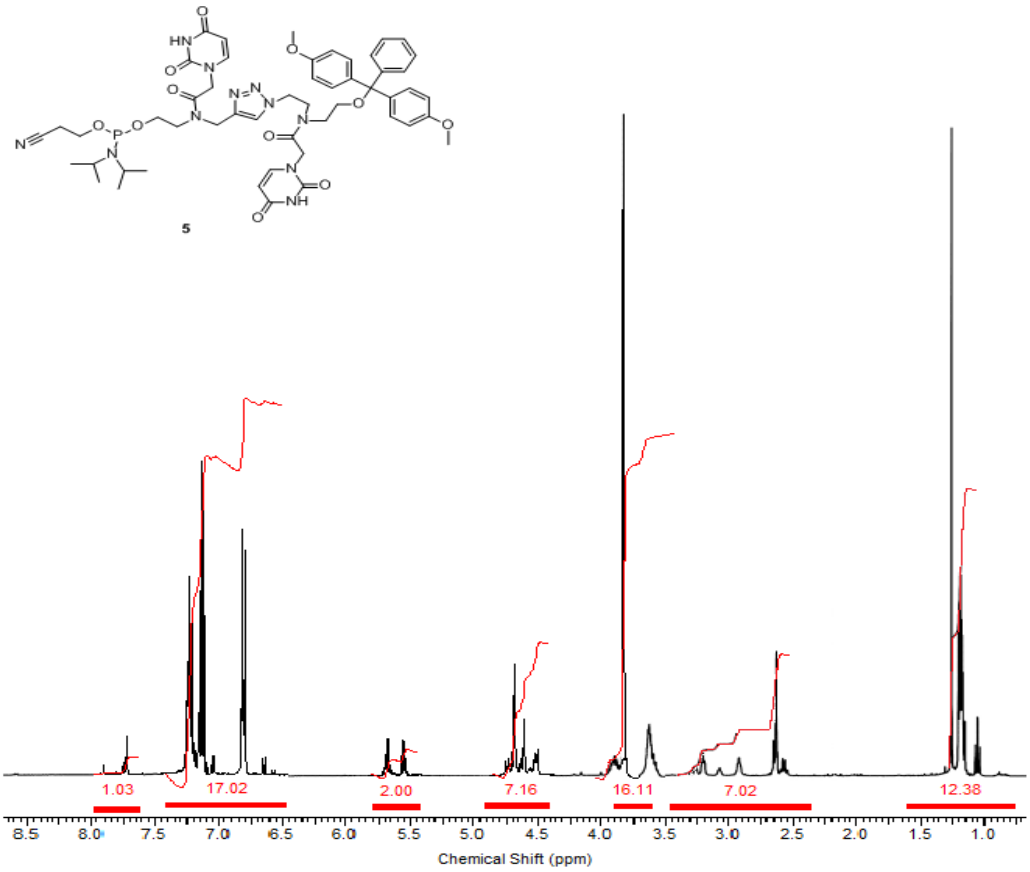

*Proton NMR Spectrum of Compound **5**. ^{1}H-NMR spectrum observed in $CDCl_3$ at 400 MHz.*